Numerical methods for optimal control problems with biological applications

Giulia Fabrini

UNIVERSITÀ DEGLI STUDI
DI GENOVA

Numerical methods for optimal control problems with biological applications

TESI DI DOTTORATO per il titolo di
Dottore di ricerca in Ingegneria delle macchine e dei sistemi
per l'energia, l'ambiente e i trasporti

THÈSE DE DOCTORAT pour le titre de
Docteur de l'Université Pierre et Marie Curie,
Sciences Mathématiques de Paris Centre.

Advisors:
Prof. PATRIZIA BAGNERINI
Prof. LUIS NEVES DE ALMEIDA
Prof. MAURO GAGGERO

Candidate:
GIULIA FABRINI

January 2017

Aknowledgements

There are a lot of people I feel the need to thank who made these three years a very special part of my life.

I want to thank my advisors who helped me during these three years of research: Patrizia Bagnerini, for her patience, her sweetness and her kindness, Luis Almeida for giving me the chance to stay in the stimulating ambient of LJLL, the time spent in Paris was a wonderful experience that gave me the opportunity to grow in the personal and professional field and Mauro Gaggero for the interesting discussions.

My deepest gratitude goes to Maurizio Falcone, for being the first person who believed in me, for his valuable advices, for his constant presence and support; in few words for being my reference point. I have always learnt a lot discussing with him thanks to his immense knowledge and entushiasm.

I would like to thank Tommaso Lorenzi for his patience, for his entuashiasm, for his perseverance, for the optimism he was always ready to inject into me even when the results of the simulations were not so encouraging, for never being tired to explain me the biological concepts and for all the laughs made in the short period we spent together at LJLL and in every skype call. I really enjoyed working with him and I am glad that our paths have crossed.

I want to thank Alessandro Alla for his support beginning from my master thesis, for all the discussions, for the always pleasent collaboration and for the welcome advices.

I would like to thank my parents for their unconditioned love, for supporting and trusting me in all my choices.

I want to thank my brothers: Lorenzo for his swetness and love and Alessandro, my favourite travel-partner, for being there everytime I needed, listening without asking. The expressions on his face to my stories are worth more than thousands of words and have always had the power to make me smile again.

Thanks to Francesca, for "being my person", nothing makes sense if is not shared with her.

Thanks to Ermanno for his constant presence in my everyday life despite the distance, for always being there cheering me up in the bad moments and sharing with me the happy ones. The importance of his friendship has never been underestimated.

Thanks to Smita, for all the never-ending skype calls, the travels and the unforgettable moments together. As you always remind me, everything happens for a reason and I will always be thankful for that evening in Paris four years ago.

I would like to thank the people I met during and thanks to my PhD, whom I became very close to: Arianna, Chiara, Laura, Silvia and Valentina.

Finally thanks to the long-term friends, in particular to Cristiana, Beatrice and Laura.

Summary

Riassunto

Questa tesi si sviluppa su due fronti: nella prima parte ci concentriamo sui metodi numerici di approssimazione di problemi di controllo ottimo, in particolare sul Principio della Programmazione Dinamica e sul Model Predictive Control (MPC), mentre nella seconda parte presentiamo applicazioni delle tecniche di controllo in campo biologico, in particolare ai modelli di evoluzione di popolazioni di cellule tumorali.
Nella prima parte della tesi consideriamo l'approssimazione di un problema di controllo ottimo ad orizzonte infinito che combina un primo passo (basato sul Model Predictive Control) allo scopo di ottenere rapidamente una traiettoria sub-ottima approssimata, e un secondo passo in cui viene risolta l'equazione di Bellman in un intorno della traiettoria di riferimento. È ben noto che la soluzione globale attraverso l'equazione di Bellman può essere piuttosto costosa poichè occorre risolvere il problema in un dominio contenente tutte le possibili condizioni iniziali per la dinamica. Occorre inoltre imporre (e scegliere) delle opportune condizioni al bordo per risolvere tale equazione. La caratteristica principale del MPC è quella di calcolare un controllo feedback approssimato per la dinamica a partire da una condizione iniziale risolvendo una sequenza di problemi di controllo ottimo ad orizzonte finito. Sembra pertanto naturale risolvere innanzitutto il problema per una condizione iniziale ottenuta applicando l'MPC, e poi calcolare la funzione valore in un intorno di tale traiettoria, riducendo di molto le dimensioni del dominio in cui l'equazione di Bellman è risolta e di conseguenza la complessità di calcolo. Il secondo passo risulta essere necessario se si vuole ottenere una soluzione stabile, dal momento che possiamo utilizzare tutte le informazioni vicine alle traiettoria di riferimento e non solo quelle su di essa.
Il secondo argomento trattato in questa tesi riguarda il controllo dell'evoluzione di un fronte descritto attraverso il metodo level set. Più nel dettaglio, consideriamo un problema di controllo ottimo in cui la dinamica è data dalla propagazione di un grafo monodimensionale controllato dalla velocità in direzione normale al fronte. Avendo fissato un target corrispondente ad una configurazione finale del fronte desiderata, l'obiettivo è quello di raggiungere tale target minimizzando un opportuno funzionale di costo. È noto che risolvere il problema di controllo ottimo attraverso l'approccio della Programmazione Dinamica soffre della così detta "curse of dimensionality", risultando pertanto impossibile applicare tale metodo alla versione semi-discreta del nostro sistema. Nonostante questa forte limitazione, siamo riusciti comunque ad applicare la programmazione dinamica grazie a una riduzione di ordine dell'equazione level-set basata sulla Proper Orthogonal Decomposition (POD). Questa tecnica permette di ottenere un nuovo sistema di dimensioni notevolmente ridotte che riesce ugualmente a descrivere la dinamica in

modo soddisfacente. Grazie alla soluzione dell'equazione di Hamilton-Jacobi Bellman con un'approssimazione POD, abbiamo potuto calcolare una legge feedback e la corrispondente traiettoria ottima per il problema non lineare che descrive la propagazione del fronte.
La seconda parte della tesi è dedicata all'applicazione dei metodi di controllo ottimo in campo biologico. Abbiamo proposto un modello che descrive l'evoluzione di una popolazione di cellule tumorali attraverso un'equazione alle derivate parziali. In tale modello è presente una funzione che modellizza il tasso di proliferazione delle cellule, una funzione che modellizza il tasso di morte dovuto alla competizione tra le cellule ed una funzione che modellizza il tasso di morte dovuto alla presenza del farmaco; infine la presenza di un coefficiente di diffusione ci permette di modellizzare il tasso di mutazione delle cellule. Abbiamo quindi messo in luce e analizzato le caratteristiche biologiche e matematiche del modello e formulato e risolto numericamente un problema di controllo ottimo: fissata una finestra temporale di 60 giorni, l'obiettivo è quello di ridurre la densità del tumore senza far aumentare troppo la resistenza. Il funzionale costo è costituito quindi da due termini moltiplicati da due coefficienti. Al variare di tali coefficienti, abbiamo analizzato e discusso i risultati delle simulazioni.

Résumé

Cette thèse se développe sur deux fronts : dans la première partie, nous nous concentrons sur les méthodes numériques des problèmes de contrôle optimal, en particulier sur le Principe de la Programmation Dynamique et sur le Model Predictive Control (MPC). Dans la deuxième partie, nous présentons des applications de techniques de controôle en biologie, en particulier pour les modèles d'évolution des populations de cellules tumorales.

Dans la première partie de la thèse, nous considérons l'approximation d'un problème de contrôle optimal avec horizon infini, qui combine une première étape, basée sur MPC permettant d'obtenir rapidement une bonne approximation de la trajectoire optimal, et une seconde étape, dans la quelle l'équation de Bellman est résolue dans un voisinage de la trajectoire de référence. Il est bien connu que l'approximation de la solution obtenue par l'équation de Bellman peut être assez coûteuse, parce que on doit résoudre le problème dans un domaine qui contient toutes les conditions initiales possibles de la dynamique. Nous devons aussi imposer (et sélectionner) des conditions aux bords appropriées pour résoudre cette équation. La caractéristique principale du MPC est de calculer un contrôle feedback approximatif pour la dynamique à partir d'une condition initiale en résolvant une séquence de problèmes de contrôle optimal à horizon fini. Il semble donc naturel de résoudre d'abord le problème pour une condition initiale obtenue avec MPC et calculer ensuite la fonction valeur dans un voisinage de cette trajectoire. De cette façon, on peux réduire une grande partie de la taille du domaine dans lequel on résout l'équation de Bellman et donc diminuer la complexité du calcul. La deuxième étape semble être nécessaire, si on veut obtenir une solution stable, puisque on peut utiliser toutes les informations voisines à la trajectoire de référence et non seulement les

informations sur la trajectoire.
Le deuxième sujet abordé dans cette thèse est le contrôle des méthodes Level Set. Plus en détail, on considère un problème de contrôle optimal, dans lequel la dynamique est donnée par la propagation d'un graphe à une dimension, contrôlé par la vitesse normale. Un état finale est fixé, correspondant à une configuration finale du front souhaité, l'objectif étant de le rejoindre en minimisant une fonction coût appropriée. Le but est de résoudre le problème de contrôle optimal avec la Programmation Dynamique, mais il est connu que cette méthode souffre de la soi-disant "curse of dimensionality". C'est donc impossible de l'appliquer à la version semi-discrète de notre système. Malgré cette importante limitation, on arrive à utiliser la programmation dynamique grâce à une réduction d'ordre de l'équation utilisant la Proper Orthogonal Decomposition (POD). Cette technique permet d'obtenir un nouvel système de dimension significativement réduite, qui décrit la dynamique de manière satisfaisante. Grâce à la solution de l'équation de Hamilton-Jacobi Bellman avec POD, nous pouvons calculer une loi feedback et la trajectoire optimale correspondante pour la résolution d'un problème non linéaire de propagation du front.
La deuxième partie de la thèse est dédiée à l'application des méthodes de contrôle en biologie. On présente un modèle décrit par une équation aux dérivées partielles qui modélise l'évolution d'une population de cellules tumorales. On analyse d'abord les caractéristiques biologiques et mathématiques du modèle. Par la suite, on formule et résout numériquement un problème de contrôle optimal concernant ce modèle, où le contrôle représente la quantité du médicament administrée. En fixant une fenêtre temporelle de 60 jours, l'objectif est de réduire la densité de la tumeur sans trop augmenter la résistance des cellules au médicament. La fonctionnelle coût est composée par deux termes pondérés par des coefficients, qu'on fait varier dans les simulations pour mieux comprendre leur rôle. Enfin, on présente et analyse les résultats obtenus.

Indice

1. Introduction

The theory of control analyzes the properties of controlled systems, *i.e.* dynamical systems on which we can act through a control. The aim is to bring the system from an initial state to a certain final state satisfying some criteria. There are many systems which can be considered: differential systems, discrete systems, systems with noise, etc. Their origins are very different: mechanics, electricity, electronics, biology, chemistry, economics, etc. The goal can be to stabilize the system so that it is insensitive to certain disturbances (stabilization), or to determine the optimal solutions for some optimization criteria (optimal control). From a mathematical point of view, a controlled system is a dynamical system depending on a term called *control*. Controls are functions or parameters usually subject to constraints. The theory of control is a continuation of the variational calculus and historically it is deeply related with the classical mechanics, in particular to the variational principles of mechanics (Fermat's principle, Huygens' principle, Euler-Lagrange equations...). In this thesis, we deal with the numerical solution of optimal control problems, which is a challenging problem for many industrial applications, *e.g.* robotics, aeronautics, electrical and aerospace engineering, but also in biology and the medical field. An interesting application concerns modeling evolutionary dynamics of tumor cells. In that case, the aim is to find an optimal dosing schedule for patients in order to eradicate the tumor or to limit its growth.
To summarize, the ultimate goal of an optimal control problem is to compute an optimal control and the corresponding optimal trajectory for the controlled system. A classical infinite horizon optimal control problem can be described as follows:

$$\begin{aligned} \inf_{u\in U} J_x(u(\cdot)) &:= \int_0^\infty L(y(s),u(s),s)e^{-\lambda s}ds \\ \text{subject to } \ \dot{y}(s) &= f(y(s),u(s),s),\ y(0)=x \end{aligned} \tag{1.1}$$

Here y is the state trajectory, x the initial condition, u denotes the control, U is the control space and $\lambda > 0$ is the discount factor. The solution for the problem (1.1) is a pair (y^*, u^*), where u^* minimizes the cost functional $J_x(u(\cdot))$ and y^* is the corresponding trajectory. One way to obtain the optimal pair is based on the Pontryagin's Maximum Principle (see [106]). It is worth to mention that the characterization via the Pontryagin principle gives only necessary conditions for the optimal trajectory and optimal open-loop control. Although from a numerical point of view the control system can be solved via shooting methods (see [85] for details) applied to the associated two point boundary value problem, in real applications a good initial guess for the adjoint equation is particularly difficult and often requires a long and tedious trial-and-error procedure to be found. Another way to solve optimal control problems and obtain open-loop controls is

using a *direct method*. It consists in discretizing directly the optimal control problem, leading to a nonlinear optimization problem, which can be solved by different algorithms (such as gradient methods, line search methods...) as shown in the book by Kelley [68] and by Nocedal and Wright [92]. An alternative way to solve optimal control problems was introduced by Bellman [16] which leads to deal with the value function $v(x)$ defined as follows:

$$v(x) = \inf_{u \in U} J_x(u(\cdot)).$$

It is well known that the Bellman's Dynamic Programming (DP) produces optimal controls in feedback form, which are more appealing in terms of robustness since they depend on the state variable. However, the synthesis of feedback controls requires the previous knowledge of the value function that is the major bottleneck for the application of DP. In fact, under suitable assumptions of regularity on the data, the value function is characterized as the unique viscosity solution of a nonlinear Hamilton-Jacobi-Bellman (HJB) equation [15]:

$$\lambda v(x) + \max_{u \in U} \{-f(x,u) \cdot Dv(x) - L(x,u)\} = 0, \qquad \text{for } x \in \mathbb{R}^d\,. \tag{1.2}$$

Due to the complexity to find an analitycal solution of the HJB equation, several approximation schemes have been proposed for this class of equations, based on finite difference [37], semi-Lagrangian [28, 43, 45] and finite volume methods [70]. These algorithms compute the solution iterating on the value space and looking for a fixed point of the equation. They converge to the value function, but the convergence is slow (see [44] for error estimates on Semi-Lagrangian schemes). A possible approach, which has a rather long history, is based on the iteration in the space of controls (or policies) for the solution of HJB equations. The Policy Iteration (PI) method, known as Howard's algorithm [65], has been investigated by Kalaba [67] and Pollatschek and Avi-Itzhak [105], who proved that it corresponds to the Newton method applied to the functional equation of dynamic programming. Later, Puterman and Brumelle [107] have given sufficient conditions for the rate of convergence to be either superlinear or quadratic. More recent contributions on the policy iteration method can be found in Santos and Rust [111] and Bokanowski *et al.* [18]. Results on its numerical implementation and diverse hybrid algorithm have been reported in Capuzzo-Dolcetta and Falcone [27], Gonzáles and Sagastizábal [59] and Grüne [56]. We mention also that an acceleration method based on the set of subsolutions has been studied in Falcone [43]. Finally Alla *et al.,* [5] have presented and accelerated algorithm for the solution of static Hamilton-Jacobi-Bellman equations related to optimal control problems. In particular, they use a classic policy iteration procedure giving a smart initial guess given by the solution of the value iteration scheme on a coarse mesh. More in general, dealing with domain decomposition methods for HJB equations, we should also mention approaches based on domain decomposition algorithms as in Falcone *et al.* [46] and more recently by Cacace *et al.* [23], on geometric considerations as in Botkin *et al.* [19].
This thesis deals also with front propagation problem described by the level set equation. The level set methods are widley used in applications such as image denoising, optimal

path planning, computing the shortest geodesic paths, optimal design. There are three main advantages of this approach: change of topology are naturally handled and surfaces automatically merge and separate; geometric quantities, like the surface normal and curvature, are easy to compute; the extension to three and even higher dimensions is conceptually straightforward.
It is well known that the level set method introduced by Osher and Sethian [94] for the study of a front evolution, produces a first order evolutive equation in the case of a normal velocity c, which only depends on space and time, *i.e.*

$$\Phi_t(x,t) + c(x,t)|\nabla\Phi(x,t)| = 0 \tag{1.3}$$

whereas it yelds a second order equation when the velocity also depends on the geometric properties of the front, typically its curvature (see the monograph [95, 115]). The front at time t is represented by the $0-$level set of the function $\Phi(x,t)$. The techniques used to approximate these problems are based on finite difference schemes, semi-Lagrangian schemes and, more recently, finite element schemes. It should also be mentioned that classical approximation methods require the computation of an approximate solution on every node of the grid at every iteration and are generally considered rather expansive. Starting with [114, 122], new methods have been proposed in order to reduce the computational effort and obtain the solution in a finite number of steps, such as Fast Marching methods [116]. This approach has shown to be very effective for level set equations related to front propagation problems, *i.e.* eikonal-type of equations. At every iteration, the scheme is applied only on a subset of nodes (localization), that are close to the front, the so-called *narrow band*. The remaining part of the grid is divided into two parts: the "accepted region", where the solution has been already computed, and the "far" region, where the solution will be computed in the following iterations. At every iteration, one node is accepted and moved from the narrow band to the accepted region; the narrow band is then updated adding the first neighbors of that node (which before were in the far region). For eikonal-type of equations, these methods converge in finite number of iterations to the correct viscosity solution and have a very low complexity (typically $\mathcal{O}(N\ln(N))$, where N is the cardinality of the grid). More recently, Cristiani *et al.* [38] introduce and analyze a fast version of the semi-lagrangian algorithm for front propagation. They use a local definition of the approximate solution typical of semi-Lagrangian schemes and redefine the set of "neighboring nodes" necessary for the Fast Marching schemes. They show that the new algorithm converges to the viscosity solution of the problem and that its complexity is $\mathcal{O}(N\ln N_{nb})$ (where N_{nb} is the number of nodes in the narrow band). In last years, several efforts have been made to extend these methods to more complex problems where the front propagation is anisotropic [117] and/or to more general HJB equations as in [10]. However, their implementation is rather delicate and their convergence to the correct viscosity solution for general HJB equations is still an open problem; we refer to [24] for an extensive discussion and several examples of these limitations. Most of the methods applied for solving the HJB equation suffer from the so called *curse of dimensionality*. This is due to the fact that the dimension of the partial differential equation characterizing the value function increases as the dimension

of the space state does. This is a major computational challenge which limits the practical implementation of numerical algorithms for optimal control design based on viscosity solutions of HJB equations.
In recent years, new tools have been developed to deal with optimal control problems for partial differential equations; the origin dates back to the monograph by J.L. Lions [80] and several books on infinite dimensional optimal control problems have appeared since then (see *e.g.* [63, 76, 77, 121]). In particular, new techniques emerged to reduce the number of dimensions in the description of dynamical systems or, more in general, of the solution of the problem to optimize. These methods are called *reduced-order methods* and include for example the Proper Orthogonal Decomposition method (POD, see [64, 118, 123]), the reduced basis approximation (see [99]) and Balance Truncation method [12]. The general idea behind these methods is that, when the solutions are sufficiently regular, one can represent them via Galerkin expansion so that the number of variables involved in this discretization will be strongly reduced. In some cases, as for the heat equation, even 1 basis function will suffice to have a rather accurate POD representation of the solution (see [72]). Following these considerations it is reasonable to follow a different approach based on DP and HJB equations. In this approach we will first develop a basis functions representation of the solution along a reference trajectory and then use this basis to set-up a control problem in the new space of coordinates. The corresponding HJB equation will just need (hopefully) $3-5$ variables to represent the state of the system. This approach has been introduced and studied starting from the seminal papers [73, 74] and has shown to be rather effective for the optimal control of parabolic and advection-diffusion equations [2]. In the above cases the solution of the dynamics is typically regular and the asymptotic behavior is easy to predict. More recently, a technique based on spectral elements has been applied to optimal control problems for the wave equation (see [71]).
As said, in many control problems it is desired to design a stabilizing feedback control, but finding analytically the closed loop solution is often unfeasible, even for the unconstrained case, since it involves the solution of the corresponding HJB equations. An alternative way to find control in feedback form are the methods known as Model Predictive Control (MPC), Moving Horizon Control or Receding Horizon Control (see the books [58, 110]). They are based on the following idea: the repeated solution of an open-loop optimal control problem for a given state. The first part of the resulting open-loop input signal is implemented and the whole process is repeated. In general, one distinguish between linear and Nonlinear Model Predictive Control (NMPC). Linear MPC refers to a family of MPC schemes in which linear models are used to predict the system dynamics and considers linear constraints on the states and inputs. Note that even if the system is linear, the closed loop dynamics are nonlinear due to the presence of constraints. NMPC refers to MPC schemes that are based on nonlinear models and/or consider a non quadratic cost-functional and general nonlinear constraints. Although linear MPC has become a technique widley used in industry, in many applications linear model are not sufficient to describe the process dynamics in a satisfactory way and nonlinear models must be applied (see [9, 48] for an introduction to NMPC). In Model Predictive Control, a crucial role is played by the prediction horizon, for instance the Quasi Infinite hori-

zon NMPC allows an efficient formulation of NMPC while guaranteeing stability and the performances of the closed-loop as shown in [8, 49] under appropriate assumptions. Since the computational complexity of MPC schemes grows rapidly with the length of the optimization horizon, estimates for minimal stabilizing horizons are crucial to ensure stability. Stability and suboptimality analysis for NMPC schemes without stabilizing constraints is presented in Chapter 6 of the book by Grüne and Panneck [58], where they prove conditions to get asymptotic stability with minimal horizon. Note that the stabilization of the problem and the computation of the minimal horizon involve the Relaxed Dynamic Programming Principle (see [57, 98]). This approach allows estimates of the horizon based on controllability properties of the system.

This thesis deals also with applications in the biological field, in particular in cancer treatment. In general mathematical modelling approaches have become rather popular in cancer research. The complexity of cancer is well suited to quantitative approaches as it provides challenges and opportunities for new developments. In turn, mathematical modelling contributes to cancer research by helping to elucidate mechanisms and by providing quantitative predictions that can be validated. The recent expansion of quantitative models addresses many questions regarding tumour initiation, progression and metastases as well as intra-tumour heterogeneity, treatment responses and resistance. Mathematical models can complement experimental and clinical studies, but also challenge current paradigms, redefine our understanding of mechanisms driving tumorigenesis and shape future research in cancer biology. In fact, mathematical models have proved useful for deriving a detailed understanding of mechanisms and processes in cancer ([11, 17]) and have been used to propose new experiments, suggest different treatment modalities and alter risk prognosis. The power of mathematical modelling lies in its ability to reveal previously unknown or counterintuitive physical principles that might have been overlooked or missed by a qualitative approach to biology. As such, mathematical modelling can test theories on quantitative grounds. At its best, modelling provides indispensable contributions to cancer research, making investigations quantitative and predictive, and hypotheses falsifiable. Furthermore, it is also interesting try to control the evolution of the tumor. The literature deals not only with cancer modeling, but it also focuses on the question of cancer treatment protocols and how to optimize them. We adress the interested reader to the book [52], Part III for an overview on cancer modeling and Part IV on cancer treatment. The aim of this kind of research is not necessarily to eradicate cancer, but to circumvent it, since it is more realistic try to contain the cancer within admissible limits for long-term survival of patients with a good quality of life. An important issue is the following: it has been observed that emergence of resistance to cytotoxic drugs in cancer cell populations is common in most cancers [112] and is one of the major pitfalls ecountered in oncology as it induces tumor recurrence in spite of therapy and limits life expectancy. In fact, although technological progress in molecular cell biology has resulted in large amounts of data documenting cancer progression, our understanding of the principles that underpin the development of resistance to anti-cancer agents and the emergence of phenotypic heterogeneity in neoplastic cell populations is filled with gaps and unresolved questions. For this reason, mathematical modelling can help to address some of these gaps in our knowledge by capturing, in abstract terms, the

crucial assumptions that underlie given hypotheses, and by offering alternative means of understanding experimental results that are currently available. In this perspective, in [75] Lorenzi *et al.* try to contribute to a systematic identification of the way in which the phenotypic distribution, the level of intrapopulation heterogeneity and the size of cancer cell populations depend on the rate of random epimutations, the strength of natural selection, the intensity of the competition for resources, and the stress exerted by cytotoxic agents. In [32] the interested reader can find a complete review on that topic. Moreover Chisolm *et al.*, focusing on intra-tumor heterogeneity, present mathematical models used to predict drug resistance in cancer and optimal control methods that can circumvent it in combined therapeutic strategies.

1.1. Contributions of this thesis

Chapter 3 is based on the idea that it can be interesting to obtain a local version of the DP method around a reference trajectory to improve a sub-optimal strategy. The reference trajectory can be obtained via the Pontryagin principle (with open-loop controls), via a Model Predictive Control approach (using feedback sub-optimal controls) or simply via the already known engineering experience. The application of DP in an appropriate neighborhood of the reference trajectory will not guarantee the global optimality of the new feedback control, but could improve the result within the given constraints. In this chapter, we focus our attention on the coupling between the MPC approach and the DP method. Although this coupling can be applied to rather general nonlinear control problems governed by ordinary differential equations, we present the main ideas of this approach using the *infinite horizon optimal control*, which is associated to the Hamilton-Jacobi-Bellman equation (1.2). For numerical purposes, the equation is solved in a bounded domain $\Omega \subset \mathbb{R}^d$, so that also boundary conditions on $\partial\Omega$ are needed. A rather standard choice when one does not have additional information on the solution is to impose state constraints boundary conditions. It is clear that the domain Ω should be large enough in order to contain as much information as possible. In general it is computed without any information about the optimal trajectory. Here we construct the domain Ω around a reference trajectory obtained by a fast solution obtained via MPC. In Chapter 4 we study an optimal control problem dealing with the dynamics given by the level set equation for front propagation problems, which have many applications in combustion, gas dynamics, fluid dynamics and image processing. The front propagation problem has solutions that are just Lipschitz continuous since singularities and topology changes in the front can appear during the evolution. Its solution must be understood in the viscosity sense. This clearly introduces some technical difficulties and makes it more complicated to construct the model reduction approximation based on the snapshots. We will use a model reduction based on POD to obtain a rather accurate approximation for the level-set dynamics in one dimension. To set the chapter into perspective, we want to mention that the problem of solving the controlled level-set equation in dimension one has been studied in [39], where the authors apply iterative descent methods for the optimization. Starting from the results obtained in [40] for the uncontrolled dynamics,

they prove the existence of optimal controls under different assumptions on the speed function (which in their case is a function of space). Concerning the solution of the control problem, they give a proof in a specific setting (see [39] for all the details). The difference here is that the control is a general function of space and time and not necessarily piecewise constant (as in [39]). Moreover in this chapter we apply the DP approach in order to obtain an approximate feedback control. The drawback is that since we are in a general setting both for the control and the profile we want to reach, there is not a theoretical result ensuring that the controllability problem has a solution. Moreover, we mention that in paper [55] the level set method is coupled to a Reduced Basis model in order to derive a rigorous approximation of the admissible region for a system characterized by several parameters.
In Chapter 6, we describe the evolution of cancer cells population through a phenotype-structured PDE. We present the main features of the model and perform an analysis under different assumptions on the cytotoxic drugs. Finallym, we formulate an optimal control problem associated with the PDE. With the aim of reducing the density of the tumor without increasing the resistance too much, we introduce an appropriate cost functional. Simulation results show the effectiveness of the proposed approach.

1.2. Organization

Tha Manuscript is divided in two parts:

Part I is more theoretical and is devoted to the numerical approximation of optimal control problem via HJB and MPC.

Chapter 2 contains some well known results on the theory of viscosity solutions and the optimal control problem. In Section 2.1 the general theory and the main results on the viscosity solution are presented. In Section 2.2 we introduce the optimal control problem, the dynamic programming principle, the algorithm for approximating the value function and an accelerated technique to speed up the convergence. Finally in section 2.3 we explain the MPC algorithm and the main results on the stability, in particular how to compute the prediction horizon which ensures the stability of the method.

Chapter 3 is organized as follows: in Section 3.1 we present the main features of the new algorithm in which we couple the MPC algorithm with the approximation of the value function via the solution of the Bellman equation. In Section 3.2 we present some numerical tests to show the efficency of the proposed algorithm.

Chapter 4 is organized as follows: in Section 4.1 we present the front propagation problem with the associated optimal control problem, in Section 4.2 we give the main features of the DP approach and we explain how to deal with the model order reduction of the level set equation. Finally, in Section 4.3 we present some numerical tests which show the efficiency of the proposed method.

Part II is more applied and related to the development of optimal control strategy to a specific biological model.

Chapter 5 is a general overview on the tumor models studied in recent years. In Section 5.1 we present some ODE model describing the evolution of the tumor growth and we give some properties and general results. Then, we introduce the therapy and its effect in the models. Starting from a general therapy, we switch to the models where the therapy is a control variable. We explain how the modelization of the tumor growth can become an optimal control problem. We introduce the target and the cost functional and finally we present some models. Section 5.2 is devoted to the presentation of PDE models. After a general introduction, we present models with natural selection, with natural selection and phenotypic variations and with natural selection, phenotypic variations and random epimutations. Finally we will explain why dealing with optimal control problem of PDE is such a challenging problem.

Chapter 6 is organized as follows: in Section 6.1 we present the model with the parameters and we give some biological motivations behind this study. In Section 6.2 we perform an analysis of the model in the absence of drugs and under the action of a constant cytotoxic drug. Then, we generalize the results presented in [75] in the case where the cytotoxic drug is a generic function of time. Finally, in Section 6.3 we present an optimal control problem and we show the results obtained with the numerical simulations.

1.2.1. Original material for this thesis

Let us briefly mention the original contributions contained in this thesis.
Chapter 3 is based on [3], to appear in Conference Proceedings of IFIP 2015.
Chapter 4 is based on the proceeding [4] submitted to Conference Proceedings of Model Reduction of Parametrized Systems III (MoRePas III).
Chapter 6 is based on the paper [42], in preparation.

Parte I.

Numerical Methods for Optimal Control Problems

2. Overview on numerical methods for optimal control problems

The aim of this chapter is to present two standard techniques, Dynamic Programming approach and Model Predictive Control, used to obtain control in feedback form as they constitute the building blocks for our new algorithm proposed in Chapter 3. Moreover, the first method together with an accelerated technique which speed up the convergence of the algorithm is applied in the simulation of Chapter 4.

2.1. Viscosity solutions

Before introducing the optimal control problem, we introduce the notion of *viscosity solution* of the Hamilton-Jacobi equation. Let us consider the equation

$$H(x, w(x), Dw(x)) = 0, \qquad x \in \Omega \tag{2.1}$$

where $\Omega \subset \mathbb{R}^n$ is an open domain and the Hamiltonian $H : \mathbb{R}^n \times \mathbb{R} \times \mathbb{R}^n \to \mathbb{R}$ is a continuous real valued function defined on $\Omega \times \mathbb{R} \times \mathbb{R}^n$. The concept of viscosity solution allows to obtain important existence and uniqueness results for some equations of the form (2.1). It is well known that this equation is in general not well-posed. It is possible to show several examples in which no classical, *e.g.* $C^1(\Omega)$, solution exists, but infinite weak solutions exists. The simplest example is the following 1-dimensional eikonal equation with a Dirichlet boundary condition

$$\begin{cases} |Dw(x)| = 1, & x \in (-1, 1) \\ w(x) = 0, & x = \pm 1 \end{cases} \tag{2.2}$$

We can find infinite multiple solution (see Figure (2.1)).

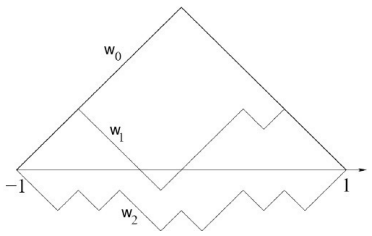

Figura 2.1.: Some solutions satisfying the equation (2.1)

From the necessity to choose an unique solution among all the possibles, the theory of

viscosity solutions was developed. In fact, it gives a criteria to select the correct physical solution. Let us recall the two definitions of viscosity solution:

Definition 2.1 *A continuous function w is a viscosity solution of the (HJ) equation if the follwing conditions are satisfied:*

i) $H(x, w(x), p) \leq 0$ *for all* $x \in \mathbb{R}^n$*, for all* $p \in D^+w(x)$ *(viscosity subsolution)*

ii) $H(x, w(x), q) \geq 0$ *for all* $x \in \mathbb{R}^n$*, for all* $q \in D^-w(x)$ *(viscosity supersolution) where* D^-, D^+ *are super and sub-differential, i.e.*

$$D^+u(x) = \left\{ p \in \mathbb{R}^n : \limsup_{y \to x} \frac{w(y) - w(x) - p \cdot (y - x)}{|y - x|} \leq 0 \right\}$$

$$D^-u(x) = \left\{ q \in \mathbb{R}^n : \liminf_{y \to x} \frac{w(y) - w(x) - p \cdot (y - x)}{|y - x|} \geq 0 \right\}.$$

Definition 2.2 *A continuous function w is a viscosity solution of the equation (2.1) if the following conditions are satisfied:*

i) for any test function $\varphi \in C^1(\Omega)$*, if* $x_0 \in \Omega$ *is a local maximum point for* $w - \varphi$*, then*

$$H(x_0, w(x_0), D\varphi(x_0)) \leq 0 \qquad \textit{(viscosity subsolution)}$$

ii) for any test function $\varphi \in C^1(\Omega)$*, if* $x_0 \in \Omega$ *is a local minimum point for* $w - \varphi$*, then*

$$H(x_0, w(x_0), D\varphi(x_0)) \geq 0 \qquad \textit{(viscosity supersolution)}$$

In addition, the viscosity solution w may be characterized as the uniform limit for $\varepsilon \to 0$ (that is $\lim_{\varepsilon \to 0^+} w^\varepsilon = w$) of the classical solution w^ε of the regularized problem

$$-\varepsilon \Delta w^\varepsilon + H(x, w^\varepsilon, Dw^\varepsilon) = 0, \qquad x \in \Omega.$$

The terminology "viscosity" solutions comes from the term $-\varepsilon \Delta w$ that corresponds to the viscosity term in fluid dynamics. This method of *vanishing viscosity* was presented in [36] by Crandall and Lions. The main issue is to prove the uniqueness of the viscosity solution, this is done via a *comparison principle*.

Theorem 2.1 *Let Ω be a bounded open subset of $\mathbb{R}^n$. Assume that $w_1, w_2 \in C(\overline{\Omega})$ are respectively a viscosity sub- and a supersolution for*

$$w(x) + H(x, Dw(x)) = 0, \qquad x \in \Omega \tag{2.3}$$

and

$$w_1 \leq w_2 \qquad \textit{on } \partial\Omega \tag{2.4}$$

Assume also that H satisfies

$$|H(x, p) - H(y, p)| \leq \omega_1(|x - y|(1 + |p|)), \tag{2.5}$$

for $x, y \in \Omega$, $p \in \mathbb{R}^n$, where $\omega_1(\cdot)$ is a modulus of continuity (i.e. $\omega : [0, +\infty) \to [0, +\infty)$ is continuous non decreasing with $\omega(0)=0$). Then, $w_1 \leq w_2$ in $\overline{\Omega}$.

Theorem 2.2 *Assume that $w_1, w_2 \in C(\mathbb{R}^n) \cap L^\infty(\mathbb{R}^n)$ are, respectively, viscosity sub and supersolution of*

$$w(x) + H(x, Dw(x)) = 0, \qquad x \in \mathbb{R}^n \tag{2.6}$$

Assume also that H satisfies (2.5) and

$$|H(x,p) - H(y,q)| \leq \omega_2(|p-q|), \qquad \text{for all } x, p, q \in \mathbb{R}^n, \tag{2.7}$$

where ω_2 is a modulus. Then $w_1 \leq w_2$ in $\mathbb{R}^n$.

Remark 2.1 *Theorem 2.2 can be generalized to cover the case of a general unbounded open set $\Omega \subset \mathbb{R}^n$. Moreover, the assumption $w_1, w_2 \in C(\mathbb{R}^n) \cap L^\infty(\mathbb{R}^n)$ can be replaced by $w_1, w_2 \in UC(\mathbb{R}^n)$.*

A comparison result can be formulated for the more general case

$$H(x, Dw(x)) = 0, \qquad x \in \Omega \tag{2.8}$$

only if we assume the convexity of H with respect to the p variable. This assumption is crucial in many theoretical results.

Theorem 2.3 *Let Ω be a bounded open subset of $\mathbb{R}^n$. Assume that $w_1, w_2 \in C(\overline{\Omega})$ are, respectively, viscosity sub- and supersolution of (2.8) with $w_1 \leq w_2$ on $\partial\Omega$. Assume also that H satisfies (2.5) and the two following conditions:*

1. *$p \to H(x,p)$ is convex on $\mathbb{R}^n$ for each $x \in \Omega$;*
2. *there exists $\varphi \in C(\overline{\Omega}) \cap C^1(\Omega)$ such that $\varphi \leq w_1$ in $\overline{\Omega}$ and $\sup_{x \in \Omega'} H(x, \nabla\varphi(x)) < 0$, for all $\Omega' \subset\subset \Omega$.*

Then $w_1 \leq w_2$ in Ω.

2.1.1. The eikonal equation

The classical model problem for (2.8) is the eikonal equation of geometric optics

$$c(x)|DT(x)| = 1, \qquad x \in \Omega \tag{2.9}$$

Theorem 2.3 applies to the eikonal equation (2.9) whenever $c(x) \in Lip(\Omega)$ and it is strictly positive. In fact, the second condition of theorem (2.3) is satisfied by taking $\varphi(x) \equiv \min_{\overline{\Omega}} w_1$. It is easy to prove that the distance function from an arbitrary set $S \subseteq \mathbb{R}^n$, $S \neq \emptyset$ defined by

$$d_S(x) = d(x, S) := \inf_{z \in S} |x - z| = \min_{z \in \overline{S}} |x - z| \tag{2.10}$$

is continuous in $\mathbb{R}^n$. Moreover, for smooth ∂S, it is smooth near ∂S and satisfies in the classical sense the equation (2.9) in $\mathbb{R}^n \setminus \overline{S}$ for $c(x) = 1$.
For a general set S, it can be shown that the function d_S is the unique *viscosity solution* of

$$|Dw(x)| = 1, \qquad x \in \mathbb{R}^n \setminus \overline{S} \tag{2.11}$$

Remark 2.2 *If we consider the eikonal equation in the form $|Dw(x)| = f(x)$, where f is a function vanishing at last in a single point in Ω, then the uniqueness result does not hold. This situation is referred to as degenerate eikonal equation. It can be proved that in this case many viscosity or even classical solution may appear. Consider for example the equation $|w'| = 2|x|$ for $x \in (-1, 1)$ complemented by Dirichlet boundary condition $w = 0$ at $x = \pm 1$. It is easy to see that $w_1(x) = x^2 - 1$ and $w_2(x) = 1 - x^2$ are both classical solutions. The case of degenerate eikonal equations was been archieved by Camilli and Siconolfi [26] and numerically by Camilli and Grüne in [25]*

2.2. Optimal control problem and Dynamic Programming Approach

We will present the main features and results, more details can be found in the original papers and in some monographs, *e.g.* in the classical books by Bellman [16], Howard [65] and for a more recent setting in framework of viscosity solutions in [27], [14] and [44].

Let the dynamics be given by

$$\begin{cases} \dot{y}(t) = f(y(t), u(t)) \\ y(0) = x \end{cases} \tag{2.12}$$

where $y \in \mathbb{R}^n$ is the state variable, $u(t)$ is the control signal, $u \in \mathcal{U} \equiv \{u : \mathbb{R}_+ \to U$, measurable$\}$ and U is a compact subset of $\mathbb{R}^m$. If $f : \mathbb{R}^n \times U \to \mathbb{R}^n$ is continuous with respect to (x, u) and Lipschitz continuous with respect to the state variable, *i.e.* there exists a constant $C_f > 0$ such that

$$|f(y_1, u) - f(y_2, u)| \leq C_f |y_1 - y_2| \qquad \text{for all } y_1, y_2 \in \mathbb{R}^n, u \in U$$

the classical assumptions for the existence and uniqueness result for the Cauchy problem (2.12) are satisfied. To be more precise, the Carathéodory theorem (see [14] or [51]) implies that for any given control $u(\cdot) \in \mathcal{U}$, there exists a unique trajectory denotated by $y_x(t; u(\cdot))$ satisfying (2.12) almost everywhere. Changing the control policy, the trajectory will change and we will have a family of infinitely many solutions of the controlled system (2.12) parametrized with respect to u.

2.2.1. Infinite horizon problem

Let us first present the method for the classical *infinite horizon problem*. Let us introduce the *cost functional* $J : \mathcal{U} \to \mathbb{R}$ which will be used to select the 'optimal trajectory'. For infinite horizon problem the functional is

$$J_x(u(\cdot)) = \int_0^\infty L(y_x(s), u(s))e^{-\lambda s}ds\,, \tag{2.13}$$

where L is Lipschitz continuous in both arguments and $\lambda > 0$ is a given parameter. The function L represents the running cost and $\lambda \in \mathbb{R}_+$ is the discount factor allowing to compare the costs at different times rescaling with the costs at time 0. From the technical point of view, the presence of the discount factor guarantees that the integral is finite whenever L is bounded, *i.e.* $||L||_\infty \leq M_L$. The goal of optimal control theory is to find an optimal pair (y^*, u^*) which minimizes the cost functional. The starting point of the Dynamic Programming is to introduce an auxiliary function, the *value function* which, in the case of infinite horizon problem, is defined as

$$v(x) = \inf_{u(\cdot)\in\mathcal{U}} J_x(u(\cdot))\,. \tag{2.14}$$

Once we compute the value function, the optimal control is defined as

$$u^*(\cdot) = arg \min_{u(\cdot)\in\mathcal{U}} J_x(u(\cdot))$$

Proposition 2.1 (Dynamic programming principle) *Under the assumption of Caratheodory theorem for all $x \in \mathbb{R}$ and $\tau > 0$ the value function satisfies:*

$$v(x) = \inf_{u\in\mathcal{U}} \int_0^\tau \left\{L(y_x(s;u), u(s))e^{-\lambda s}ds + e^{-\lambda\tau}v(y_x(\tau;u))\right\}$$

It is well known that passing to the limit in the Dynamic Programming Principle (DPP), one can obtain a characterization of the value function in terms of the following first order non linear Bellman equation

$$\lambda v(x) + \max_{u\in U}\{-f(x,u)\cdot Dv(x) - L(x,u)\} = 0, \quad \text{for } x \in \mathbb{R}^n\,. \tag{2.15}$$

Several approximation schemes on a fixed grid G have been proposed for (2.15). Here, we will use a semi-Lagrangian approximation based on a Discrete Time Dynamic Programming Principle. This leads to

$$v_{\Delta t}(x) = \min_{u\in U}\{e^{-\lambda\Delta t}v_{\Delta t}\left(x + \Delta t f\left(x,u\right)\right) + \Delta t L\left(x,u\right)\}\,, \tag{2.16}$$

where $v_{\Delta t}(x)$ converges to $v(x)$ when $\Delta t \to 0$. A natural way to solve (2.16) is to write it in fixed point form (see [44] for more details) as in the following algorithm:

Algorithm 1: Value Iteration for infinite horizon optimal control **(VI)**

Data: Mesh G, Δt, initial guess V^0, tolerance ϵ.
while $||V^{k+1} - V^k|| \geq \epsilon$ **do**
  forall the $x_i \in G$ **do**
    $$V_i^{k+1} = \min_{u \in U} \{ e^{-\lambda \Delta t} I \left[V^k \right] (x_i + \Delta t f(x_i, u)) + \Delta t L(x_i, u) \} \tag{2.17}$$
  end
  $k = k + 1$
end

Here V_i^k represents the values at a node x_i of the grid at the k-th iteration and I is an interpolation operator acting on the values of the grid; without loss of generality, we will assume that the numerical grid G is a regular equidistant array of points with mesh spacing denoted by Δx, and we consider a multilinear interpolation operator. Extensions to nonuniform grids and high-order interpolants can be performed in a straightforward manner.
Algorithm 1 is referred in the literature as the *value iteration method* because, starting from an initial guess V^0, it modifies the values on the grid according to the nonlinear rule (2.17). It is well-known that the convergence of the value iteration can be very slow, since the contraction constant $e^{-\lambda \Delta t}$ is close to 1 when Δt is close to 0. This means that a higher accuracy will also require more iterations. For this reason, there is a need for an acceleration technique in order to cut the link between accuracy and complexity of the value iteration.

2.2.2. Minimum time problem

For sake of clarity, the above framework has been presented for the infinite horizon optimal control problem. However, similar ideas can be extended to other classical control problems with small changes. Let us present how to deal with the minimum time problem. In the minimum time problem one has to drive the controlled dynamical system (2.12) from its initial state to a given target $\mathcal{T}$. Let us assume that the target is a compact subset of $\mathbb{R}^n$ with non empty interior and piecewise smooth boundary. The major difficulty dealing with this problem is that the time of arrival to the target starting from the point x

$$t_x(u(\cdot)) := \begin{cases} \inf\limits_{u \in \mathcal{U}} \{ t \in \mathbb{R}_+ : y(t, u(\cdot)) \in \mathcal{T} \} & \text{if } y(t, u(t)) \in \mathcal{T} \text{ for some } t, \\ +\infty & \text{otherwise,} \end{cases} \tag{2.18}$$

can be infinite at some points. As a consequence, the minimum time function defined as

$$T(x) = \inf_{u \in \mathcal{U}} t_x(u(\cdot)) \tag{2.19}$$

is not defined everywhere if some controllability assumptions are not introduced. In general, this is a free boundary problem where one has to determine at the same time,

the couple (T, Ω), *i.e.* the minimum time function and its domain.

Definition 2.3 *The reachable set is* $\mathcal{R} := \{x \in \mathbb{R}^n : T(x) < +\infty\}$ *i.e., it is the set of starting points from which it is possible to reach the target.*

We remark that the reachable set depends on the target, the dynamics and on the set of admissible controls and it is not a datum in our problem.

Proposition 2.2 *For all* $x \in \mathcal{R}$, $0 \leq t < T(x)$, *so that* $x \notin \mathcal{T}$, *the value function satisfies*

$$T(x) = \inf_{u(\cdot)\in\mathcal{U}} \{t + T(y(t; u(\cdot)))\}. \tag{2.20}$$

Let us derive formally the Hamilton-Jacobi-Bellman equation associated to the minimum time problem from the DPP. We rewrite the equation (2.20)

$$T(x) - \inf_{u(\cdot)\in\mathcal{U}} T(y(t; u(\cdot))) = t$$

and divide by $t > 0$

$$\sup_{u(\cdot)\in\mathcal{U}} \left\{ \frac{T(x) - T(y(t; u(\cdot)))}{t} \right\} = 1 \qquad \text{for all } t < T(x).$$

We want to pass the limit as $t \to 0^+$. Assume that T is differentiable at x and $\lim_{t\to 0^+}$ commutes with $\sup_{u(\cdot)}$. Then, if $\dot{y}(0; u(\cdot))$ exists,

$$\sup_{u(\cdot)\in\mathcal{U}} \{-Dt(x) \cdot \dot{y}(0; u(\cdot))\} = 1$$

so that, if $u(0) = u_0$, we get

$$\max_{u_0\in U} \{-DT(x) \cdot f(x, u_0)\} = 1. \tag{2.21}$$

We remark that in the equation (2.21) the maximum is taken over U and not on the set of measurable controls $\mathcal{U}$.

Proposition 2.3 *If* $\mathcal{R} \setminus \mathcal{T}$ *is open and* $T \in C(\mathcal{R} \setminus \mathcal{T})$, *then* T *is a viscosity solution of*

$$\max_{u\in U} \{-f(x, u) \cdot \nabla T(x)\} - 1 = 0 \qquad x \in \mathcal{R} \setminus \mathcal{T}. \tag{2.22}$$

Natural boundary conditions associated to the equation (2.21) are

$$\begin{cases} T(x) = 0 & x \in \partial\mathcal{T} \\ \lim_{x\to\partial\mathcal{R}} T(x) = +\infty \end{cases} \tag{2.23}$$

In order to achieve uniqueness of the viscosity solution of equation (2.22) is useful an exponential transformation named *Kruzkhov transform*

$$v(x) \equiv \begin{cases} 1 - \exp(-T(x)) & \text{for } T(x) < +\infty \\ 1 & \text{for } T(x) = +\infty \end{cases} \tag{2.24}$$

Formally it easy to check that if T is a solution of (2.22) then v is a solution of

$$v(x) + \max_{u \in U}\{-f(x,u) \cdot Dv(x)\} = 1 \tag{2.25}$$

The transformation has many advantages:

1. The equation for v has the form (2.3), so that we can apply the uniqueness result already developed in this chapter.
2. v takes value in $[0,1]$ whereas T is generally unbounded (for example if f vanishes in some points) and this helps in the numerical approximation.
3. The domain in which the equation has to be solved is no more unknown.
4. It is always possible to reconstruct T and $\mathcal{R}$ from v by relations

$$T(x) = -\ln(1 - v(x)), \qquad \mathcal{R} = x : v(x) < 1.$$

Proposition 2.4 *v is the unique viscosity solution of*

$$\begin{cases} v(x) + \sup_{u \in U}\{-f(x,u) \cdot Dv(x)\} = 1 & \text{in } \mathcal{R} \backslash \mathcal{T} \\ v(x) = 0 & \text{on } \partial\mathcal{T}\,. \end{cases} \tag{2.26}$$

Then, the application of the semi-Lagrangian method presented for the infinite horizon optimal control problem together with a value iteration procedure, leads to following iterative scheme:

Algorithm 2: Value Iteration for minimum time optimal control **(VI)**

Data: Mesh G, Δt, initial guess V^0, tolerance ϵ.
while $||V^{k+1} - V^k|| \geq \epsilon$ **do**
  forall the $x_i \in G$ **do**

$$V_i^{k+1} = \min_{u \in U}\{e^{-\Delta t} I\left[V^k\right](x_i + \Delta t f(x_i, u)) + 1 - e^{-\Delta t}\} \tag{2.27}$$

  end
  $k = k + 1$
end

The numerical implementation is closed with the boundary conditions $v(x) = 0$ at $\partial\mathcal{T}$ (and inside the target as well), and with $v(x) = 1$ at other points outside the computational domain (we refer the reader to [13] for more details on the approximation of minimum time problems).

2.2.3. Accelerated policy iteration algorithm

As we mentioned, there are some techniques for speed-up the convergence of the algorithms presented above. A more efficient formulation of the (VI) algorithm is the so-called *policy iteration algorithm* (PI), which starting from an initial guess u_i^0 of the control at every node, performs the following iterative procedure:

$$[V^k]_i = e^{-\lambda \Delta t} I_1[V^k](x_i + \Delta t f(x_i, u_i^k)) + hL(x_i, u_i^k)$$
$$[u^{k+1}]_i = \underset{u \in \mathcal{U}}{\operatorname{argmin}} \{e^{-\lambda \Delta t} I_1[V^k](x_i + \Delta t f(x_i, u)) + \Delta t L(x_i, u)\},$$

where we first have to solve a linear system, since we freeze the control, in order to find the value function corresponding to the given control and then update the control. We iterate until convergence to the value function. The PI algorithm has a quadratic convergence provided a good initial guess is given and its convergence is only local (as for the Newton method), so there is a need for good initialization. In order to provide a smart initial guess for the algorithm, it was proposed in [5] an acceleration mechanism based on a (VI) solution on a coarse grid, which is used to generate an initial guess for (PI) on the fine grid (see Algorithm 3). The proposed coupling aims at efficiency and robustness. We remark that in Chapter 4 we adopt the Accelerated Policy Iteration method (shortly API) for the approximation of the HJB equation.

Algorithm 3: Accelerated Policy Iteration **(API)**

Data: Coarse mesh G_c, Δt_c, fine mesh G_f and Δt_f, initial coarse guess V_c^0, coarse-mesh tolerance ε_c, fine-mesh tolerance ε_f.

begin
- Coarse-mesh value iteration step: perform Algorithm 1
- **Input**: $G_c, \Delta t_c, V_c^0, \varepsilon_c$
- **Output**: V_c^*
- **begin**
  - **forall the** $x_i \in G_f$ **do**
  - $V_f^0(x_i) = I_1[V_c^*](x_i)$
  - $U_f^0(x_i) = arg\min_{u \in U}\{e^{-\lambda \Delta t} I_1[V_f^0](x_i + f(x_i, u)) + \Delta t L(x, u)\}$
- **end**
- Fine-mesh policy iteration step: perform Algorithm 3
- **Input:** $G_f, \Delta t_f, V_f^0, U_f^0, \varepsilon_f$
- **Output:** V_f^*

end

2.3. The NMPC approximation

Nonlinear model predictive control (NMPC) is an optimization based method for the feedback control of nonlinear systems. It consists in solving iteratively a finite horizon open loop optimal control problem subject to system dynamics and constraints involving

states and controls.
Let us consider the controlled system:

$$\begin{cases} \dot{y}(t) = f(y(t), u(t)) \\ y(0) = y_0 \end{cases} \tag{2.28}$$

where $y \in Y \subseteq \mathbb{R}^n$ and $u \in \mathcal{U}$ are the set of admissible control already defined in the previous section. We want to select a control $u \in \mathcal{U}$ such that the associated trajectory defined as $y_{[u,t_0,y_0]}$ follows a given desired state $\overline{y}$ as good as possible. This problem is known as *tracking problem* and if $\overline{y} = 0$ holds, a *stabilization problem.* The aim is to find control in feedback form, *i.e.* we want to determine a mapping $\mu : Y \to U$ with $u(t) = \mu(y(t_n))$ for $t \in [t_n, t_n + 1]$. We want to solve the following infinite horizon problem:

$$\min_{u \in \mathcal{U}} = \int_{t_0}^{\infty} L(y_{[u,t_0,y_0]}, u(t))dt$$

with a quadratic running cost:

$$L(y, u) = (\|y - \overline{y}\|^2 + \gamma \|u\|^2)$$

Note that, here, we are not dealing with a discount factor. The standard MPC is often presented in without it. Let us denote $\mu : Y \to U$ the feedback law we want to find, if we insert μ in (2.28), we obtain the closed loop system:

$$\begin{cases} \dot{y}(t) = f(y(t), \mu(y(t))) & \text{for } t \in (t_n, t_{n+1}] \quad \text{and } n = 0, 1, ... \\ y(0) = y_0 \end{cases} \tag{2.29}$$

The infinite horizon problem is computationally unfeasible, therefore we fix an horizon length N and we solve a sequence of finite horizon problems. In order to formulate the algorithm, we need to introduce the finite horizon quadratic cost functional in the following way; we set $y_0 \in Y$, $u \in \mathcal{U}$

$$J_{y_0}^N(u(\cdot)) = \int_{t_0}^{t_0^N} L(y_{[u,t_0,y_0]}, u(t))e^{-\lambda t}dt$$

where N is a natural number, $t_0^N = t_0 + N\Delta t$ is the final time, $N\Delta t$ denotes the length of the prediction horizon for the chosen time step $\Delta t > 0$. We also define the set of admissible control:

$$\mathcal{U}^N := \{u \in U^N | u \in U\}$$

with $U^N \subseteq R^N$, with $N \in \mathbb{N}$ fixed. The method works as follows: in each iteration over n we store the optimal control on the first time interval $[t_n, t_{n+1}]$ and the associated optimal trajectory of the sampling time. Then, we initialize a new finite horizon optimal control problem whose initial condition is given by the optimal trajectory $y_{[\mu^N(y_0),t_0,y_0]}$ at $[t_0 + \Delta t]$ using the optimal control $u(t) = \mu^N(y_0)$ and we iterate this process.

Algorithm 4: NMPC Algorithm

1: **D**ata: fix a time step $\Delta t > 0$, a finite horizon $N \in \mathbb{N}$, a weighted parameter $\lambda > 0$
2: **for** $n = 0, 1, 2, \ldots$ **do**
3: Measure the current state $y(t_n) \in Y$ of the system at $t_n = n\Delta t$.
4: Set $t_0 = t_n = n\Delta t$, $y_0 := y(t_n)$ and compute the open-loop solution of

$$\min J_{y_0}^N(u) \qquad \text{s.t. } u \in \mathcal{U}^N \tag{2.30}$$

We denote the obtained optimal control by u_n^*
5: Define the NMPC feedback value $\mu^N(y(t_n)) := u_n^*(t_n)$,
6: Compute the associated state $y_n = y_{[u_n,t_0,y_0]}$ by solving (2.30) in the next sampling period $[t_0, t_0 + \Delta t]$
7: **end for**

In general, one can obtain a better feedback approximation increasing the prediction horizon, but this will of course make the CPU time grow. Typically, one is interested in short prediction horizons (or even horizon of minimal length), which can guarantee stabilization properties of the MPC scheme. The problem is that when the horizon N is too short we will loose these properties (see [58] Example 6.26). In the following, we will recall estimates on the minimum value for N ensuring asympotitic stability based on the relaxed dynamic programming principle. The interested reader can find all the details and proofs in [58] and the references therein.

Dynamic Programming and Asymptotic stability

First of all, let us introduce the value function for an infinite horizon optimal control problem:

$$v_\infty(y_0) := \inf_{u(\cdot)\in\mathcal{U}} J_{y_0}^\infty(u).$$

Let $N \in \mathbb{N}$ be chosen. For any $k \in \{0, ..., N\}$ the value function v satisfies the dynamic programming principle:

$$v(y_0) = \inf_{u\in\mathcal{U}^k(t_0)} \left\{ \int_{t_0}^{t_0+k\Delta t} L(y_{[u,t_0,y_0]})(t), u(t))dt \right\} + v(y_{[u,t_0,y_0]}(t_0 + k\Delta t)).$$

In the same way we define the value function for the finite horizon problem in the following way:

$$v_N(y_0) = \inf_{u(\cdot)\in\mathcal{U}^N} J_{y_0}^N(u).$$

The value function v^N satisfies the DPP for the finite horizon problem for $t_0 + k\Delta t$, $0 < k < N$:

$$v^N(y_0) = = \inf_{u\in\mathcal{U}^k(t_0)} \left\{ \int_{t_0}^{t_0+k\Delta t} L(y_{[u,t_0,y_0]}(t), u(t))dt + v^N(y_{[u,t_0,y_0]}(t_0 + k\Delta t)) \right\}.$$

To introduce the concept of asymptotic stability of an equilibrium, we have to define a special class of functions:

Definition 2.4 *We define the following classes of comparison functions:*

$$\begin{aligned}
\mathcal{K} &:= \left\{\alpha : \mathbb{R}_0^+ \to \mathbb{R}_0^+ \,|\, \alpha \text{ is continuous, strictly increasing and } \beta(0) = 0\right\},\\
\mathcal{K}_\infty &:= \left\{\alpha : \mathbb{R}_0^+ \to \mathbb{R}_0^+ \,|\, \alpha \in \mathcal{K},\ \alpha \text{ unbounded}\right\},\\
\mathcal{L} &:= \left\{\alpha : \mathbb{R}_0^+ \to \mathbb{R}_0^+ \,|\, \alpha \text{ is continuous, strictly decreasing, } \lim_{t\to\infty} \alpha(t) = 0\right\},\\
\mathcal{KL} &:= \left\{\beta : \mathbb{R}_0^+ \times \mathbb{R}_0^+ \to \mathbb{R}_0^+ \,|\, \beta \text{ is continuous, } \beta(\cdot, t) \in \mathcal{K}, \beta(r, \cdot) \in \mathcal{L}\right\}
\end{aligned}$$

Definition 2.5 *Let u be the solution of* (2.29) *and y_* an equilibrium for* (2.29)*, i.e. it states $f(y_*, \mu(y_*)) = 0$. Then, we say that y_* is* locally asymptotically stable *if there exists a constant $\eta > 0$ and a function $\beta \in \mathcal{KL}$ such that the inequality*

$$\|y_{[\mu(\cdot),t_0,y_0]}(t) - y_*\| \leq \beta(\|y_0 - y_*\|, t) \tag{2.31}$$

holds for $y_0 \in Y$ satisfying

$$\|y_0 - y_*\| < \eta$$

and $t \geq t_0$. In (2.31) we denote by $y_{[\mu(\cdot),t_0,y_0]}$ the solution to (2.29).

Thanks to the DPP and the comparison functions in Definition 2.4, we are able to prove the following result (see [58]):

Proposition 2.5 *We consider the prediction horizon $N \in \mathbb{N}$ and the feedback mapping μ^N computed by means of the Algorithm 1. Let us assume there exists an $\alpha^N \in (0, 1]$ such that for all $(t_0, y_0) \in \mathbb{R}_0^+ \times Y$ the relaxed DPP inequality holds:*

$$v^N(y_0) \geq v^N(t_0 + \Delta t, y_{[\mu^N(y_0),t_0,y_0]}(t_0 + \Delta t)) + \alpha L(y_0, \mu^N(y_0)) \tag{2.32}$$

Moreover, we have for all $(t_0, y_0) \in \mathbb{R}_0^+ \times Y$:

$$\alpha v(y_0) \leq \alpha J_{y_0}^N(\mu^N(y_0)) \leq v^N(y_0) \leq v(y_0), \tag{2.33}$$

where $y_{[\mu^N(y_0),t_0,y_0]}$ solves the closed-loop dynamics (2.29) with $\mu = \mu^N$. If, moreover, there exists an equilibrium $y_* \in Y$ and $\alpha_2, \alpha_3 \in \mathcal{K}_\infty$ such that the inequalities

$$L_*(y_0) = \min_{u \in \mathcal{U}} L(y_0, u) \geq \alpha_1(\|y_0 - y_*\|),$$

$$\alpha_2(\|y_0 - y_*\|) \geq v^N(y_0)$$

holds for all $(t_0, y_0) \in \mathbb{R}_0^+ \times Y$, then y_* is a globally asymptotically stable equilibrium for (2.29) with the feedback map $\mu = \mu^N$ and value function v^N.

We now present a result which tells how to choose the prediction horizon in order to guarantee the stabilization of the problem. The computation of the constant α in (2.32) plays a crucial role. We first require the following controllability property of the system:

Definition 2.6 *We call the system* (2.28) *exponentially controllable with respect to the runninc cost L, if for each $(t_0, y_0) \in \mathbb{R}_0^+ \times H$ there exists constants $C \geq 0$ and $\sigma \in [0, 1)$ and an admissible control $u \in \mathcal{U}$ such that*

$$L(y_{[u,t_0,y_0]}(t), u(t)) \leq C\sigma^{t-t_0} L^*(y_0) \qquad a.e.\ t \geq t_0. \tag{2.34}$$

Thanks to this definition, we can compute α in (2.32) as suggested by the following theorem:

Theorem 2.4 *Assume that the system* (2.28) *and L satisfy the controllability contition* (2.34) *and let the optimization horizon N be given. Then, the suboptimality degree α^N from* (2.32) *is given by:*

$$\alpha^N := \alpha = 1 - \frac{(\gamma_N - 1)\prod_{i=2}^{N}(\gamma_i - 1)}{\prod_{i=2}^{N}\gamma_i - \prod_{i=2}^{N}(\gamma_i - 1)} \tag{2.35}$$

with $\gamma_i = C\dfrac{1-\sigma^i}{1-\sigma}$.

As a consequence of Theorem 2.4, the closed loop system is asymptotically stable and the sub-optimality estimate (2.33) holds whenever α is positive. The minimal horizon that guarantees stability is the smallest $N \in \mathbb{N}$ with $\alpha^N > 0$.

3. Coupling MPC and DP methods in optimal control problems.

In this chapter we study the approximation of optimal control problems via the solution of a Hamilton-Jacobi equation in a tube around a reference trajectory obtained by solving a Model Predictive Control problem. The coupling between the two methods is introduced to improve the initial local solution and to reduce the computational complexity of the Dynamic Programming algorithm. We present some features of the method and show the results obtained via this technique showing that it can produce an improvement with respect to the two uncoupled methods. The main results on Dynamic Programming and Model Predictive Control are summarized in Chapter 2, so in the following we will start presenting the novelty of the coupling of the two methods.

3.1. Coupling MPC with Bellman Equation

The idea behind the coupling is to combine the advantages from both methods. The Dynamic Programming approach is global and gives an information on the value function in a domain, provided we solve the Bellman equation. It gives the feedback synthesis in the whole domain. Model Predictive control is local and gives an approximate feedback control just for a single initial condition. Clearly MPC is faster, but does not give the same amount of information.
In many real situations, we need a control to improve the solution around a reference trajectory, $\overline{y}_x(\cdot)$, starting at x so we can reduce the domain to a neighborhood of $\overline{y}_x(\cdot)$. Now, let us assume that we are interested in the approximation of feedbacks for an optimal control problem given the initial condition x. First of all we have to select a (possibly small) domain where we are going to compute the approximate value function and to this end we need to compute a first guess that we will use as reference trajectory.

MPC can provide quickly a reasonable reference trajectory $\overline{y}_x(\cdot) := y^{MPC}(\cdot)$, but this trajectory is not guaranteed to be globally optimal (or have the required stabilization properties). In our approach, we can choose a rather *short* prediction horizon in order to have a fast approximation of the initial guess. This will not give the final feedback synthesis, but will be just used to build the domain Ω_ρ, where we are going to apply the DP approach. It is clear that MPC may provide inaccurate solutions if N is too short, but its rough information about the trajectory y^{MPC} will be later compensated by the knowledge of the value function obtained by solving the Bellman equation. We construct a domain Ω_ρ as a tube of radius ρ around y^{MPC} defining

$$\Omega_\rho := \{x \in \Omega : dist(x, y^{MPC}) \leq \rho\} \tag{3.1}$$

This tube can be actually computed via the eikonal equation, *i.e.*, solving the Dirichlet problem

$$|\nabla v(x)| = 1, \quad x \in \mathbb{R}^N \backslash \mathcal{T}, \qquad \text{with } v(x) = 0, \quad x \in \mathcal{T}, \tag{3.2}$$

where the target is $\mathcal{T} := \{y^{MPC}(t), t \in [0, T]\}$. We just want to mention that for this problem several fast methods are available (e.g. Fast Marching [115] and Fast Sweeping [125]) so this step can be solved very efficiently. The interested reader can find in [47] many details on numerical approximation of the weak solutions to the eikonal equation.

By solving the eikonal equation (3.2) (in the viscosity sense), we obtain the distance function from the target. Then, we choose a radius $\rho > 0$ in order to build the tube Ω_ρ. In this way the domain of the HJB is not built by scratch but taking into account some information on the controlled system. To localize the solution in the tube we impose state constraints boundary conditions on $\partial\Omega_\rho$, penalizing in the scheme (2.17) the points outside the domain. It is clear that a larger ρ will allow for a better approximation of the value function, but at the same time, enlarging ρ we will lose the localization around the trajectory, increasing the number of nodes (and the CPU time). Finally, we compute the optimal feedback from the value function computed and the corresponding optimal trajectories in Ω_ρ. The algorithm is summarized below:

Algorithm 5: Localized DP algorithm (LDP)

1: *Start:* Initialization
2: **Step 1:** Solve MPC and compute y_x^{MPC} starting at x
3: **Step 2:** Compute the distance from y_x^{MPC} via the Eikonal equation
4: **Step 3:** Select the tube Ω_ρ of radius ρ centered at y_x^{MPC}
5: **Step 4:** Compute the constrained value function v^{tube} in Ω_ρ via HJB
6: **Step 5:** Compute the optimal feedbacks and trajectory using v^{tube}
7: *End*

3.2. Numerical tests

In this section we present some numerical tests both for the infinite horizon problem and the minimum time problem to illustrate the performances of the proposed algorithm. However, the localization procedure can be applied to more general optimal control problems.
All the numerical simulations have been realized on a MacBook Pro with 1 CPU Intel Core i5 2.4 GHz and 8GB RAM. The codes used for the simulations are written in Matlab.

Test 1: 2D Linear Dynamics Let us consider the following controlled dynamics:

$$\begin{cases} \dot{y}(t) = u(t) \quad t \in [0, T] \\ y(0) = x \end{cases} \tag{3.3}$$

where $u = (u_1, u_2)$ is the control, $y : [0, T] \to \mathbb{R}^2$ is the dynamic and x is the initial condition. The cost functional we want to minimize is:

$$J_x(u) := \int_0^\infty \min\{|y(t;u) - P|^2, |y(t;u) - Q|^2 - 2\}\, e^{-\lambda t}\, dt \tag{3.4}$$

where $\lambda > 0$ is the discount factor.
In this example, the running cost has two local minima in P and Q. We set $P := (0, 0)$ and $Q := (2, 2)$ so that the value of the running cost is 0 at P and -2 at Q. Note that we have included a discount factor λ, which guarantees the integrability of the cost functional $J_x(u)$ and the existence and uniqueness of the viscosity solution. The main task of the discount factor is to penalize long prediction horizons. Since we want to make a comparison, we introduce it also in the setting of MPC, although this is not a standard choice. As we mentioned, MPC will just provide a first guess used to define the domain where we solve the HJB equation.
In this test the chosen parameters are: $u \in [-1, 1]^2$, $\rho = 0.2$, $\Omega = [-4, 6]^2$, $\Delta t_{MPC} = 0.05 = \Delta t_{HJB}$, $\Delta x_{HJB} = 0.025$, $\Delta\tau = 0.01$ (the time step to integrate the trajectories). In particular, we focus on $\lambda = 0.1$ and $\lambda = 1$. The number of controls are 21^2 for the value function and 3^2 for the trajectories. Note that the time step used in the HJB approach for the approximation of the trajectory ($\Delta\tau$) is smaller than the one used for MPC: this is because MPC leads to have a rough and quick approximation of the solution. In Figure 3.1, we show the results of MPC with $\lambda = 0.1$ on the left and $\lambda = 1$ on the

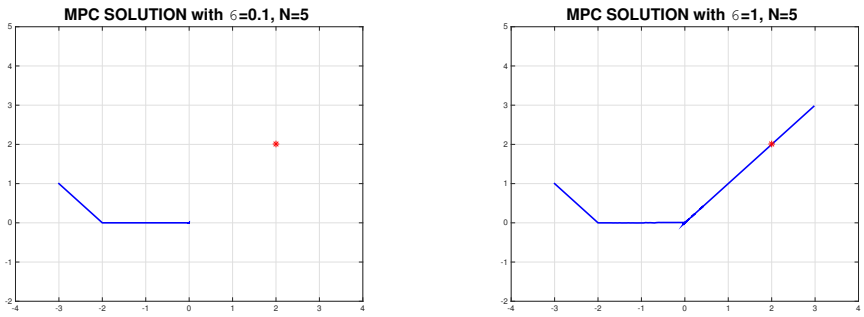

Figura 3.1.: Test 1: MPC solver with $\lambda = 0.1$ (left) and $\lambda = 1$ (right)

right. As one can see, none of them is an accurate solution. In the first case, the solution goes to the local minimum $(0, 0)$ and is trapped there, whereas when we increase λ, the optimal solution does not stop at the global minimum y_2. On the other hand, these two approximations help us to localize the behavior of the optimal solution in order to apply the Bellman equation in a reference domain Ω_ρ.
In Figure 3.2, we show the contour lines of the value function in the whole interval Ω for $\lambda = 1$ and the corresponding value function in Ω_ρ. Finally, the optimal trajectories for $\lambda = 1$ are shown in Figure 3.3. In the right part of the figure we propose the optimal solution obtained by the approximation of the value function in Ω whereas, on the left, we can see the first approximation of the MPC solver (red line), the tube (purple lines)

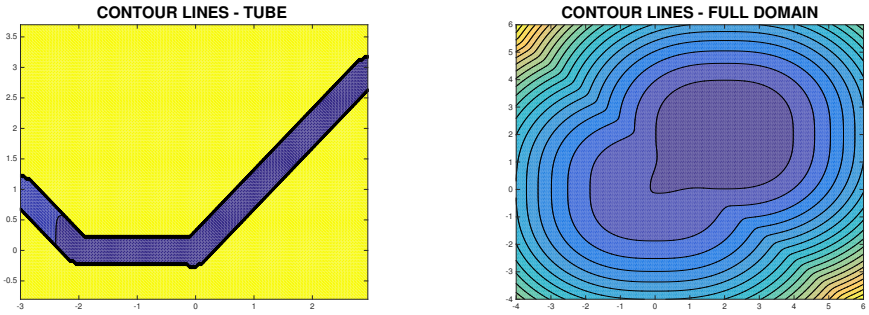

Figura 3.2.: Test 1: Contour lines of the value function in the tube Ω_ρ (left) and in Ω (right).

and the optimal solution via Bellman equation (blu line). As we can see in the pictures, the solutions provided from the DP approach in Ω and Ω_ρ are able to reach the global desired minimum y_2. In Table 3.3, we present the CPU time and the evaluation of the

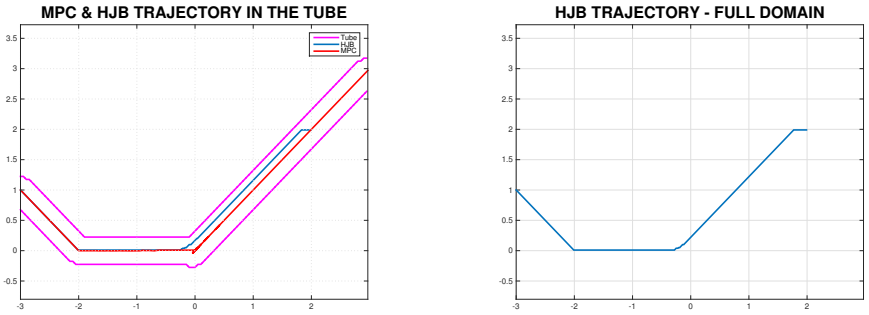

Figura 3.3.: Test 1: Optimal trajectory via MPC (red line) and via HJB (blu line) in the tube (purple lines) (left), optimal trajectory via HJB in Ω (right).

$\lambda = 1$	**MPC N=5**	**HJB in Ω_ρ**	**HJB in Ω**
CPU	16s	239s	638s
$J_x(u)$	5.41	5.33	5.3

Tabella 3.3.: A comparison of CPU time (seconds) and values of the cost functional.

cost functional for different tests. As far as the CPU time is concerned, in the fourth column we show the global time needed to get the approximation of the value function in the whole domain and the time to obtain the optimal trajectory, whereas the third column shows the global time needed to compute all the steps of LDP algorithm: the

trajectory obtained via MPC, the computation of the tube, the computation of the value function in the reduced domain and the computation of the optimal trajectory. As we expected, the value of the cost functional is lower when we compute the value function in the whole domain (because $\Omega_\rho \subset \Omega$). It is important to note that the approximation in Ω_ρ guarantees a reduction of the CPU time of the 62.5%.

Test 2: Infinite Horizon Problem for the Van der Pol dynamics. In this test we consider the two-dimensional nonlinear system dynamics given by the Van Der Pol oscillator:

$$\begin{cases} \dot{x}(t) = y(t) \\ \dot{y}(t) = (1 - x(t)^2)y(t) - x(t) + u(t) \\ x(0) = x_0,\ y(0) = y_0. \end{cases} \tag{3.5}$$

The cost functional we want to minimize with respect to u is:

$$J_x(u) := \int_0^\infty (x^2 + y^2)e^{-\lambda t}\, dt. \tag{3.6}$$

We are dealing with a standard tracking problem where the state we want to reach is the origin. The chosen parameters are: $\lambda = \{0.1, 1\}$, $u \in [-1, 1]$, $\rho = 0.4$, $\Omega = [-6, 6]^2$, $\Delta t_{MPC} = 0.05 = \Delta t_{HJB}$, $\Delta x_{HJB} = 0.025$, $\Delta\tau = 0.01$, $x_0 = -3$, $y_0 = 2$. We took 21 controls for the approximation of the value function and 3 for the optimal trajectory. In Figure 3.4, we present the optimal trajectory: on the right, the one obtained solving

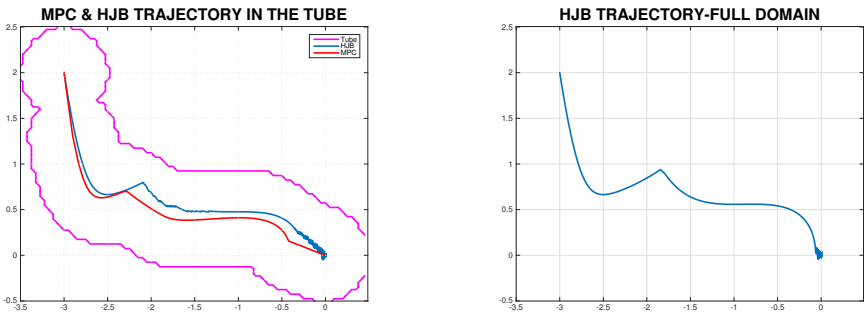

Figura 3.4.: Test 2: Optimal trajectory via MPC (red line) and via HJB (blu line) in the tube Ω_ρ (left) and in Ω (right) for $\lambda = 0.1$.

the HJB equation in the whole domain, on the left, the one obtained applying the LDP algorithm.

In Table 3.4 we present the CPU time and the evaluation of the cost functional with $\lambda = 0.1$ and $\lambda = 1$. In both case we can observe that the algorithm we propose is faster than solving HJB in the whole domain and the cost functional provides a value that improves the one obtained with the MPC algorithm.

$\lambda = 0.1$	**MPC N=10**	**HJB in Ω_ρ**	**HJB in Ω**
CPU	79s	155s	228s
$J_x(u)$	14.31	13.13	12.41

$\lambda = 1$	**MPC N=10**	**HJB in Ω_ρ**	**HJB in Ω**
CPU	23s	49s	63s
$J_x(u)$	6.45	6.09	6.07

Tabella 3.4.: Test 2: A comparison of CPU time (seconds) and values of the cost functional for $\lambda = \{0.1, 1\}$.

Test 3: Minimum Time Problem for the Van Der Pol dynamics We consider again the dynamics given by (3.5). In this test we are dealing with a minimum time problem where the target is a neighborhood of the origin. It is well-known that the minimum time problem is tricky to solve via MPC. We try to improve its solution by adding a running cost which penalizes the distance from the desired target. This will turn out to be absolutely relevant for the MPC solver, and as a consequence in the algorithm we propose. The cost functional we want to minimize is:

$$J_x(u) := \int_0^\infty L(x(t), y(t), u(t))\chi_{\mathcal{T}}(t)\, dt \tag{3.7}$$

with $\mathcal{T} = B_\varepsilon(0)$, $\varepsilon = 0.1$, and the running cost is

$$L(x, y, u) = (x^2 + y^2)e^{-\lambda t}.$$

We remark that dealing with the standard minimum time problem means to consider $L(x, y, u) \equiv 1$.
In Figure 3.5 we show, on the left, the uncontrolled solution of equation (3.5) with initial condition $x = 3, y = 2$. As we can see the solution is not going to the origin but it provides the so called *limit cycles*. Our aim is to steer the solution close to the origin. However, the uncontrolled solution may suggest the interval where we could compute the value function: $\Omega \equiv [-4, 4] \times [-4, 4]$ and it gives the optimal trajectory shown on the right of Figure 3.5 via Bellman's equation without running cost.
We can see in Table 3.5 that this approach is not very efficient. As we can see in the middle of Figure 3.5, the MPC solver is not able to steer the solution close to the origin. So we can get just a rough idea of the controlled solution leading a smaller interval for HJB and we also need to consider the origin in the interval. In Table 3.5, we show the efficiency of the LDP method. The cost functionals evaluated from the solution of HJB provide the same value and both are lower than the one obtained by MPC.
In Figure 3.6 we show the value function in the whole domain on the left and the reduced value function on the right.
Then, we switch to the minimum time problem with running cost. The running cost helps the MPC solver to penalize solutions far from the target. The parameters chosen for the simulations are: $U = [-1, 1], \rho = 0.4, \Omega = [-6, 6]^2, x = 3, y = 2, \Delta t_{MPC} =$

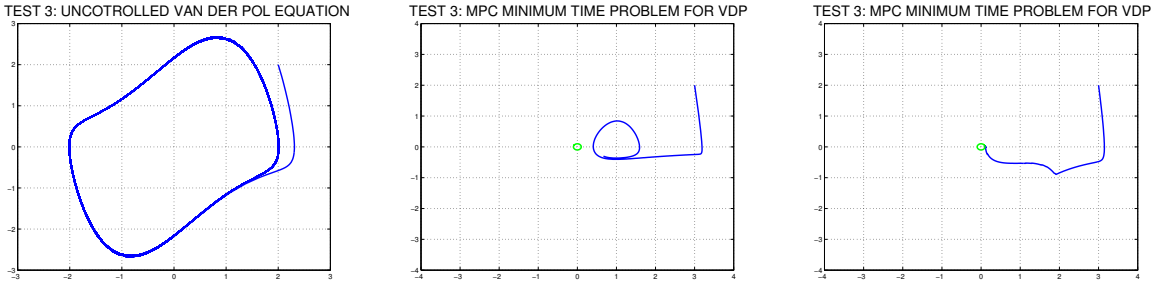

Figura 3.5.: Test 3 (without running cost): Uncontrolled solution (left), optimal trajectory via MPC (middle), optimal trajectory via HJB (right).

	MPC N=5	**HJB in Ω_ρ**	**HJB in Ω**
CPU	3.19s	11.82s	12.74s
$J_x(u)$	1.02	1	1

Tabella 3.5.: Test 3 (without running cost): A comparison of CPU time (seconds) and values of the cost functional.

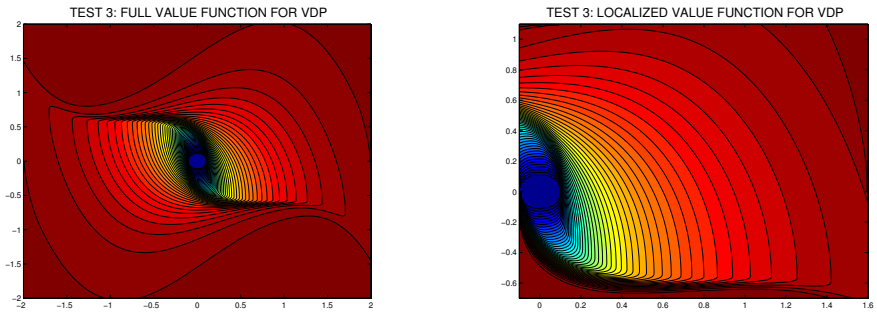

Figura 3.6.: Test 3 (without running cost): Contour lines of the value function in a tube (left), and in a full domain (right).

$0.05 = \Delta t_{HJB}, \Delta x_{HJB} = 0.025, \Delta\tau = 0.01, \lambda = \{0.1, 1\}$. We took 21 controls for the approximation of the value function and 3 for the optimal trajectory. In Figure 3.7, we show the contour lines of the value function obtained solving the HJB equation in the full domain and in a reduced domain with two different parameters λ.

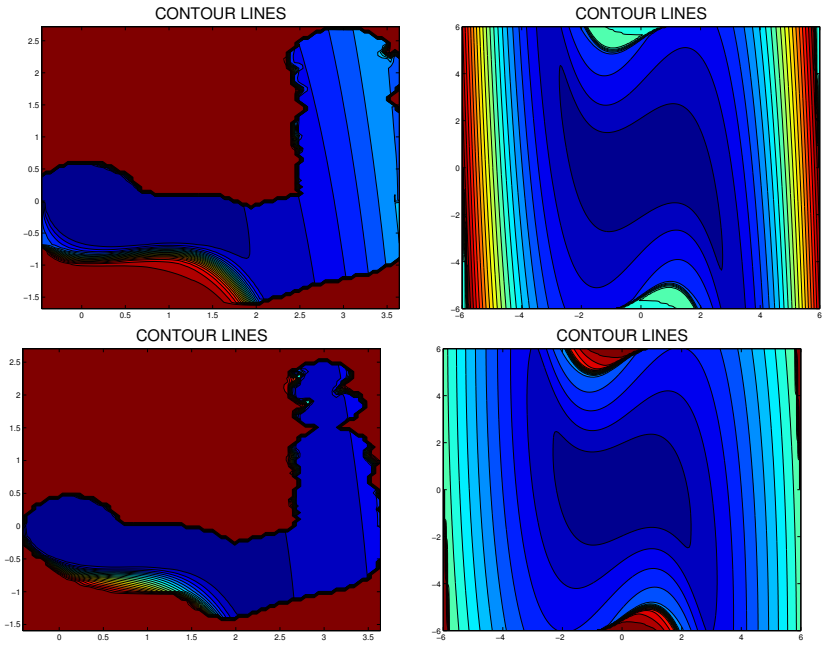

Figura 3.7.: Test 3 (with running cost): Contour lines of the value function in a tube (left), and in a full domain (right), with $\lambda = 0.1$ (top), and $\lambda = 1$ (bottom)

In Figure 3.8, we present the optimal trajectories. We see how the MPC solver is able to reach the target when we provide the running cost with an additional term that takes into account the distance from the desired point. In Figure 3.2 we show the contour lines of the distance function from the target, which is a crucial point of our algorithm.

Finally, in Table 3.9, we present the evaluation of the cost functional and CPU time. In both cases $\lambda = 0.1$ and $\lambda = 1$, the approximation in the reduced domain is faster than the approximation of HJB in the full domain. We want to emphasize that the MPC solver, with a running cost, provides reasonable values of the cost functional, which is definitely improved thanks to Bellman's equation.

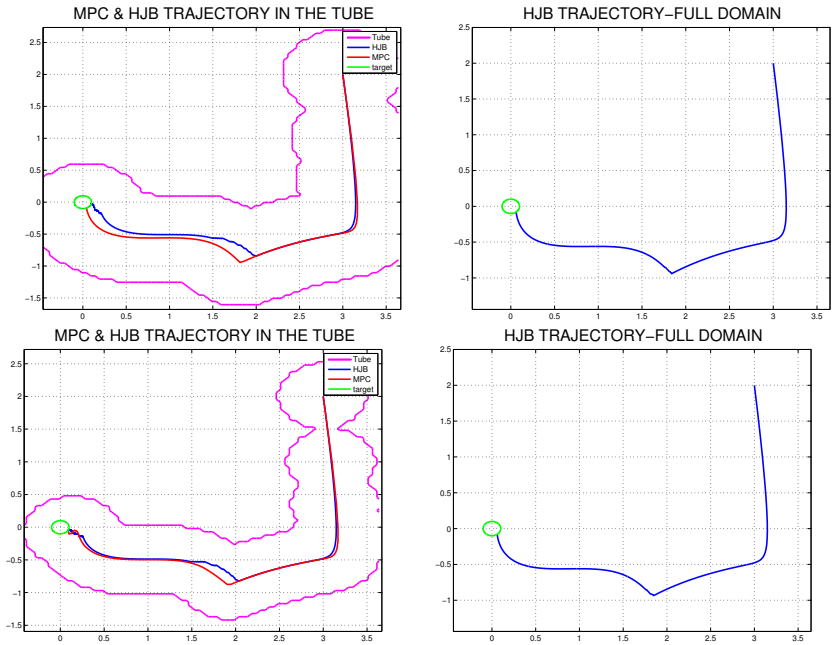

Figura 3.8.: Test 3 (with running cost): Left: Optimal trajectory via MPC (red) and via HJB (blue) in a tube (purple) on the left, optimal trajectory via HJB in the chosen full domain (right) with $\lambda = 0.1$(top) and $\lambda = 1$ (bottom)

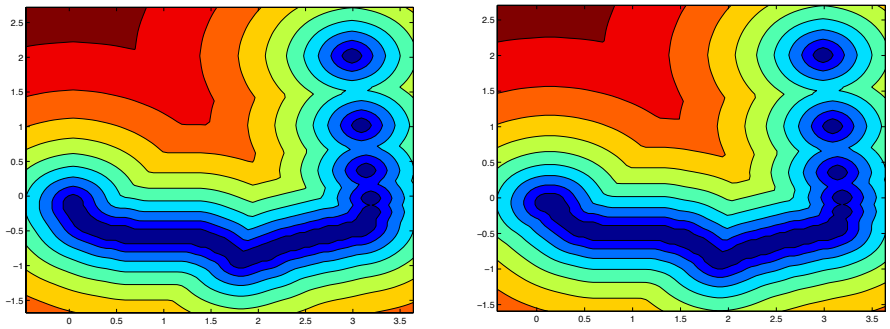

Figura 3.9.: Test 3: Contour lines of the solution of the eikonal equation.

$\lambda = 0.1$	**MPC N=20**	**HJB in Ω_ρ**	**HJB in Ω**
CPU	34s	58s	169s
$J_x(u)$	19.84	19.73	19.43

$\lambda = 1$	**MPC N=20**	**HJB in Ω_ρ**	**HJB in Ω**
CPU	51s	67s	80s
$J_x(u)$	8.52	8.2	8.19

Tabella 3.9.: Test 3 (with running cost): CPU time and evaluation of the cost functional with $\lambda = 0.1$ and $\lambda = 1$.

Test 4: Zermelo navigation problem We consider the minimum time problem for the Zermelo dynamics, which is given by:

$$\begin{cases} \dot{x}(t) = 1 + V_b \cos(u) \\ \dot{y}(t) = V_b \sin(u) \end{cases} \tag{3.8}$$

where $V_b \in \mathbb{R}$. As we discussed in the previous example, we add a running cost penalizing the distance from the target in order to help the MPC solver. Therefore, the cost functional we want to minimize is:

$$J_x(u) := \int_0^\infty L(x, y, u)\chi_{\mathcal{T}}(t)\, dt \tag{3.9}$$

with $\mathcal{T} = B_\varepsilon(0)$, $\varepsilon = 0.2$, running cost

$$L(x, y, u) = (x^2 + y^2)e^{-\lambda t}$$

In our simulations we fix $\lambda = 0.1$ and we focus our attention on two different values of V_b, $V_b = \{0.6, 1.4\}$. The parameters chosen are: $U = [-\pi, \pi], \rho = 0.4, \Omega = [-2, 2]^2, x_0 - 1, y_0 = -0.5, \Delta t_{MPC} = 0.05 = \Delta t_{HJB}, \Delta x_{HJB} = 0.04, \Delta\tau = 0.01$. We took 72 controls for the approximation of the value function and the same for the optimal trajectory.
In Figure 3.10 we show the optimal trajectory obtained via HJB in the full domain as well as the countour lines for two different choices of V_b.
In Figure 3.11 we show the trajectory obtained solving the HJB equation in a tube built around the MPC trajectory (left). Note that the radius of the tube is quite big ($\rho = 0.4$) as if we take a smaller ρ the target will not be in the tube; as a consequence, the trajectory would never be able to reach it. In the middle we show the contour lines of the value function in the reduced domain. On the right we can see the contour lines obtained solving the eikonal equation where the target is the trajectory given by MPC (this is an important step of our algorithm in order to build the tube).

Finally, we present the results of our simulation in the Table 3.11. Note that in both cases ($V_b = 0.6$ and $V_b = 1.4$) the algorithm we propose is faster than solving HJB in the full domain (it takes less than half of the time); concerning the evaluation of the cost functional, the value we obtain applying the LDP algorithm is lower than the one obtained with the MPC solver and it is close to the value obtained solving HJB in the

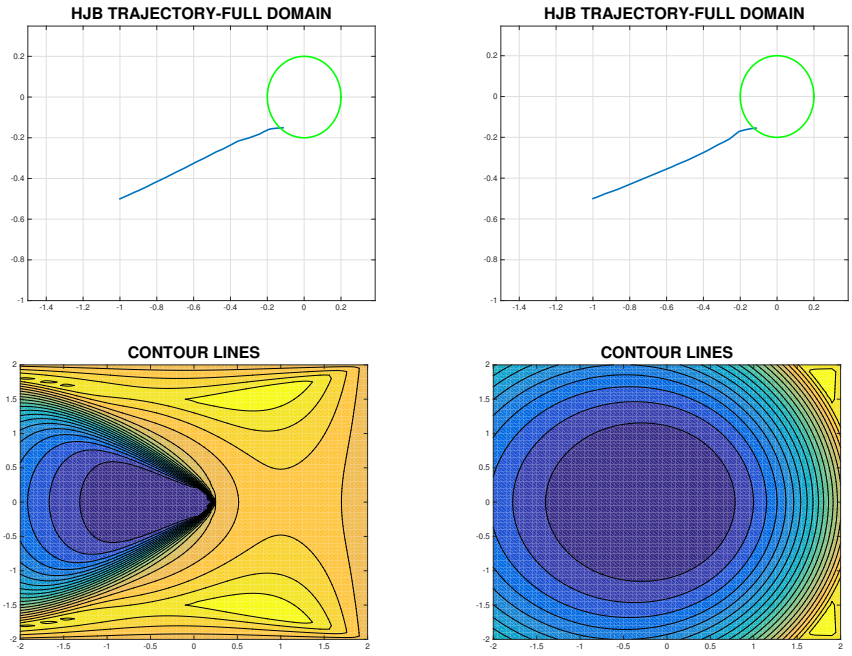

Figura 3.10.: Test 4: optimal trajectory via HJB (top: left $V_b = 0.6$, right $V_b = 1.4$), contour lines in the full domain (bottom, left $V_b = 0.6$, right $V_b = 1.4$)

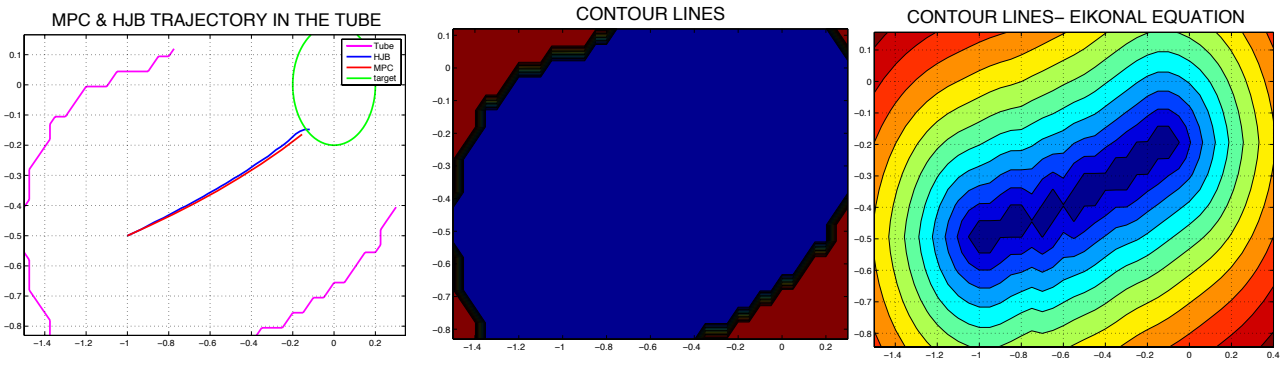

Figura 3.11.: Test 4: optimal trajectory in the tube (left), contour lines of the value function in the reduced domain (middle), contour lines of the value function obtained solving the eikonal equation (right), with $\lambda = 0.1$, $V_b = 0.6$

full domain.

$V_b = 0.6$	**MPC**	**HJB in Ω_ρ**	**HJB in Ω**
CPU	1.36s	11.15s	24.47s
$J_x(u)$	0.35	0.34	0.34
$V_b = 1.4$	**MPC**	**HJB in Ω_ρ**	**HJB in Ω**
CPU	0.92s	6.39s	17.61s
$J_x(u)$	0.23	0.2	0.2

Tabella 3.11.: Test 5 CPU time and evaluation of the cost functional with $\lambda = 0.1$ and $V_b = \{0.6, 1.4\}$

4. A HJB-POD approach to the control of the level set equation

In this chapter we consider an optimal control problem where the dynamics is given by the propagation of a one-dimensional graph controlled by its normal speed. A target corresponding to the final configuration of the front is given and we want to minimize the cost to reach the target. We want to solve this optimal control problem via the dynamic programming approach, but it is well known that these methods suffer from the "curse of dimensionality", so that we can not apply the method to the semi-discrete version of the dynamical system. However, this is made possible by a reduced-order model for the level set equation based on Proper Orthogonal Decomposition. This results in a new low-dimensional dynamical system that is sufficient to track the dynamics. By the numerical solution of the Hamilton-Jacobi-Bellman equation related to the POD approximation, we can compute the feedback law and the corresponding optimal trajectory for the nonlinear front propagation problem. We discuss some numerical issues of this approach and present numerical examples.

4.1. A front propagation problem with target

Let us first introduce our problem, the interested reader is referred to [95] for more details on the topic. The dynamics will describe the front propagation of an interface via the level-set equation in $\mathbb{R}^n$. The typical situation is the following: an initial position for the front $\Gamma(0) = \Gamma_0$ (*i.e.*, an initial surface in $\mathbb{R}^n$) is given and the front evolves driven by a force always directed in the normal direction to every point of the front. The velocity in the normal direction will be denoted by V_Γ and the scalar speed $a(x,t)$ must keep the same sign during the evolution (let us choose the positive sign to fix ideas). Note that in the general case the speed can also depend on the position x and the time t, although also the case of a piecewise constant speed is interesting (and we will use it in the sequel). To summarize, we will have in general

$$V_\Gamma = a(x,t), \qquad a : \mathbb{R}^n \times \mathbb{R}_+ \to \mathbb{R}_+. \tag{4.1}$$

The initial configuration of the front is

$$\Gamma(0) = \Gamma_0 \tag{4.2}$$

and Γ_0 can be a single closed curve or the union of many finite closed curves without intersections. The evolutive equation describes the propagation of the front $\Gamma(t)$ in time.

This problem can produce singularities for a single smooth curve Γ_0 even in the particular case of a constant speed. It is well known that a powerful method to track this evolution, even when one has singularities and topology changes (*e.g.*, when the front $\Gamma(t)$ starting from Γ_0 can produce intersections at time t), is the level set method. In this case one describes $\Gamma(t)$ as the 0-level set of a continuous function solving the Cauchy problem

$$\begin{cases} \Phi_t(x,t) + a(x,t)|\nabla\Phi(x,t)| = 0 & \text{in } \mathbb{R}^n \times \mathbb{R}_+ \\ \Phi(x,0) = \Phi_0(x) & \text{in } \mathbb{R}^n \end{cases} \tag{4.3}$$

where Φ_0 is a representation function for Γ_0 (*i.e.*, a continuous function changing sign across Γ_0) and $a(x,t)$ is assumed to be known. By solving (4.3), one can obtain $\Phi(x,t)$ and recover the position of the front $\Gamma(t)$ as

$$\Gamma(t) := \{x \in \mathbb{R}^n : \Phi(x,t) = 0\}. \tag{4.4}$$

The Cauchy problem (4.3) has a unique viscosity solution under rather general assumptions (see [15]).
Since here we just want to describe our technique, we will consider the evolution of a graph, *i.e.*, the dimension will be $n = 1$ and we look for the front

$$\Gamma(t) := \{(x, y(x,t)) | x \in \mathbb{R}\} \subset \mathbb{R}^2.$$

In this particular case the dynamics will be given by

$$\begin{cases} y_t = a(x,t)\sqrt{1+y_x^2}, & (x,t) \in \mathbb{R} \times [0,T], \\ y(x,0) = y_0(x), & x \in \mathbb{R}. \end{cases} \tag{4.5}$$

Many numerical schemes have been proposed so far to solve the level set equation (4.5). In particular we refer to [115] for monotone and consistent schemes based on finite difference approximation and to [47] for semi-Lagrangian schemes. In the present work, we will adopt an explicit finite difference scheme. We closely follow the scheme used in [40]; we choose space and time steps, Δx and Δt respectively and let

$$x_j = j\Delta x,\ j \in \mathbb{Z}, \quad t_n = n\Delta t,\ 0 \le n \le N,$$

where $N\Delta t = T$. We denote by y_j^n the numerical approximation of $y(x_j, t_n)$. We approximate the solution of equation (4.5) using the following up-wind scheme: let $y_j^0 = y_0(x_j)$, $j \in \mathbb{Z}$ and for $n = 0, ..., N-1$

$$y_j^{n+1} = y_j^n + \Delta t\, a(x_j,t_n)\sqrt{1 + \max\left\{\left(\frac{y_{j-1}^n - y_j^n}{\Delta x}, \frac{y_{j+1}^n - y_j^n}{\Delta x}\right)\right\}^2} \quad j \in \mathbb{Z}.$$

Let us remark that we must work on a bounded interval $\Omega := (a,b)$ for numerical purposes. Then, the grid will have only a finite number of nodes $a = x_0 < x_1 < \ldots < x_d = b$ and, in order to give enough freedom to the front evolution, we impose homogeneous

zero Neumann boundary conditions (see [115] for more details on the implementation).

Let us introduce the control problem for the front propagation. Now the speed function $a(x,t)$ will not be fixed, but will be our control function that we can vary in order to steer the solution as close as possible to a particular desired configuration of the front, *e.g.*, our *target* denoted by $\bar{y}$. In this framework, the speed $a(x,t)$ will be denoted as $u(x,t)$, adopting the classical notation for control problems. In conclusion, we have a control problem for a first order nonlinear partial differential equation of Hamilton-Jacobi type, which can develop singularities during the evolution. This is known to be a difficult problem for the lack of regularity of the solution. Note that another important issue is the reachability of the target: we are not aware of any theoretical result which ensure us that the target is reachable in finite time, so it is natural to set the problem as an infinite horizon problem. We will use the corresponding cost functional with a quadratic running cost in order to penalize the distance from the target:

$$J_p(y_0, u(t)) = \int_0^\infty \|y(x,t) - \bar{y}\|_p^2 \chi_{\bar{y}}(x) e^{-\lambda t} dt, \tag{4.6}$$

where $y(x,t)$ is the solution of (4.5), ε is a positive parameter and

$$\chi_{\bar{y}}(x) = \begin{cases} 1 & if\ \|y(x,t) - \bar{y}\|_p > \varepsilon \\ 0 & otherwise. \end{cases} \tag{4.7}$$

Note that there is a strong dependence of the cost function from the initial condition $y_0(x)$ and from the norm of the running cost p. In fact, we want to solve an infinite horizon optimal control problem with a running cost which penalizes the distance in L^p-norm (where $p = 1, 2, \infty$) from our target which is a stripe of radius ε centered in the profile we want to reach $\bar{y}$. For a given time $t > 0$ and $\Omega = [a, b] \subset \mathbb{R}$ we define the L^∞-error as

$$||y(x,t) - \bar{y}||_\infty := \max_{x \in \Omega} |y(x,t) - \bar{y}|$$

and the L^p-error ($p = 1, 2$) as

$$||y(x,t) - \bar{y}||_p := \left(\int_\Omega |y(x,t) - \bar{y}|^p dx \right)^{\frac{1}{p}}.$$

Let us also observe that the characteristic function (4.7) makes the costs vanish whenever we enter a neighborhood of the target. The reachability of the target is an interesting open problem which we will not address even in the numerical examples the neighborhood is always reachable.

4.2. An HJB-POD method for the control of the level-set equation

Since the main features of the dynamic programming principle are presented in Chapter 2, here we just recall the main features of Proper Orthogonal Decomposition (POD) and we explain the coupling of the two methods. The interested reader can found more details in [73, 6].
We just mention that we are dealing with an optimal control problem of the form:

$$\min_{u \in \mathcal{U}} J(y_0, u(t)) := \int_0^\infty L(y(s), u(s))\, e^{-\lambda s}\, ds \tag{4.8}$$

constrained by the nonlinear ordinary differential equation:

$$\begin{cases} \dot{y}(t) = f(y(t), u(t)), & t > 0, \\ y(0) = y_0 \end{cases} \tag{4.9}$$

with system dynamics in $\mathbb{R}^n$ and a control signal $u(t) \in \mathcal{U} \equiv \{u(\cdot)\,\text{measurable}\,, u : [0,T] \to U\}$, where U is a compact subset of $\mathbb{R}^m$; we assume $\lambda > 0$, while $L(\cdot,\cdot)$ and $f(\cdot,\cdot)$ are Lipschitz-continuous, bounded functions. We address the reader to the Chapter 2 for all the details on the discretization and the numerical approximation. Finally, let us observe that our optimal control problem fits into the general framework if we define in (4.8) and (4.9), respectively:

$$L(y(t), u(t)) := \|y(t) - \bar{y}\|_p^2 \chi_{\bar{y}}$$

$$f(y_j^n, u) := u(x_i, t)\sqrt{1 + \max\left\{\left(\frac{y_{j-1}^n - y_j^n}{\Delta x}, \frac{y_{j+1}^n - y_j^n}{\Delta x}\right)\right\}^2}$$

4.2.1. POD approximation of the control problem

In this section, we explain the POD method for the approximate solution of the optimal control problem. The approach is based on projecting the nonlinear dynamics onto a low dimensional manifold utilizing projectors which contain information of the dynamics. A common approach in this framework is based on the snapshot form of POD proposed in [118], which works as follows.
The snapshots are computed by the numerical approximation of (4.9) for $y(t_i) \in \mathbb{R}^n$ for given time instances and a reference control. Its choice turns out to be very important in order to build accurate surrogate model and may provide basis functions which are not able to capture the desired dynamics.
We define the POD ansatz of order ℓ for the state y as

$$y(t) \approx \bar{y} + \sum_{i=1}^{\ell} y_i^\ell(t)\psi_i\,. \tag{4.10}$$

where $\bar{y} \in \mathbb{R}^n$ is our target. We define the snapshot matrix $Y = [y(t_0) - \bar{y}, \dots, y(t_n) - \bar{y}]$ and determine its singular value decomposition $Y = W\Sigma V$. The POD basis functions $\Psi = \{\psi_i\}_{i=1}^{\ell}$ of rank ℓ are the first ℓ columns of the matrix W. The reduced optimal control problem is obtained through replacing (4.9) by a dynamical system obtained from a Galerkin approximation with basis functions $\{\psi_i\}_{i=1}^{\ell}$ and ansatz (4.10) for the state. This leads to an $\ell-$dimensional system for the unknown coefficients $\{y_i^{\ell}\}_{i=1}^{\ell}$, namely

$$\dot{y}^{\ell}(t) = \Psi^T f(\Psi y^{\ell}, u(t)), \quad y^{\ell}(0) = y_0^{\ell}. \tag{4.11}$$

where $y_0^{\ell} = \Psi^T(y_0 - \bar{y}) \in \mathbb{R}^{\ell}$. The error of the Galerkin projection is governed by the singular values associated to the truncated states of the singular value decomposition (SVD).
The POD-Galerkin approximation leads to the optimization problem

$$\inf_{u \in \mathcal{U}} J_{y_0^{\ell}}^{\ell}(u) := \int_0^{\infty} L(y^{\ell}(s), u(s)) e^{-\lambda s}\, ds, \tag{4.12}$$

where $u \in \mathcal{U}$, y^{ℓ} solves the reduced dynamics (4.11) . The value function v^{ℓ}, defined for the initial state $y_0^{\ell} \in \mathbb{R}^{\ell}$ is given by

$$v^{\ell}(y_0^{\ell}) = \inf_{u \in \mathcal{U}} J_{y_0^{\ell}}^{\ell}(u)\,.$$

Note that the resulting HJB equations are defined in $\mathbb{R}^{\ell}$, but for computational purposes we need to restrict our numerical domain to a bounded subset of $\mathbb{R}^{\ell}$. We refer the interested reader to [2] for details on this issue.

4.3. Numerical tests

In this section we describe our numerical tests. The aim is to drive an initial front profile to a desired final configuration that will be our target (no final time is given). We compute the snapshots with an initial guess for the control inputs. We remark that it is rather crucial to obtain snapshots simulating the desired trajectory. In the current work, we could observe the sensitivity of the surrogate model with respect to the choice of the initial input. However, we found very helpful to enrich the snapshot set with the desired configuration $\bar{y}$. A study of basis generation in this framework may be found in [7]. To apply model order reduction we assume that the control may be rewritten as follows:

$$u(x,t) := \sum_{i=1}^{M} u_i(t) b_i(x) \tag{4.13}$$

where $u_i : [0, +\infty] \to U$ are the control inputs, M is the finite number of control functions used to reconstruct $u(x,t)$ and the coefficients $b_i : \mathbb{R}^n \to \mathbb{R}$ are the so-called shape functions, which model the actions that we can apply to the system governed by

the model. The dynamics is given by (4.5) and we performed the simulations choosing different norms in the cost functional in (4.6).
To show the effectiveness of the method we compute the error in different norms between the final configuration of the front and the given target. We define the error as follows:

$$\mathcal{E}_p = \|y_f(x) - \bar{y}\|_p, \qquad p = 1, 2, \infty \tag{4.14}$$

where we denote $y_f(x)$ the final configuration of the front. All the numerical simulations have been realized on a MacBook Pro with 1 CPU Intel Core i5 2.4 GHz and 8GB RAM. The codes used for the simulations are written in Matlab.

4.3.1. Test 1: Constant final configuration

In this test we choose the initial profile $y_0(x) = 1 + \dfrac{cos(2\pi(1-x))}{2}$ in (4.5) with $x \in [0, 1]$. We want to steer the front toward the target $\bar{y}(x) = 2.5$. We compute the snapshots with a finite difference explicit scheme with a space step $\Delta x = 0.05$, time step $\Delta t = 0.01$ and a given input $u(x,t) = 0.42e^{-(x-0.5)^2}$. The shape functions in (4.13) are $b_1(x) = y_0(x), b_2(x) = e^{-(x-0.5)^2}$ and the control set is $U = [-2, 2]$. In this test the chosen parameters for the value function are: $\Delta x = 0.1, \varepsilon = 0.01, \lambda = 1, \ell = 5, \Delta\tau = 0.01$ (the time step to integrate the trajectories). The set U is discretized into 9 equidistant elements for the value function and 21 for the trajectories.
In the left panel of Figure 4.1 we show the controlled evolution of the front. We can observe that the final configuration of the front is in a neighborhood of the desired configuration. In the right panel of Figure 4.1 we compare the controlled front's configuration, obtained with the L^2-norm with the target and the uncontrolled front.

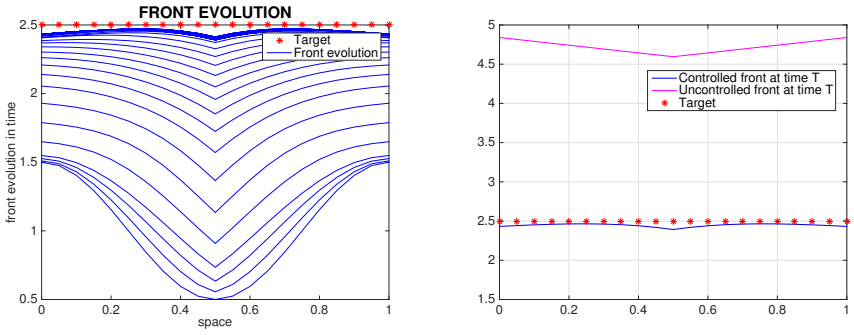

Figura 4.1.: Test 1: evolution of the controlled front in the phase-plane with the target (left), final controlled and uncontrolled front profile with the target (right) with $p = 2$.

Figure 4.2 shows the same comparison where the optimal configuration is computed with L^1 and $L^\infty-$ norm. Although the classical choice for the norm in the cost functional is $p = 2$, we obtain better results for $p = 1$. We also consider $p = \infty$.

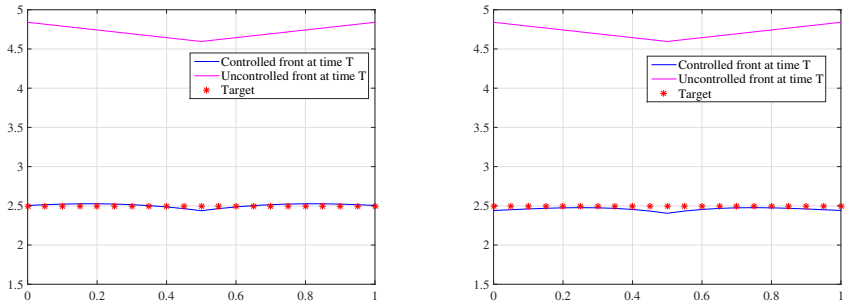

Figura 4.2.: Test 1: Final controlled and uncontrolled front's profile and target using the norm $p = 1$ (left) and the norm $p = \infty$ (right).

	$p = 1$	$p = 2$	$p = \infty$
$\mathcal{E}_p$	0.0214	0.0584	0.0949
$J_p(y_0, u)$	0.3326	0.3185	0.5832

Tabella 4.2.: Test 1: Error between final and desired configuration and evaluation of the cost functional for $\varepsilon = 0.01$

In Table 4.2 we compute the quantity $\mathcal{E}_p$ to evaluate the distance between the controlled final configuration and the desired one in different norms. We also evaluate the cost functional with different choices of p. It turns out that the norm with $p = 1$ provides the most accurate final configuration, whereas the norm $p = 2$ has lower value of the cost functional. We note that the evaluation of the cost functional takes into account the whole history of the trajectories and not just the final configuration.

4.3.2. Test 2: Constant initial configuration

In this test we choose a constant initial profile $y_0(x) \equiv 0$ in (4.5) with $x \in [-1, 1]$. The target is $\bar{y}(x) = 0.2 + e^{-(x-0.5)^2}$. We compute the snapshots with a finite difference explicit scheme with a space step $\Delta x = 0.05$, time step $\Delta t = 0.01$ and velocity $u(x, t) = 0.2 + e^{-(x-0.5)^2}$.
In this test the parameters for the value function are: $\Delta x = 0.1, \varepsilon = 0.01, \lambda = 1, U \equiv [0, 2], b(x) = 0.2+e^{-(x-0.5)^2}, \ell = 4, \Delta\tau = 0.01$ (the time step to integrate the trajectories).

The number of controls are 11 for the value function and 21 for the trajectories.
In Figure 4.3 we show the evolution of the controlled front where the final profile is steered close to the target. For the sake of completeness we also show the optimal control in Figure 4.4.

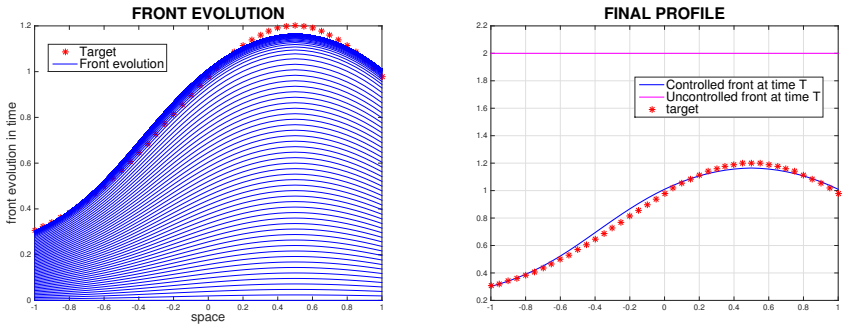

Figura 4.3.: Test 2: evolution of the front in the phase-plane with the target (left), final controlled and uncontrolled front's profile with the target (right) with $p = 2$.

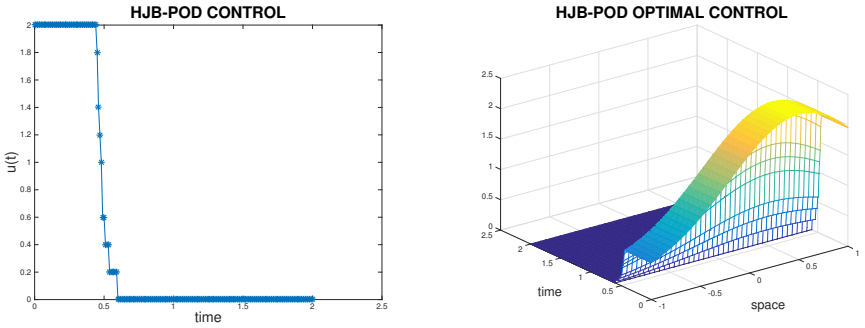

Figura 4.4.: Test 2: evolution of HJB-POD control in time $u(t)$ (left), evolution of hjb-pod control $u(x,t)$ (right)

As explained in Test 1, we perform the simulations using different norms in the cost functional ($p = 1, 2, \infty$). Table 4.4 shows the distance between the controlled solution and the desired configuration and the evaluation of the cost functional. Here, we can see that the choice of $p = 2$ in the norm for the cost functional provides the most accurate final configuration, whereas $p = \infty$ provides a lower value for the cost functional.

	$p=1$	$p=2$	$p=\infty$
$\mathcal{E}_p$	0.0526	0.0439	0.0617
$J_p(y_0,u)$	0.2561	0.2562	0.2218

Tabella 4.4.: Test 2: Error between final and desired configuration and evaluation of the cost functional for $\varepsilon = 0.01$

4.4. Test 3: A non-regular target

Here we consider a final configuration which is not-regular. Let us define the target as:

$$\bar{y}(x) = \begin{cases} x & x > 0 \\ 0 & x \leq 0. \end{cases}$$

The constant initial profile is $y_0(x) \equiv 0$ in (4.5) with $x \in [-1, 1]$. We compute the snapshots with a finite difference explicit scheme with a space step $\Delta x = 0.05$, time step $\Delta t = 0.01$ and velocity $u(x,t) = 0\chi_{x\leq 0} + x\chi_{x>0}$.
In this test the parameters for the value function are: $\Delta x = 0.1, \varepsilon = 0.01, \lambda = 1, U \equiv [0,3], b(x) = 0\chi_{x\leq 0} + x\chi_{x>0}$ (shape function), $\ell = 4$ (POD basis's rank) $\Delta\tau = 0.01$ (the time step to integrate the trajectories). The number of controls are 21 for the value function and for the trajectories. In Figure 4.5 we show the evolution of the controlled front where the final profile is steered close to the target. We also show the optimal control in Figure 4.6.

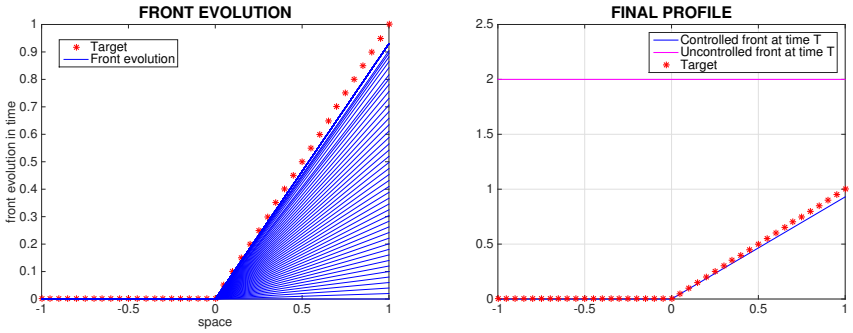

Figura 4.5.: Test 3: evolution of the front in the phase-plane with the target (left), final controlled and uncontrolled front's profile with the target (right) with $p = 2$.

In Table 4.6, as we did for the previous tests, we show the distance between the controlled solution and the desired configuration and the evaluation of the cost functional

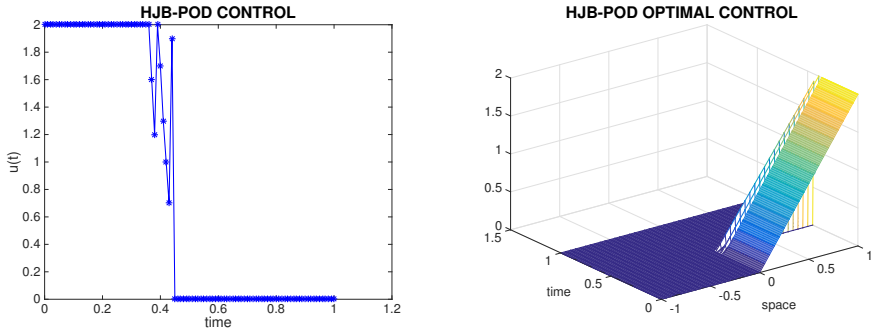

Figura 4.6.: Test 3: evolution of HJB-POD control in time $u(t)$ (left), evolution of hjb-pod control $u(x,t)$ (right)

for different choices of the norm in the cost functional. Despite the non-regularity of the target, we obtain satisfactory results. Here, we can see that the choice of $p = 1$ in the norm for the cost functional provides the most accurate final configuration, whereas both $p = 1$ and $p = 2$ provide a lower value for the cost functional.

	$p = 1$	$p = 2$	$p = \infty$
$\mathcal{E}_p$	0.0367	0.0419	0.0699
$J_p(y_0, u)$	0.0537	0.0537	0.1496

Tabella 4.6.: Error between final and desired configuration and evaluation of the cost functional for $\varepsilon = 0.01$

4.4.1. Test 4: A discountinuous target

Here we consider a final configuration which is less regular than the one presented before, since we have a jump. To this end, let us define

$$\bar{y}(x) := C_1 \chi_{[a,\overline{x}]}(x) + C_2 \chi_{[\overline{x},b]}(x). \tag{4.15}$$

The constant initial profile is $y_0(x) \equiv 0$ in (4.5) with $x \in [0, 1]$. We compute the snapshots with a finite difference explicit scheme with a space step $\Delta x = 0.05$, time step $\Delta t = 0.01$ and velocity $u(x,t) = C_1 \chi_{[0,\overline{x}]} + C_2 \chi_{[\overline{x},1]}$, with $C_1 = 0.5, C_2 = 0.8.\overline{x} = 0.5$.
In this test the parameters for the value function are: $\Delta x = 0.1, \varepsilon = 0.01, \lambda = 1, U \equiv [0, 3], b_1(x) = \chi_{[0,\overline{x}]}, b_2 = \chi_{[\overline{x},1]}$ (shape functions), $\ell = 4$ (POD basis's rank) $\Delta\tau = 0.01$ (the time step to integrate the trajectories). The number of controls are 16 for the value function and 31 for the trajectories.
In Figure 4.7 we show the evolution of the controlled front where the final profile is steered close to the target with $p = 2$.

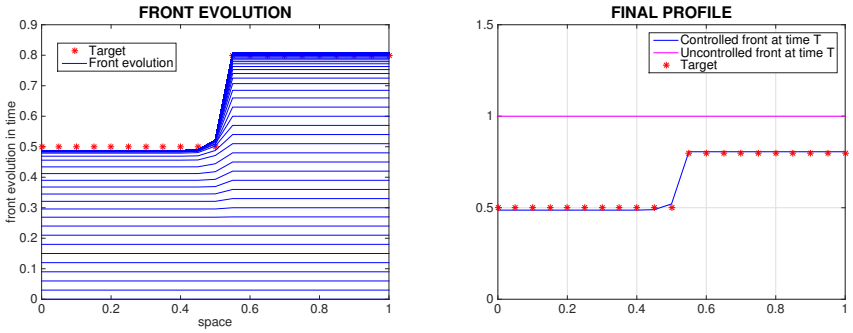

Figura 4.7.: Test 4: evoultion of the front in the phase-plane with the target (left), final controlled and uncontrolled front's profile with the target (right) with $p = 2$.

Then, the results with $p = 1, +\infty$ are displayed in Figure 4.8.

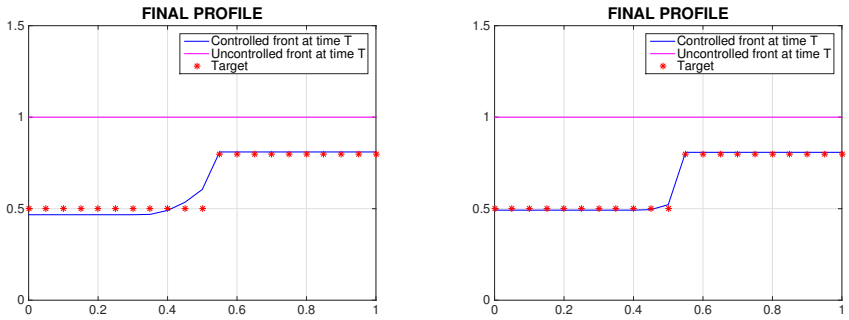

Figura 4.8.: Test 4: Final controlled and uncontrolled front's profile and target using the norm $p = 1$ (left) and the norm $p = \infty$ (right).

Finally, in Figure 4.9 we also show the optimal control.

An analysis of the distance between the controlled and desired configuration is provided in Table 4.9. In this example, we can see that the norm with $p = 2$ provides the most accurate solution for the final configuration and the cost functional.

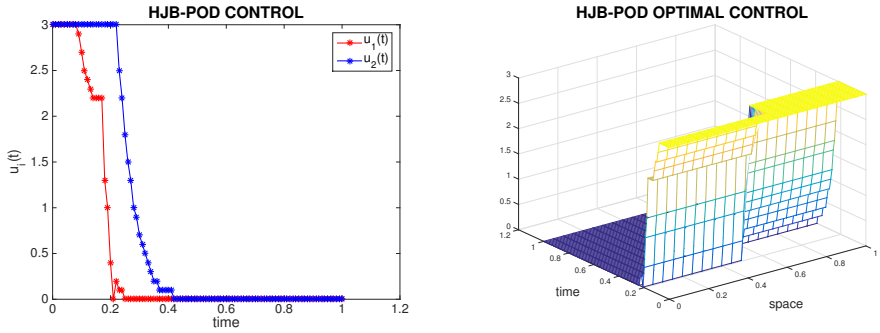

Figura 4.9.: Test 4: evolution of hjb-pod control in time $u(t)$ (left), evolution of hjb-pod control $u(x,t)$ (right).

	$p=1$	$p=2$	$p=\infty$
$\mathcal{E}_p$	0.0256	0.011	0.0218
$J_p(y_0,u)$	0.0382	0.0366	0.0568

Tabella 4.9.: Test 4: Error between final and desired configuration and evaluation of the cost functional with $\varepsilon = 0.01$.

4.4.2. Test 5: Experiments with uniform noise

In this test we deal with the two dynamics considered in Test 1 and Test 2 and we add noise to the optimal trajectory. Our goal is to show the efficiency of the feedback control, which is able to steer the solution to the target under some perturbations of the system. We remark that the value function in both cases is stored from the system without perturbation, but the reconstruction of the feedback control is affected by uniform noise $\eta(x)$ between $[-1,1]$ in every sampling time instances. In both cases we can observe that even under some disturbances, the feedback control is almost able to steer the solution to the target. As we did for the previous cases we computed the error tables for the tests with uniform noise (Table 4.10). If we compare the results obtained in this case with the results of Table (4.2 4.4) we can observe that the error and the evaluation of the cost functional are quite close despite the introduction of the noise.

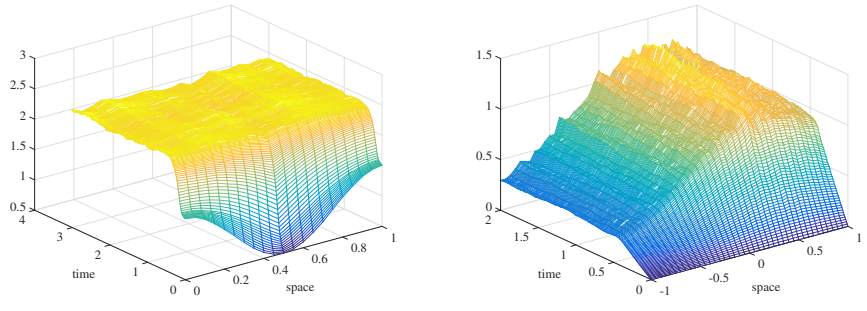

Figura 4.10.: Optimal HJB-POD state for Test 1 with $|\eta(x)| \leq 0.5\%$ at every 10 time step and for Test 2 with $|\eta(x)| \leq 1\%$ in every time step.

	$p = 1$	$p = 2$	$p = \infty$
$\mathcal{E}_p$	0.0374	0.1095	0.2425
$J_p(y_0, u)$	0.3388	0.3296	0.5897

Tabella 4.10.: Test 5: Error between final and desired configuration with different norms for Test 1 with noise $|\eta(x)| \leq 0.5\%$ at every 10 time step.

	$p = 1$	$p = 2$	$p = \infty$
$\mathcal{E}_p$	0.1078	0.0861	0.1559
$J_p(y_0, u)$	0.2550	0.2578	0.2274

Tabella 4.10.: Test 5:Error between final and desired configuration and evaluation of the cost functional with $\varepsilon = 0.01$ for Test 2 with noise $|\eta(x)| \leq 1\%$ in every time step.

Parte II.

Optimal Control in Biology

5. Overview of mathematical models for evolutionary dynamics in cancer cell populations

The evolutionary dynamics of cancer cell populations and their interaction with therapeutic agents are complex biological processes, which can be described in mathematical terms by means of different modelling approaches. The type of model depends on the representation scale which is selected. At the microscopic scale, cells in the population are seen as single individuals whose dynamics can be described in mathematical terms through the algorithmic rules of individual-based (IB) models. On the contrary, at the macroscopic scale, the cell population is seen as a whole and, in the absence of any spatial structure, the dynamics of observable quantities can be described in terms of ordinary differential equations (ODEs). Due to the very large number of biological elements at play in cancer cell populations, dealing with single individuals, as at the microscopic scale, can be mathematically unwieldy. On the other hand, the macroscopic description hides a number of relevant cell properties. Such limitations can be overcome by observing the dynamics of cell populations at the mesoscopic scale. At this scale, the state of the whole population is characterized by a suitable function, or a set of functions, describing the distribution of cells over the microscopic states, and macroscopic quantities are naturally recovered as successive moments of these functions. Models at the mesoscopic scale are stated in terms of partial differential equations (PDEs), where even integral terms can be included, which describe the evolution of this function, or these functions, on the basis of microscopic interactions. In this chapter we will provide a short summary of ODE models (Section 5.1) and PDE models (Section 5.2) that have been developed in the last years to study the evolutionary dynamics of cancer cell populations.

5.1. ODE Models

The first models of tumor growth were developed to reproduce and explain experimentally observed tumor growth curves and they are based on birth and death processes. These kinds of phenomena are described by general Lotka-Volterra equations

$$\frac{d}{dt}N(t) = N(t)\big(b(t) - d(t)\big), \qquad N(0) = N_0, \tag{5.1}$$

where $N(t)$ represents the total population density of cells, $b(t)$ is the birth rate and $d(t)$ the death rate. Access to nutrients and space availability control cell proliferation and death. For this reason, b and d are usually taken as nonlinear functions of N, leading to

the equation

$$\frac{d}{dt}N(t) = N(t)R\big(N(t)\big) \tag{5.2}$$

where R is the mass growth rate. Indicating by $r > 0$ the intrinsic birth rate in condition where nutrients and space are avalaible without limitations, R satisfies one of the two following conditions:

$$R(0) = r > 0, \quad R'(\cdot) < 0, \quad R(N) \to 0 \quad \text{as } N \to \infty \text{ (unlimited growth)}$$

$$R(0) = r > 0, \quad R'(\cdot) < 0, \quad R(K) = 0 \text{ for some } K > 0 \text{ (maximal tumor size).}$$

Several nonlinearities are proposed in the literature which satisfies one of these two conditions. The most common ones are the *logistic growth*, where

$$R(N) = r\left[1 - \left(\frac{N}{K}\right)^a\right], \qquad a > 0,\, K > 0$$

and the *Gompertz law*

$$R(N) = b\ln\left(\frac{N}{K}\right), \qquad 0 < N(0) < K. \tag{5.3}$$

These models take into account the possibile limitation of growth due to a lack of space resources, assuming that the instantaneous growth rate $\frac{1}{N}\frac{dN}{dt}$ depends on the carrying capacity of the environment K. Indipendently from the non-linearity appearing in $R(\cdot)$, it can be proven that the solutions of (5.1) are always monotonic. With these types of models, all cells are duplicating. This behavior is not realistic, since observations show that most of the cells are in a quiescent state and only a part of them is in proliferative state. Transitions between these two states depend on various environmental conditions such as space availability and nutrients. Starting from this observation, we distinguish between two states of cells: proliferative and quiescent. This leads to write the following model:

$$\begin{cases} \dot{P} = F(P) - bP + cQ \quad \text{(proliferative cells)} \\ \dot{Q} = bP - cQ - dQ \quad \text{(quiescent cells)} \end{cases} \tag{5.4}$$

with, for instance, a logistic growth

$$F(P) = rP\left(1 - \left(\frac{P}{K}\right)^a\right). \tag{5.5}$$

The size of the tumor is defined as

$$N(t) = P(t) + Q(t).$$

The coefficients $b > 0$ and $c > 0$ represent the transfer from one compartment to another and $d \geq 0$ is the death rate of quiescent cells. We remark that the dynamics (5.4) preserves positivity, *i.e.*,

$$P^0 > 0,\, Q^0 > 0 \Longrightarrow P(t) > 0, Q(t) > 0 \quad \forall t > 0.$$

Moreover the dynamics (5.4) is a "monotonic operator", which means

$$\dot{P}(t=0) > 0,\, \dot{Q}(t=0) > 0 \Rightarrow \dot{P}(t) > 0,\, \dot{Q}(t) > 0 \quad \forall t > 0.$$

An important observation is about the linear stability of the two steady states. In fact, for d small, the non-zero steady state is linearly stable, *i.e.*

$$\overline{P} = p_0 K, \quad p_0 = \left(1 - \frac{bd}{r(c+d)}\right)^{\frac{1}{a}} \qquad \overline{Q} = \frac{b}{c+d}\overline{P}. \tag{5.6}$$

The steady state $(0,0)$ is linearly unstable if $r > b$.

An important mathematical result concerning the global stability for this kind of ODE system is the following.

Theorem 5.1 *Assume $d = 0$. For $P(0) \geq 0, Q(0) \geq 0$ and $(P(0), Q(0)) \neq (0,0)$, the solution of the system (5.4)-(5.5) satisfies*

$$\lim_{t\to\infty} P(t) = K, \qquad \lim_{t\to\infty} Q(t) = \frac{b}{c}K.$$

The Gompertz law (5.3) for tumor growth has been extended in the angiogenesis framework by Hanfeldt *et al.* in [61]. They propose a two-variable model that includes a variable "carrying capacity" depending on access to nutrient. They obtain the following model:

$$\begin{cases} \dfrac{d}{dt}N(t) = bN(t)\ln\left(\dfrac{K(t)}{N(t)}\right) \\ \\ \dfrac{d}{dt}K(t) = cN(t) - (dN(t)^{2/3})K(t) \end{cases} \tag{5.7}$$

where the term $cN(t)$ takes into account the stimulation by VEGF (Vascular Endothelial Growth Factors emitted by the necrotic cells) and the negative term takes into account tumor surface *vs* tumor volume for the inhibition.
If we reduce the analysis to $N > 0$ and $K > 0$, the unique steady state is

$$\overline{N} = \overline{K} = \left(\frac{c}{d}\right)^{3/2}$$

Theorem 5.2 *If $N^0 > 0$ and $K^0 > 0$, then for all times $N(t) > 0$ and $K(t) > 0$. and $(N(t), K(t)) \to (\overline{N}, \overline{K})$ as $t \to \infty$.*

The interested reader can find the proofs of the previous results in [101] and in the reference therein.

5.1.1. ODE models with therapy

In this section we introduce the effects of the therapy in the model presented in the last section, and we see how it acts on the evolution of the tumor. It is usual to consider that the "effective concentration" of therapy $c(t)$ that is infused in a tumor acts as a death term. Using the equation (5.2), we can write

$$\frac{d}{dt}N(t) = N(t)R\big(N(t)\big) - c(t)N(t), \qquad N(0) = N_0 > 0. \tag{5.8}$$

We define "bolus" a therapeutic protocol which consists in giving the highest possible amount in a single dose and repeat injection in a periodic way

$$c_{\text{bolus}} := \sum_{k\geq 0} \delta(t - kT)C_M,$$

where C_M is the maximum dose allowed, due to side effects on healthy tissues. If we insert the bolus in our model, under suitable assumptions, we obtain the following

$$\begin{cases} \dfrac{d}{dt}\bar{N}(t) = \bar{N}(t)R(\bar{N}(t)), \qquad \bar{N}(0) = N_0, \\ \\ N(T^+) = N(T^-)e^{-C_M} \end{cases} \tag{5.9}$$

Theorem 5.3 *Assume that $R'(N) \leq 0$ in (5.8), then the bolus at time T (a certain degradation/elimination time) is an optimal therapy.*

Before introducing the therapy for the equation (5.4), we explain briefly which kind of drugs we can administer to the patient. We make a distinction between *cytotoxic* and *cytostatic* drugs, which acts differently on the cells. Cytotoxic drugs kill the proliferative cells while cytostatic drugs just block proliferation. If we denote by c_k and c_b the concentration of cytotoxic and cytostatic drugs, a simple option for introducing the drug in the model is the following:

$$\begin{cases} \dot{P} = F(P) - (b + c_b)P + cQ - c_kP \quad \text{(proliferative cells)} \\ \\ \dot{Q} = (b + c_b)P - cQ - dQ \quad \text{(quiescent cells)} \end{cases} \tag{5.10}$$

Choosing $a = 1$ to simplify the steady states (5.6), we observe that cytostatic drugs only increase the value of b and decrease the proliferative compartment, but increasing the number of quiescent cells. For $\frac{d}{r} \ll 1$, the total tumor size increases.
Cytotoxic drugs are always efficient because we find:

$$\bar{P} = K\left(1 - \frac{c_t}{r} - \frac{bd}{r(c+d)}\right) \bar{Q} = \frac{b}{c+d}\bar{P}, \quad \bar{N} = K\left(1 - \frac{c_t}{r} - \frac{bd}{r(c+d)}\right)\left(1 + \frac{b}{c+d}\right).$$

Finally, we remark that the ODE models assume large number of cells, the number of tumor cells can decrease exponentially fast, but cannot vanish exactly. The interested reader can find the proofs of the previous results in [101] and in the reference therein.

5.1.2. Optimal control for ODE models

After simulating the evolution of the disease and introducing the effects of treatment in (5.10) another big challenge is to study the effects of the drugs in the model and try to find the best way to administer the drugs minimizing an objective function. Optimization of cancer treatments can be represented as an optimal control problem on the controlled dynamical system. Before presenting some models, we will briefly discuss how the effects of different types of treatment can be included and which is the cost functional to minimize. Then, we will present examples of objective functions considered in the literature on cancer treatment.

Possible therapies and drugs

The first distinction to be made is between the type of therapy: chemotherapy and immunotherapy. Immunotherapy is a treatment based on the stimulation of the ability of the immune system to fight infection and disease. The therapy is thus any form of treatment that uses the body's natural abilities constituting the immune system to fight infection and disease or protecting the body from some of the side effects of treatment. On the other hand, chemotherapy is a category of cancer treatment that uses chemical substances, especially one or more anti-cancer drugs (chemotherapeutic agents) that are given as part of a standardized chemotherapy regimen. Focusing on the second kind of therapy, we have already introduced the distinction between cytotoxic and cytostatic drugs. Another important issue is how they enter in the dynamic of the tumor growth and in which sense they affect the tumor growth. Once the drugs are introduced in the system, their behavior can be modeled by a *pharmacokinetics* ODEs for their concentrations. Sometimes their behavior can also be represented by spatial PDEs with boundary conditions. In the framework of optimal control problems, there are also some constraints that arise due to the administration of drugs:

- **Toxicity constraints** A crucial issue in cancer treatment is due to the fact that drugs usually exert their effects not only on cancer cells, but also on healty cells. Obviously a simple way to reduce the size of the tumor is to administer a high dose of drug to the patient, who will consequently be exposed at high letal risk. To overcome this problem the idea is to put some constraints on the amount of drugs that can be delivered. We can set the upper bound on the maximum dose of drug allowed per day or on the total amount of drugs, or even on both of them. The drawback is that this kind of costraints does not take into account specificities of the patient's metabolism and response to the treatment. Often in chemotherapy optimization protocols the bang-bang controls are very interesting. These kind of controls are defined in a way that at each time we give either the minimum amount of drugs allowed (*i.e.*, zero) or the maximum.

- **Drug resistance** Another big issue we have to deal with when we administer drugs to the patient is the emergence of cells resistant to the treatment. A classical solution is to forbid too low drug concentrations that are supposed to create environmental conditions favorable to the development of drug resistant cell populations without killing them. Assuming that there exists a resistant cell population at the beginning of the treatment. Then, delivering high drug doses often produces the effect to kill all sensitive cells, giving a comparative fitness advantage to resistant cells, that subsequently become very hard to eradicate. The following strategy has been proposed at least in slowly developping cancers: trying to control the tumor growth by killing just some cancer cells and letting enough of these drug sensitive cancer cells to oppose by competition for space, the thriving resistant cells that are supposed to be less fit.

Introduction of the target

An optimization problem consists in maximizing or minimizing a given real-valued objective function modeling the objective we want to reach. In the framework of cancer treatment, the main purpose is to minimize the number of cancer cells. If we take into account the number of cancer cells directly, the objective function is the value of the coordinate of the state variable corresponding to the number of cancer cells at time T, where T can be fixed or controlled. We can also formulate the optimization problem as the minimization of the asymptotic growth rate of the cancer cell population.

Many models are based on the Gompertz law (5.3). Murray [89, 90] considers a two population Gompertz growth model with a loss term modeling the effect of the cytotoxic drug. He considers both tumor and normal cells, and the drug acts with exactly the same effectiveness on both normal and tumor cell populations. Murray's aim is to minimize the size of the tumor at the end of the treatment period maintaining a normal cell population above a lower level as a limit of toxicity. What happens is that the optimal drug dose is maximal at the beginning, so that the normal cell population is driven down to its lower level, and then the drug level is chosen in order to mantain the normal cell population there until the end of treatment. The number of tumor cells is always decreasing. In [83], Martin develops an optimal control model of cancer chemotherapy, where the aim is to reduce the size of the tumor after a fixed period of treatment has elapsed. Martin imposes a constraint so that the tumour size must decrease at or faster than a specified rate. What the author obtaines from the numerical simulations is that the best way of reducing the size of the tumor after a fixed period, is to keep the rate of decrease of the tumor size to a minimum initially and then give high-intensity treatment until the end of the time.

Ledzewicz *et al.* give a big contribution in the field of optimal control of ODE cancer

models. In [79], Ledzewicz *et al.* consider the following model:

$$\begin{cases} \dot{P} = -\xi P \ln\left(\dfrac{P}{Q}\right) - \phi P c_k \\ \\ \dot{Q} = bQ^{2/3} - dQ^{4/3} - \mu Q - \gamma c_b - \eta q c_k \end{cases} \tag{5.11}$$

where the coefficients ϕ, γ and η are non-negative constants that relate the dosages of respective agents to their effectiveness and c_b and c_k represent, respectively, the doses of anti-angiogenic drug and of cytotoxic drug. The optimal control problem considered by Ledzewicz *et al.* consists in minimizing the tumor cell mass under constraints on the amount of drug to be delivered. Mathematically, Ledzewicz *et al.* propose an optimal control problem with free terminal time T and constraints that limit the quantities for the agents to be given

$$\int_0^T c_b(t)dt \leq A \qquad \text{and} \qquad \int_0^T c_k(t)dt \leq B.$$

In [97], Panetta *et al.* propose the following model:

$$\begin{cases} \dot{P} = (\alpha - \mu - \eta)P + \beta Q \\ \dot{Q} = \mu P - (\beta + \gamma)Q \end{cases} \tag{5.12}$$

where P represents the proliferative cell mass and Q the quiescent mass, the parameteres are all constant positive and defined as follows: α is the proliferating growth rate, μ is the transition rate from proliferating to resting, η is the natural decay of proliferating cells, β is the transition rate from resting to proliferating, γ is the natural decay of resting cells. Adding a drug-induced death term in the equation on cycling cells, Panetta *et al.* investigated the effects on tumor growth of two kinds of periodic chemoterapies: a pulsed one and a piecewise continuous one. Starting from this model, some authors have determined optimal chemotherapy schedules [50, 78].
In [50], Fister *et al.* propose the following model:

$$\begin{cases} \dot{P} = (\alpha - \eta - \mu - sc(t))P + \beta Q, \quad P(0) = P_0 \\ \dot{Q} = \mu P - (\gamma + \beta)Q, \quad Q(0) = Q_0 \end{cases} \tag{5.13}$$

where all the constants are the same defined for the previous model and s is the effectiveness of the treatment. The cost functional to maximize is the following

$$J(c) = \int_0^T \left[a(P+Q) - \frac{b}{2}(1 - c(t))^2\right] dt, \qquad \text{with } a, b \in \mathbb{R}_+$$

The aim is to give as much drug as possible while not killing all healthy cells. Starting from [50], Ledzewicz *et al.* add to the model a pharmacokinetic equation modeling the time evolution of the drug's concentration in the body/plasma. Ledzewicz *et al.* propose

a bilinear system of the form

$$\dot{c} = -(f + ug) + hu \qquad c(0) = 0,$$

where u is the drug dosage ($u = 1$ maximal dose and $u = 0$ denotes no treatment), and f, g, h are positive constant parameters representing the dynamics for the drug concentration c in the plasma. While Panetta *et al.* in [50] use a quadratic cost functional to prove the existence and uniqueness of the control, Ledzewicz *et al.* [78], to be more realistic from a modeling perspective, decide to use an objective cost that is linear in the control:

$$J(c) = r_1 P(T) + r_2 Q(T) + \int_0^T [q_1 P(t) + q_2 Q(t) + bc(t)]\, dt,$$

with $r_1, r_2, q_1, q_2 \in \mathbb{R}_+$. They stress the fact that the choice of a quadratic control term in the objective undermines the negative effects of the drug. In fact, for example half of a dose is only measured as a quarter due to the prensence of the quadratic term in the cost. Such an optimal solution will have the tendency to give partial doses of the drug. Choosing a cost linear in the control does not provide such an incentive and leads to a bang-bang control which means treatment protocols that alternate between intervals when a full dose is given and intervals where no drugs are administered. In this cost functional appears also a term that tries to keep the number of healty cells high. Ledzewicz *et al.* also add a final term representing a weighted average of the total bone marrow at the end of an assumed fixed therapy interval $[0, T]$, in such a way they prevent that the bone marrow would be depleted too much towards the end of the therapy interval. Since the aim of the chemotherapy is to kill cancer cells, they also want to maximize the amount of drug given which acts against the maximization of bone marrow cells.

5.2. PDE Models

During the last fifty years, partial differential equations for populations structured by physiological traits have been extensively used to achieve a better understanding of a wide range of ecological phenomena [100, 102]. These equations describe population dynamics in terms of the evolution of population densities across phenotypic spaces, and can be derived from individual-based models through suitable asymptotic limits [30, 31, 33]. However, unlike IB models, which can be explored mainly through numerical simulations only, PDEs for populations structured by physiological traits make it possible to integrate numerical simulations with rigorous analysis, in order to achieve more robust biological conclusions.

A growing body of evidence indicates that cancer progression at the cellular level is, in essence, an evolutionary process [1, 41, 54, 69, 87, 93]. During cancer progression, novel phenotypic variants emerge via heritable changes in gene expression. Subsequently, phenotypic variants are subject to natural selection – they survive, reproduce, and die

– under the action of the tumour microenvironment and anti-cancer agents. The scenario is further complicated by cell-to-cell variability in gene expression, which gives rise to phenotypic differences between cancer cells of the same population. This phenotypic heterogeneity is a dynamic source of therapeutic resistance that needs to be accounted for when investigating effective anti-cancer therapeutic protocols [84]. Novel phenotypic variants in cancer cell populations originate mainly from mutations (*i.e.*, genetic modifications). However, novel phenotypic variants can also emerge due to epimutations (*i.e.*, heritable changes in gene expression that leave the sequence of bases in the DNA unaltered) [22, 53, 60, 91, 108]. For instance, recent experiments using fluorescent-activated cell sorting have demonstrated that non-genetic instability mediated by fluctuating protein levels allows cancer cells to reversibly transition between different phenotypic states [29, 103, 113]. Such non-genetic source of phenotypic variability has been increasingly recognised as integral to the development of resistance to cytotoxic agents in cancer cell populations [32, 66]. Moreover in the presence of the stress exerted by the drugs, cells are led to "actively" modify their phenotype state through a stress induced phenotypic variation in order to survive. For instance, in recent experiments on isogenetic cancer cell lines, it was observed that exposure to high doses of anti-cancer drugs can induce the emergence of a subpopulation of weakly-proliferative and drug-tolerant cells, that displays markers associated with cancer stem cells. After a period of time, some of the surviving cells were observed to change their phenotype to resume normal proliferation, and eventually repopulate the sample.

5.2.1. Natural selection

First of all, we present a simple integro-differential model in which the effects of phenotypic variations are not included. We indicate with $x \in \mathbb{R}^d$ the cells phenotypic state and with $n(x,t) \geq 0$ the population density of cancer cells (*i.e.*, the number of cells that at time t are in the phenotypic state x), so that the total number of cells at time t is computed as

$$\rho(t) = \int_{\mathbb{R}^d} n(x,t)\, \mathrm{d}x, \tag{5.14}$$

while the average phenotypic state at time t is computed as

$$\mu(t) = \frac{1}{\rho(t)} \int_{\mathbb{R}^d} x\, n(x,t)\, \mathrm{d}x. \tag{5.15}$$

The evolution of the cell population density $n(x,t)$ is described by the following equation:

$$\frac{\partial n}{\partial t}(x,t) = \underbrace{R\left(x, \rho(t), c(t)\right) n(x,t)}_{\text{natural selection}}. \tag{5.16}$$

Natural selection is driven by the function $R\big(x, \rho(t), c(t)\big)$, which represents the fitness of cancer cells in the phenotypic state x at the time t, given the total number of cells

$\rho(t)$ and the concentration of cytotoxic drug $c(t)$, and is defined as follows:

$$R\big(x, \rho(t), c(t)\big) := p(x) - \mu\rho(t) - k(x)c(t). \tag{5.17}$$

Definition (5.17) relies on the idea that a higher total number of cells corresponds to less avalaible resources. Therefore, we let cells inside the population die at rate $\mu\rho(t)$, where the parameter $\mu > 0$ models the rate of death due to intrapopulation competition. The function $p(x)$ stands for the net proliferation rate of cancer cells in the phenotypic state x, while the function $k(x)$ is the rate of death caused by the cytotoxic drug.

5.2.2. Natural selection and random phenotypic variations

To reduce biological complexity to its essence, we make the *prima facie* assumption that random epimutations yield infinitesimally small phenotypic modifications. Therefore, we model the effects of phenotypic variations through a diffusion operator. We consider the following model:

$$\frac{\partial n}{\partial t}(x,t) = \underbrace{R\left(x, \rho(t), c(t)\right) n(x,t)}_{\text{natural selection}} + \underbrace{\beta \Delta n(x,t)}_{\text{random variations}} \quad . \tag{5.18}$$

where the diffusion coefficient $\beta > 0$ stands for the rate of epimutation of cancer cells, which is assumed to be constant. Focusing on a one-dimensional case and considering R in the form (5.17), Lorenzi *et al.* [75] assume that the phenotypic state $x = 1$ corresponds to the highest level of cytotoxic-drug resistance and let the function k be strictly convex with minimum in $x = 1$. Furthermore, because the death rate of cancer cells will increase as the concentration of the cytotoxic drug increases, the same authors assume that k is an increasing function of c. On the other hand, under the assumption that the phenotypic state $x = 0$ corresponds to the highest level of proliferative potential when there are no cytotoxic drugs (*i.e.*, when $c(\cdot) = 0$), Lorenzi *et al.* let the function p be a strictly concave function with maximum in $x = 0$. The convexity and concavity assumptions, on p and k, respectively, lead naturally to smooth fitness landscapes which are close to the approximate fitness landscapes inferred from experimental data through regression techniques (see for instance, [96] and references therein). In the same paper the authors demonstrate that higer doses of cytotoxic drugs reduce the size of cancer cell populations at the cost of promoting the selection of more resistant phenotypic variants.

5.2.3. Natural selection, random and stressed induced phenotypic variations

In this section we present a class of models which takes into account also the effect of stress induced variations through a drift term. Models belonging to this class read as:

$$\frac{\partial n}{\partial t}(x,t) + \underbrace{\nabla \cdot [v(x, c(t))n(x,t)]}_{\text{stress-induced variations}} = \underbrace{R(x, \rho(t), c(t))n(x,t)}_{\text{natural selection}} + \underbrace{\beta \Delta n(x,t)}_{\text{random variations}} \quad . \tag{5.19}$$

where v represents the rate at which cells in the phenotypic state x undergo phenotypic variations in response to the drug (*i.e.*, v is the rate of stress induced phenotypic variations). The dependence of v on the concentration of cytotoxic drugs $c(t)$ accounts for the fact that the rate of stress-induced phenotypic variations depends on the level of stress exerted by the cells' local environment. In fact, a higher concentration of drug will exert more stress on the cell population, and will thus increase the rate of stress-induced phenotypic variations. In [35], Chisholm *et al.* focus on a two-dimensional case and set $x = (x_1, x_2)$ with x_1 being the normalized expression levels of the survival-potential and x_2 the proliferation-potential traits. The outcomes of the model suggest that selection, random phenotypic variations, stress-induced variations and the interplay between these mechanisms can push an actively proliferating cell population into a weakly-proliferative phenotype, due to selection pressure and phenotypic fluctuations. Moreover, in the paper the authors highlight how the transient appearance of the weakly proliferative and drug-tolerant cells is related to the use of high-dose therapy.

5.2.4. Mathematical formalization of natural selection in cancer cell populations

In the mathematical framework of equation (5.16), the dynamics of cancer cells in the limit of many generations can be characterized by rescaling the time line with respect to a small parameter $\varepsilon > 0$ to obtain

$$\varepsilon \frac{\partial n_\varepsilon}{\partial t}(x,t) = R(x, \rho_\varepsilon(t), c_\varepsilon(t)) n_\varepsilon(x,t) \tag{5.20}$$

and then studying the behaviour of the population density $n_\varepsilon(x,t)$ in the limit $\varepsilon \to 0$. Under the same time rescaling, noting that

- phenotypic variations are less frequent than proliferation and death events
- stress-induced phenotypic variations occur on a timescale which is faster than that of random phenotypic variations,

equations (5.18) and (5.19) can be rewritten, respectivelly, as

$$\varepsilon \frac{\partial n_\varepsilon}{\partial t}(x,t) = R(x, \rho_\varepsilon(t), c_\varepsilon(t)) n_\varepsilon(x,t) + \varepsilon^2 \Delta n_\varepsilon(x,t) \tag{5.21}$$

and

$$\varepsilon \frac{\partial n_\varepsilon}{\partial t}(x,t) + \varepsilon \nabla_x \cdot (v(x) n_\varepsilon(x,t)) = R(x, \rho_\varepsilon(t), c_\varepsilon(t)) n_\varepsilon(x,t) + \varepsilon^2 \Delta n_\varepsilon(x,t). \tag{5.22}$$

In the case in which the concentration of cytotoxic drug is kept constant over time, say $c_\varepsilon(t) \equiv C$ with $C \geq 0$, under assumptions which are biologically relevant, the solutions of the above equations are expected to concentrate as sums of weighted Dirac masses [34, 82]. From a biological point of view, the positions of the Dirac masses (*i.e.*, the

concentration points) can be understood as the fittest phenotypic states within the cancer cell population, whilst the weights identify the proportions of cells in these states. Therefore, analysing the evolution of the concentration points and the related weights is equivalent to describing evolutionary dynamics. The mathematical interest lies in the fact that it is far from obvious how the concentration points and the weights evolve. This problem can be solved by using a Hamilton-Jacobi approach [34, 82], that is, recasting the original problem in terms of a constrained Hamilton-Jacobi equation that characterizes the dynamics of the concentration points and the related weights.

5.2.5. Optimal control for PDE models

We have seen that in the field of optimal control theory for ODE models a lot of theory is available and in many cases an analytical study can be done, also for most of the biological models. Unfortunately, when we switch to the PDE case things are much more complicated. In general, solving optimization problems subject to constraints given in terms of partial differential equations with additional constraints on the controls and/or states is one of the most challenging problem in the context of industrial, medical and economical applications. In recent years, new tools have been developed to deal with optimal control problems in high dimension (see for instance the book by Lions [80] or by Hinze *et al.* [63]). Optimization problems with PDE-constraints are posed in infinite dimensional spaces. Therefore, functional analytic techniques, function space theory, as well as existence and uniqueness results for the underlying PDE are essential to study the existence of optimal solutions and to derive optimality conditions. In particular in [80] a detailed analysis of control systems governed by elliptic, parabolic and hyperbolic PDEs can be found. The book of Hinze *et al.* [63] is mostly focused on the optimization methods available.
The PDE model considered in the next chapter is much more complicated due to the presence of the integral in the equation (leading to an integro-differential equation). Therefore, in our case it is difficult to carry out a rigorous analysis and this is the reason why we decided to focus on the numerical approach.

6. Optimal dosing schedules in cancer cell populations

6.1. Methods

In this chapter we study evolutionary dynamics in a well-mixed population of cancer cells that is structured by the expression level $y \in \mathbb{R}_+$ of a gene which is linked to both the cellular levels of cytotoxic-drug resistance and proliferative potential – such as ALDH1, CD44, CD117 or MDR1 [62, 86]. In the line of Pisco and Huang [104], we assume that there is a level of expression y^H which endows cells with the highest level of cytotoxic-drug resistance, and a level of expression $y^L < y^H$ conferring the highest proliferative potential when there are no xenobiotic agents. In this framework, we characterise the phenotypic state of each cell by means of the variable $x \in \mathbb{R}$ with

$$x = \frac{y - y^L}{y^H - y^L},$$

so that the state $x = 1$ corresponds to the highest level of cytotoxic-drug resistance, while the state $x = 0$ corresponds to the highest level of proliferative potential in the absence of xenobiotic agents.

Cells inside the population proliferate or die, compete for limited resources, and undergo variation in phenotype due to random epimutation events. Furthermore, a cytotoxic drug can be present, which acts by increasing the death rate of cancer cells. The function $n(x,t) \geq 0$ stands for the population density, so that the total number of cells at time t is computed as

$$\rho(t) = \int_{\mathbb{R}} n(x,t)\ \mathrm{d}x, \tag{6.1}$$

while the average phenotypic state and the related variance at time t are computed, respectively, as

$$\mu(t) = \frac{1}{\rho(t)} \int_{\mathbb{R}} x\ n(x,t)\ \mathrm{d}x, \qquad \sigma^2(t) = \frac{1}{\rho(t)} \int_{\mathbb{R}} x^2\ n(x,t)\ \mathrm{d}x - \mu(t)^2. \tag{6.2}$$

In this mathematical framework, the function $\sigma^2(t)$ provides a measure of the level of intrapopulation heterogeneity at time t. Also, since the phenotypic state $x = 0$ corresponds to the highest level of proliferative potential in the absence of xenobiotic agents and the phenotypic state $x = 1$ corresponds to the highest level of cytotoxic-drug resistance, we expect the value of $\mu(t)$ to be between 0 and 1. Hence, the function $\mu(t)$ provides a measure of the average level of resistance to the cytotoxic drug at time t.

Finally, we introduce the function $c(t) \geq 0$ to model the instantaneous concentration of cytotoxic drug.

6.1.1. The model

We describe the evolution of the cell population density $n(x,t)$ by means of the following phenotype-structured PDE

$$\frac{\partial n}{\partial t}(x,t) = \underbrace{\beta \, \frac{\partial^2 n}{\partial x^2}(x,t)}_{\substack{\text{non-genetic} \\ \text{instability}}} + \underbrace{R\left(x, \rho(t), c(t)\right) n(x,t)}_{\text{natural selection}}, \tag{6.3}$$

which we complete with the boundary conditions

$$n(x,\cdot) \to 0 \quad \text{and} \quad \frac{\partial^q n}{\partial x^q}(x,\cdot) \to 0 \text{ for all } q \in \mathbb{N} \quad \text{as } |x| \to \infty \tag{6.4}$$

and the initial condition

$$n(x,0) \in L^1 \cap L^\infty(\mathbb{R}), \quad n(x,0) > 0 \text{ a.e. on } \Omega \subset \mathbb{R}. \tag{6.5}$$

In the above equation, Ω is a compact subset of $\mathbb{R}$. Eq. (6.3) relies on the assumptions and the modelling strategies presented in the following subsections.

Mathematical modelling of non-genetic instability

To reduce biological complexity to its essence, we make the *prima facie* assumption that random epimutations yield infinitesimally small phenotypic modifications. Therefore, we model the effects of non-genetic instability through a diffusion operator. The diffusion coefficient $\beta > 0$ in Eq.(6.3) stands for the rate of epimutation of cancer cells, which is assumed to be constant.

Mathematical modelling of natural selection

Natural selection is driven here by the function $R\big(x, \rho(t), c(t)\big)$, which represents the fitness of cancer cells in the phenotypic state x at the time t, given the total number of cells $\rho(t)$ and the concentration of cytotoxic drug $c(t)$. In the following we make use of the following definition:

$$R\big(x, \rho(t), c(t)\big) := p(x) - d\rho(t) - k(x, c(t)). \tag{6.6}$$

Definition (6.6) relies on the idea that a higher total number of cells corresponds to less available resources; therefore, we let cells inside the population die at rate $d\rho(t)$, where the parameter $d > 0$ models the rate of death due to intrapopulation competition. The function $p(x)$ stands for the net proliferation rate of cancer cells in the phenotypic state x, while the function $k(x, c(t))$ is the rate of death caused by the cytotoxic drug. Since

the phenotypic state $x = 1$ corresponds to the highest level of cytotoxic-drug resistance, we assume that the function k is strictly convex with minimum in $x = 1$. Furthermore, because the death rate of cancer cells will increase as the concentration of the cytotoxic drug increases, we assume that k is an increasing function of c. On the other hand, to take into account the fact that the phenotypic state $x = 0$ corresponds to the highest level of proliferative potential when there are no xenobiotic agents (*i.e.*, when $c(t) = 0$), we assume that p is a strictly concave function with maximum in $x = 0$. In this setting, we follow the modelling strategies presented in [75, 81] and define the functions p and k as:

$$p(x) := \gamma - \eta\, x^2, \qquad k(x; c) := c(t)\, (x - 1)^2. \tag{6.7}$$

In the above definitions, the parameter $\gamma > 0$ corresponds to the maximum fitness of cancer cells, and the non-linear selection gradient $\eta > 0$ provides a measure of the strength of natural selection in the absence of xenobiotic agents.

6.1.2. Cost functional and optimal control problem

If we define t_f as the final time of the anti-cancer treatment, achieving this goal is equivalent, in the framework of our model, to find a control function $c \in L^\infty(0, t_f)$ which minimize the following cost functional:

$$J := \frac{\alpha_1}{t_f} \int_0^{t_f} \frac{\rho(t)}{K}\, \mathrm{d}t + \frac{\alpha_2}{t_f} \int_0^{t_f} \mu(t)\, \mathrm{d}t, \qquad \alpha_1, \alpha_2 \in [0, 1]. \tag{6.8}$$

and it satisfies the constraints:

$$0 \leq c(t) \leq C_1 \quad \text{and} \quad \int_0^{t_f} c(t)\, \mathrm{d}t \leq C_2 \tag{6.9}$$

In the definition (6.8), the first term accounts for the normalised average number of cancer cells inside the population during the time interval $[0, t_f]$, whereas the second term considers the related average level of resistance. The population size $\rho(t)$ is divided by the parameter K, which stands for the carrying capacity of the cell population in the absence of xenobiotic agents and without epimutations (*i.e.*, when $c(\cdot) = 0$ and $\beta = 0$), to have the same order of magnitude of $\mu(t)$ (as we expect the value of $0 \leq \mu(t) \leq 1$). The weights α_1 and α_2 are used to identify different biological scenarios. For instance, the choice $\alpha_1 = 1$ and $\alpha_2 = 0$ reproduces the case where, not being concerned at all about the emergence of cytotoxic-drug resistance, we look for dosing schedules which minimise the average size of the cancer cell population as much as possible.

6.1.3. Model parametrisation and setup of numerical simulations

We numerically solve the mathematical problem defined by completing equation (6.3) with boundary conditions (6.4) and the following initial condition

$$n(x,0) = n^0(x) := a_0 e^{-b_0 x^2} \quad \text{with } a_0 \; s.t. \quad \int_\Omega n^0(x)\,\mathrm{d}x < K, \tag{6.10}$$

where $\Omega \subset \mathbb{R}$. The above definition represents an initial population mainly composed of cells in the phenotypic state $x = 0$. Numerical computations are performed in MATLAB. We select a uniform discretisation consisting of 500 points on the interval $\Omega \equiv [-5, 5]$ as the computational domain. The method for calculating numerical solutions is based on a time splitting scheme between the conservative part and the reaction term. As for the conservative part, we approximate the diffusion term through a three-point explicit scheme, while we use an implicit finite difference scheme for the reaction term.

Numerical scheme for equation (6.3)

We discretize the intervals Ω and $[0, T]$, respectively, with a constant space step dx and time step dt

$$\begin{cases} x_j = x_0 + j\,dx & j = 0, ..., M \\ t_i = t_0 + i\,dt & i = 0, ..., N \end{cases} \tag{6.11}$$

where M is the number of nodes in the space grid, while N the number of nodes in the time grid. We denote with $n_j(t) := n(x_j, t)$ and $R_j(\rho(t), c(t)) := R(x_j, \rho(t), c(t))$, respectively, the solution and the natural selection term evaluated in the point x_j at time t. We obtain the following system of ODE (on the points $1, ..., M-1$ since we know the value of the solution on the boundary):

$$n_j'(t) = \beta \frac{n_{j-1}(t) - 2n_j(t) + n_{j+1}(t)}{dx^2} + \big[R_j(\rho(t), c(t))\big] n_j(t), \qquad j = 2, ..., M-1.$$

We use the implicit Euler scheme, so denoting with $n_j^i = n(x_j, t_i)$ and $R_j^i := R(x_j, \rho(t_i), c(t_i))$, we obtain for $i = 0, ..., N-1$ the fully discrete scheme:

$$n_j^{i+1} = n_j^i + \beta\lambda\big[n_{j-1}^{i+1} - 2n_j^{i+1} + n_{j+1}^{i+1}\big] + dt\, n_j^{i+1} R_j^{i+1} \qquad \text{with } \lambda := \frac{dt}{dx^2}.$$

So, at each iteration we have to solve the following linear system:

$$-\lambda\beta n_{j-1}^{i+1} + \Big(1 + 2\lambda\beta - dt R_j^{i+1}\Big) n_j^{i+1} - \lambda\beta n_{j+1}^{i+1} = n_j^i,$$

which written in matrix form becomes:

$$\begin{pmatrix} 1 & 1 & 0 & 0 & 0 & 0 \\ -\beta\lambda & 1 - dtR_j^{i+1} + 2\beta\lambda & -\beta\lambda & 0 & 0 & 0 \\ 0 & \ddots & \ddots & \ddots & 0 & 0 \\ 0 & 0 & 0 & -\beta\lambda & 1 - dtR_j^{i+1} + 2\beta\lambda & -\beta\lambda \\ 0 & 0 & 0 & 0 & 1 & 1 \end{pmatrix} \begin{pmatrix} n_0 \\ n_1 \\ \vdots \\ n_{M-1} \\ n_M \end{pmatrix} = \begin{pmatrix} 0 \\ n_1^i \\ \vdots \\ n_{M-1}^i \\ 0 \end{pmatrix}.$$

For all simulations, we set the time step $dt = 0.1$. Concerning the solution of the ODE system (6.33), we make the following choice for the initial conditions: we set the density equal to the equilibrium value, $r_0 = (\gamma - \sqrt{\beta\eta})/d$, $\mu_0 = 0$ and $f_0 = \eta$. We approximate the system with an explicit Euler scheme with a time step such that it ensures numerical stability to the scheme (*i.e.*, $dt = 0.01, 0.005$ for different cases). We set the maximum fitness $\gamma = 0.66$, so that the doubling time of cells in the highly proliferative state $x = 0$ is about 25 hours (*cf.* data in [119]). Furthermore, the *in vitro* experiments presented in [103] on the phenotypic evolution of HL60 leukemic cells exposed to vincristine have shown that, in absence of xenobiotic agents, highly cytotoxic-drug resistant cells take approximatively 18 days to accomplish the repopulation of the equilibrium cell distribution observed without xenobiotic agents. Also, according to the same experiments, the ratio between the proliferation rate of the cells with the highest level of cytotoxic-drug resistance and the proliferation rate of the cells with the highest proliferative potential is equal to 5. Therefore, we choose the non-linear selection gradient η and the rate epimutation β to be such that, when $c(\cdot) = 0$, it takes approximatively 18 days for an initial population mainly composed of cells in the phenotypic state $x = 1$ to reconstitute the equilibrium phenotypic distribution corresponding to $c(\cdot) = 0$, with the value of η constrained by the condition $p(x = 0)/p(x = 1) = 5$. Moreover, in agreement with previous reports [20, 21], we define the average rate of death due to intrapopulation competition as $d := \gamma/K$, so that the equilibrium value of the total number of cells in the absence of xenobiotic agents and without epimutation (*i.e.*, when $c(\cdot) = 0$ and $\beta = 0$) is equal to the carrying capacity $K = 10^8$. Based on these considerations, we perform numerical simulations using the parameter values listed in Table 6.0. Finally, the concentration of cytotoxic drug is expressed in terms of the LC_a – *i.e.*, the constant value of c that is required to reduce the equilibrium value of the total number of cells by $a\%$.

Tabella 6.0.: Values of the parameters used to perform numerical simulations.

Parameter	Biological meaning	Value
γ	Maximum fitness	0.66 per day
η	Selection gradient	0.132 per day
d	Rate of death due to intrapopulation competition	0.66×10^{-8} per day
β	Rate of epimutation	0.001 per day

Concerning the optimal control problem, we use a method based on the interior-

point algorithm available within the FMINCON routine of the MATLAB OPTIMISATION TOOLBOX. We perform the simulation in a time window of 60 days and we divide the interval $[0, t_f]$ in sub-intervals T_i composed by 7 days. In each period we alternate four days of therapy with three days of rest. This is done imposing an L^∞ constraint on the control variable:

$$\begin{cases} 0 \leq c(t) \leq C_1 & \text{at day } 1,2,3,4 \text{ of each } T_i \\ c(t) = 0 & \text{elsewhere} \end{cases} \tag{6.12}$$

Moreover we impose an L^1-constraint on each interval, *i.e.*:

$$\int_{T_i} c(t)\, \mathrm{d}t \leq C_2. \tag{6.13}$$

In order to use a meaningful value for the constant C_1 and C_2, we compute the LC and we set $C_1 = C_2 = LC_a$. We tested the code for different choices of LC (from $LC20$ to $LC80$). We remark that from a numerical point of view, it is natural to introduce an upper bound, whereas the biological meaning of these constraints are the following: the L^∞-bound represents the maximum dose avaiable that we can administer to the patient, while the L^1-bound is the total amount of drugs allowed in each period.

6.2. Results and discussion

In this section we analyse the cell dynamics under the action of different infusion of cytotoxic drug. In the first two sub-section we briefly present the results estabilished in [75], while in the last sub-section we perform an analysis in the most general case.

6.2.1. Cell dynamics in the absence of cytotoxic drug

In the framework of our model, the total number of cells $\rho(t)$, the average phenotypic state $\mu(t)$ and the level of intrapopulation heterogeneity $\sigma^2(t)$ are computed according to equations (6.1)-(6.2). Then, in the absence of xenobiotic agents (*i.e.*, when $c(\cdot) = 0$), a complete characterisation of the cancer cell population at equilibrium is provided by the following theorem:

Theorem 6.1 *Let $c(\cdot) = 0$, and denote by $\overline{n}(x)$ the equilibrium population density for $c(\cdot) = 0$. Then:*

(i) if $\gamma - (\beta\eta)^{1/2} \leq 0$,

$$\rho(t) \to 0, \qquad \text{as } t \to \infty; \tag{6.14}$$

(ii) if $\gamma - (\beta\eta)^{1/2} > 0$,

$$\rho(t) \to \overline{\rho} = \frac{1}{d}\Big[\gamma - (\beta\eta)^{1/2}\Big], \qquad \text{as } t \to \infty \tag{6.15}$$

and

$$\overline{n}(x) = \overline{\rho}\,\frac{(\eta/\beta)^{1/4}}{(2\pi)^{1/2}}\exp\Big[-\frac{1}{2}\Big(\frac{\eta}{\beta}\Big)^{1/2}x^2\Big], \tag{6.16}$$

so that

$$\mu(t) \to \overline{\mu} = 0 \quad \textit{and} \quad \sigma^2(t) \to \overline{\sigma}^2 = \sqrt{\frac{\beta}{\eta}}, \qquad \textit{as } t \to \infty. \tag{6.17}$$

Proof 6.1 *When $c(\cdot) = 0$, plugging definitions* (6.6)-(6.7) *into equation* (6.3) *we obtain*

$$\frac{\partial n}{\partial t}(x,t) = \beta\,\frac{\partial^2 n}{\partial x^2}(x,t) + \Big[\gamma - \eta\,x^2 - d\,\rho(t)\Big]\,n(x,t). \tag{6.18}$$

The proof of Theorem 1 follows from a more general analysis developed in [33, 81], and it uses the results established by the following two lemmas:

Lemma 6.1 *If $\gamma > (\beta\eta)^{1/2}$, the problem defined by completing* (6.18) *with* (6.4)-(6.5) *admits a unique non-negative nontrivial equilibrium solution $\overline{n}(x)$ which is given by* (6.16).

Proof of Lemma 6.1. *Consider the PDE problem*

$$\begin{cases} \beta\,\overline{n}''(x) + \Big[\gamma - \eta\,x^2 - d\,\overline{\rho}\Big]\,\overline{n}(x) = 0, \qquad x \in \mathbb{R}, \\ \\ \overline{\rho} = \displaystyle\int_{\mathbb{R}} \overline{n}(x)\,dx. \end{cases} \tag{6.19}$$

Writing

$$\overline{n}(x) = Y(z), \qquad z = \Big(\frac{4\eta}{\beta}\Big)^{1/4}x,$$

we find that $Y(z)$ satisfies the differential equation

$$Y''(z) - \Big(\frac{z^2}{4} + a\Big)Y(z) = 0, \tag{6.20}$$

with

$$a = \frac{d}{2(\beta\eta)^{1/2}}\Big(\overline{\rho} - \frac{\gamma}{d}\Big).$$

It is known that equation (6.20) *has solutions that are bounded for all z if and only if $a = -m - 1/2$, where m is a non-negative integer [88, 120]. These bounded solutions are the Gaussians $\exp(-z^2/4)$ multiplied by polynomials of degree m, which form an orthogonal set of functions, and so are everywhere non-negative if and only if $m = 0$. Therefore, the existence of a nontrivial non-negative solution of the PDE problem* (6.19) *requires $a = -1/2$. This implies that to have a nontrivial non-negative equilibrium solution the condition*

$$\overline{\rho} = \frac{1}{d}\Big[\gamma - (\beta\eta)^{1/2}\Big]$$

must be satisfied. If this condition is met, for some $A \in \mathbb{R}_+$

$$\overline{n}(x) = A \exp\Big\{-\frac{1}{2}\Big(\frac{\eta}{\beta}\Big)^{1/2} x^2\Big\}. \tag{6.21}$$

The constant A *can be evaluated in terms of* $\overline{\rho}$ *by integrating equation* (6.21)*. We find that*

$$\overline{n}(x) = \overline{\rho}\, \frac{(\eta/\beta)^{1/4}}{(2\pi)^{1/2}} \exp\Big\{-\frac{1}{2}\Big(\frac{\eta}{\beta}\Big)^{1/2} x^2\Big\},$$

and this concludes the proof of Lemma 6.1.

□

Lemma 6.2 *The integral* $\rho(t)$ *of the solution of the problem defined by completing* (6.18) *with* (6.4)-(6.5) *has the following long-time behaviour:*

$$\lim_{t\to\infty} \rho(t) = \begin{cases} \dfrac{1}{d}\Big[\gamma - (\beta\eta)^{1/2}\Big] & \text{if} \quad \gamma > (\eta\beta)^{1/2}, \\ \\ 0 & \text{if} \quad \gamma \le (\eta\beta)^{1/2}. \end{cases} \tag{6.22}$$

Proof of Lemma 6.2. *Following the method of proof that we presented in [33], it is possible to prove that, for all non-negative initial conditions* $n(x,0)$ *such that* $0 < \rho(0) < \infty$*,*

$$\rho(t) = \frac{g(t)\rho(0)}{g(0) + d\ \rho(0) \int_0^t g(\tau)\ d\tau},$$

with the function $g(t)$ *satisfying*

$$g(t) \sim \frac{2\beta}{(2\pi)^{1/2}} \int_0^\infty \exp\Big[-\frac{z^2}{4}\Big(\frac{4\eta}{\beta}\Big)^{1/4} z\Big]\ dz \exp\Big\{\Big[\gamma - (\beta\eta)^{1/2}\Big]t\Big\}, \quad \text{as } t \to \infty.$$

In the limit $t \to \infty$*:*

- *if* $\gamma < (\beta\eta)^{1/2}$*, then* $g(t) \to 0$ *exponentially rapidly;*

- *if* $\gamma = (\beta\eta)^{1/2}$*, then* $g(t)$ *converges to a positive constant;*

- *if* $\gamma > (\beta\eta)^{1/2}$*, then* $g(t) \to \infty$ *exponentially rapidly.*

Therefore:

- *if* $\gamma < (\beta\eta)^{1/2}$*, then* $\lim_{t\to\infty} \rho(t) = 0$*;*

- *if* $\gamma = (\beta\eta)^{1/2}$, *then* $\lim_{t\to\infty} \rho(t) = 0$;

- *if* $\gamma > (\beta\eta)^{1/2}$, *then* $\lim_{t\to\infty} \rho(t) = \frac{1}{d}\Big[\gamma - (\beta\eta)^{1/2}\Big]$.

This concludes the proof of Lemma 6.2.

□

Taken together, Lemma 6.1 and Lemma 6.2 allow to reach the following conclusions:

(i) if $c(\cdot) = 0$ *and* $\gamma - (\beta\eta)^{1/2} \leq 0$, *then*

$$\rho(t) \to 0, \qquad \text{as } t \to \infty; \tag{6.23}$$

(ii) if $c(\cdot) = 0$ *and* $\gamma - (\beta\eta)^{1/2} > 0$, *then*

$$\rho(t) \to \overline{\rho} = \frac{1}{d}\Big[\gamma - (\beta\eta)^{1/2}\Big], \qquad \text{as } t \to \infty$$

and

$$\overline{n}(x) = \overline{\rho}\,\frac{(\eta/\beta)^{1/4}}{(2\pi)^{1/2}} \exp\Big[-\frac{1}{2}\Big(\frac{\eta}{\beta}\Big)^{1/2} x^2\Big].$$

This establishes the claims of Theorem 6.1.

6.2.2. Cell dynamics under the action of constant cytotoxic drug

In the case where the drug concentration is $c(\cdot) = C$ a complete characterisation of the cancer cell population at equilibrium is provided by the following theorem:

Theorem 6.2 *Let* $c(\cdot) = C > 0$ *define*

$$\gamma_c := \gamma - \frac{\eta\, C}{\eta + C}, \qquad \eta_c := \eta + C, \tag{6.24}$$

and denote by $\overline{n}_c(x)$ *the equilibrium population density for* $c(\cdot) = C$. *Then:*

(i) if $\gamma_c - (\beta\eta_c)^{1/2} \leq 0$,

$$\rho(t) \to 0, \qquad \text{as } t \to \infty; \tag{6.25}$$

(ii) if $\gamma_c - (\beta\eta_c)^{1/2} > 0$,

$$\rho(t) \to \overline{\rho}_c = \frac{1}{d}\Big[\gamma_c - (\beta\eta_c)^{1/2}\Big], \qquad as\ t \to \infty \tag{6.26}$$

and

$$\overline{n}_c(x) = \overline{\rho}_c\ \frac{(\eta_c/\beta)^{1/4}}{(2\pi)^{1/2}} \exp\Big\{-\frac{1}{2}\Big(\frac{\eta_c}{\beta}\Big)^{1/2}\big[x - \overline{x}_c\big]^2\Big\}, \tag{6.27}$$

with

$$\overline{x}_c := \frac{C}{\eta + C}, \tag{6.28}$$

so that

$$\mu(t) \to \overline{\mu}_c = \overline{x}_c \quad and \quad \sigma^2(t) \to \overline{\sigma}_c^2 = \sqrt{\frac{\beta}{\eta_c}}, \qquad as\ t \to \infty. \tag{6.29}$$

The proof of Theorem 6.2 follows the method of proof of Theorem 6.1.

Proof 6.2 *When* $c(\cdot) = C > 0$, *plugging definitions* (6.6)-(6.7) *into equation* (6.3) *we obtain*

$$\frac{\partial n}{\partial t}(x,t) = \beta\ \frac{\partial^2 n}{\partial x^2}(x,t) + \Big[\gamma - \eta\ x^2 - d\ \rho(t) - C\ (x-1)^2\Big]\ n(x,t).$$

Defining

$$\gamma_c := \gamma - \frac{\eta\ C}{\eta + C}, \qquad \eta_c := \eta + C \quad and \quad \overline{x}_c := \frac{C}{\eta + C},$$

we can rewrite the above equation as

$$\frac{\partial n}{\partial t}(x,t) = \beta\ \frac{\partial^2 n}{\partial x^2}(x,t) + \Big[\gamma_c - \eta_c\ (x - \overline{x}_c)^2 - d\ \rho(t)\Big]\ n(x,t). \tag{6.30}$$

Since $x \in \mathbb{R}$, *there is no loss of generality in translating coordinates so that* $\overline{x}_c = 0$. *Hence, to adapt the method of proof of Theorem 6.1 to prove Theorem 6.2 is purely technical. For this reason, we do not give further details.*

6.2.3. Cell dynamics under the action of time dependent cytotoxic drug

We consider the general case in which the cytotoxic drug $c(t)$ is a generic function of time. Substituting the definitions (6.6) and (6.7) into equation (6.3) and defining

$$\gamma_c(t) := \gamma - \frac{\eta\ c(t)}{\eta + c(t)}, \quad \eta_c(t) := \eta + c(t) \quad \text{and} \quad \varphi_c(t) := \frac{c(t)}{\eta + c(t)},$$

we can rewrite equation (6.3) as

$$\frac{\partial n}{\partial t}(x,t) = \Big[\gamma_c(t) - \eta_c(t)\ (x - \varphi_c(t))^2 - d\ \rho(t)\Big]\ n(x,t) + \beta\ \frac{\partial^2 n}{\partial x^2}(x,t). \tag{6.31}$$

In this setting, a characterisation of the phenotypic evolution of the cancer cell population is provided by the following proposition, whose proof relies on a suitable generalisation of the method of proof that has been used in a recent paper [81]:

Proposition 6.1 *The problem defined by equations* (6.3), (6.4), (6.5) *admits solutions of the form*

$$n(x,t) = \frac{\varrho(t)}{\sqrt{2\pi}}\Big(\frac{f(t)}{\beta}\Big)^{1/4}\exp\Big\{-\frac{1}{2}\Big(\frac{f(t)}{\beta}\Big)^{1/2}\big[x-\mu(t)\big]^2\Big\}, \tag{6.32}$$

where $\rho(t)$, $\mu(t)$ *and* $f(t)$ *satisfies the following system of ODEs*

$$\begin{cases} f'(t) = 4[\beta f(t)]^{1/2}\big[\eta_c(t) - f(t)\big], \\ \\ \mu'(t) = 2\Big[\dfrac{\beta}{f(t)}\Big]^{1/2}\eta_c(t)\big[\varphi_c(t)-\mu(t)\big], \\ \\ \dfrac{\rho'(t)}{\rho(t)} = Q(t) - d\rho(t), \\ \\ Q(t) := \gamma_c(t) - \eta_c(t)\,\Big[\varphi_c(t)-\mu(t)\Big]^2 - \eta_c(t)\Big[\dfrac{\beta}{f(t)}\Big]^{1/2}. \end{cases} \tag{6.33}$$

Proof 6.3 *We introduce the following trial solution:*

$$\mathcal{N}(x,t) = \frac{\varrho(t)}{\sqrt{\pi}}\Big(\frac{f(t)}{4\beta}\Big)^{1/4}\exp\Big\{-\Big(\frac{f(t)}{4\beta}\Big)^{1/2}\big[x-\mu(t)\big]^2\Big\}, \tag{6.34}$$

with

$$\rho(t) = \int_{\mathbb{R}}\mathcal{N}(x,t)\,\mathrm{d}x \quad \textit{and} \quad \mu(t) = \frac{1}{\rho(t)}\int_{\mathbb{R}} x\,\mathcal{N}(x,t)\,\mathrm{d}x.$$

Since

$$\log[\mathcal{N}] = \log[\varrho(t)] + \frac{1}{4}\,\log\Big[\frac{f(t)}{4\beta}\Big] - \Big(\frac{f(t)}{4\beta}\Big)^{1/2}\big[x-\mu(t)\big]^2 + \textit{constant},$$

it follows that

$$\begin{aligned} \frac{1}{\mathcal{N}}\frac{\partial\mathcal{N}}{\partial t} &= \frac{\varrho_i'(t)}{\varrho(t)} + \frac{1}{4}\frac{f'(t)}{f(t)} - \frac{1}{4}\frac{f'(t)}{\sqrt{\beta f(t)}}\big[x-\mu(t)\big]^2 - \Big(\frac{f(t)}{\beta}\Big)^{1/2}\big[x-\mu(t)\big]\mu'(t) \\ \frac{1}{\mathcal{N}}\frac{\partial\mathcal{N}}{\partial x} &= -\Big(\frac{f(t)}{\beta}\Big)^{1/2}\big[x-\mu(t)\big], \\ \frac{1}{\mathcal{N}}\frac{\partial^2\mathcal{N}}{\partial x^2} &= -\Big(\frac{f(t)}{\beta}\Big)^{1/2} + \frac{f(t)}{\beta}\big[x-\mu(t)\big]^2. \end{aligned}$$

Hence, substituting $\mathcal{N}(x,t)$ to Eq. (6.31) as a trial solution, we require the following equation to hold as an identity:

$$\frac{\varrho'(t)}{\varrho(t)} + \frac{1}{4}\frac{f'(t)}{f(t)} - \frac{1}{4}\frac{f'(t)}{\sqrt{\beta f(t)}}\big[x-\mu(t)\big]^2 - \Big(\frac{f(t)}{\beta}\Big)^{1/2}\big[x-\mu(t)\big]\mu'(t) = \\ \beta\Big\{-\Big(\frac{f(t)}{\beta}\Big)^{1/2} + \frac{f(t)}{\beta}\big[x-\mu_i(t)\big]^2\Big\} + \gamma_c(t) - \eta_c(t)\big[x-\varphi_c(t)\big]^2 - d\varrho(t).$$

If we expand both sides in powers of x, then the coefficients of the terms in x^2, x^1 and x^0, respectively, give us three differential equations:

$$\begin{cases} f'(t) = 4\eta_c(t)\big[\beta f(t)\big]^{1/2} - 4\beta^{1/2}\big[f(t)\big]^{3/2} \\ \mu'(t) = 2\eta_c\Big[\dfrac{\beta}{f(t)}\Big]^{1/2}\varphi_c(t) - \dfrac{1}{2}\dfrac{f'(t)}{f(t)}\mu(t) - 2[\beta f(t)]^{1/2}\mu(t) \\ \qquad = 2\Big[\dfrac{\beta}{f(t)}\Big]^{1/2}\eta_c(t)\big[\varphi_c(t)-\mu(t)\big] \\ \dfrac{\rho'(t)}{\rho(t)} = Q(t) - d\rho(t) \end{cases} \tag{6.35}$$

The results of Proposition 6.1 are illustrated by the plots of Figure (6.1) and Figure (6.2).

6.3. Optimal dosing schedules

In this section we present the results of numerical simulations obtained by minimizing the cost functional (6.8) under the constraints on the control variable given by (6.12), (6.13). We want to study the reaction of the tumor cells to different protocols in a fixed time window of 60 days (approximately two months of treatment). We remark that with the choice of the constraints on the control variable made there are two possible "extreme" strategies: giving to the patient the maximum dose allowed concentrated in one day, or spread the amount of drugs during the whole period. In the following, we will analyze how the optimal protocol changes if in the cost functional we give more importance to a term with the respect to the other (*i.e.* we tested different values of α_1 and α_2). In a therapy it is reasonable to alternate periods in which we administer a certain amount of drugs with periods of rest. For this reason in our simluations we alternate 4 days of therapy with 3 days of rest (as we point out in the previous section each period T_i is composed of 7 days); we start giving the therapy on day $1, 8, 15, 22, 29, 36, 43, 50, 57$. In the figures below we show the results of our tests. We remark that we do not observe any meaningful change in the shape of the control varying the values of the LC from $LC40$ to $LC80$ in (6.12),(6.13). So, in the following, we present the results obtained choosing

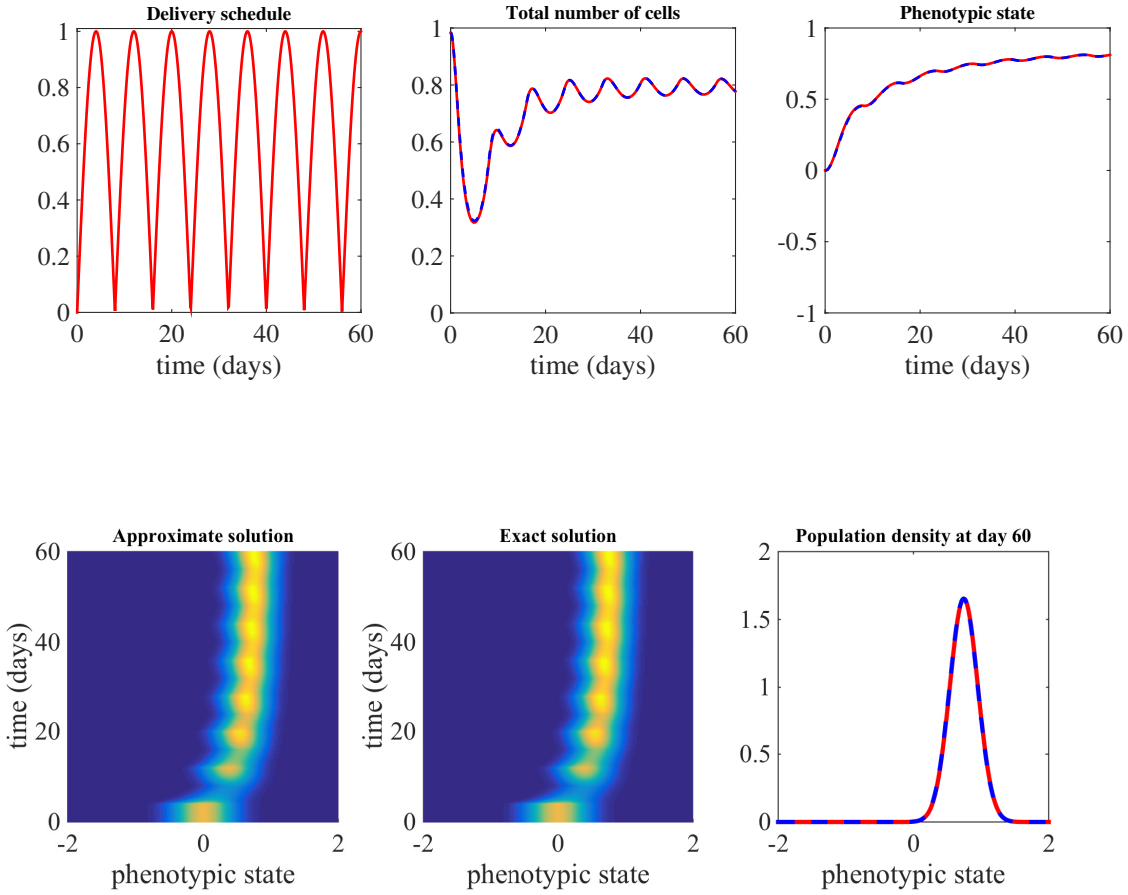

Figura 6.1.: Top row: dosing schedule (left); dynamics of the corresponding total number of cells $\rho(t)$ (middle); dynamics of the corresponding average phenotypic state $\mu(t)$ (right). The red line correspond to the exact solution obtained solving numerically the system (6.33), while the blu dashed line refers to the numerical solution of the PDE (6.3). Bottom line: evolution of the cells population $n(t, x)$ in space and time numerically solving the PDE (6.3) (left), the same plot, but solving numerically the system of ODEs (6.33), distribution of the population density at the last day (right). The red line is the exact solution computed solving the system (6.33), while the blu dashed line refers to the numerical solution of the PDE (6.3).

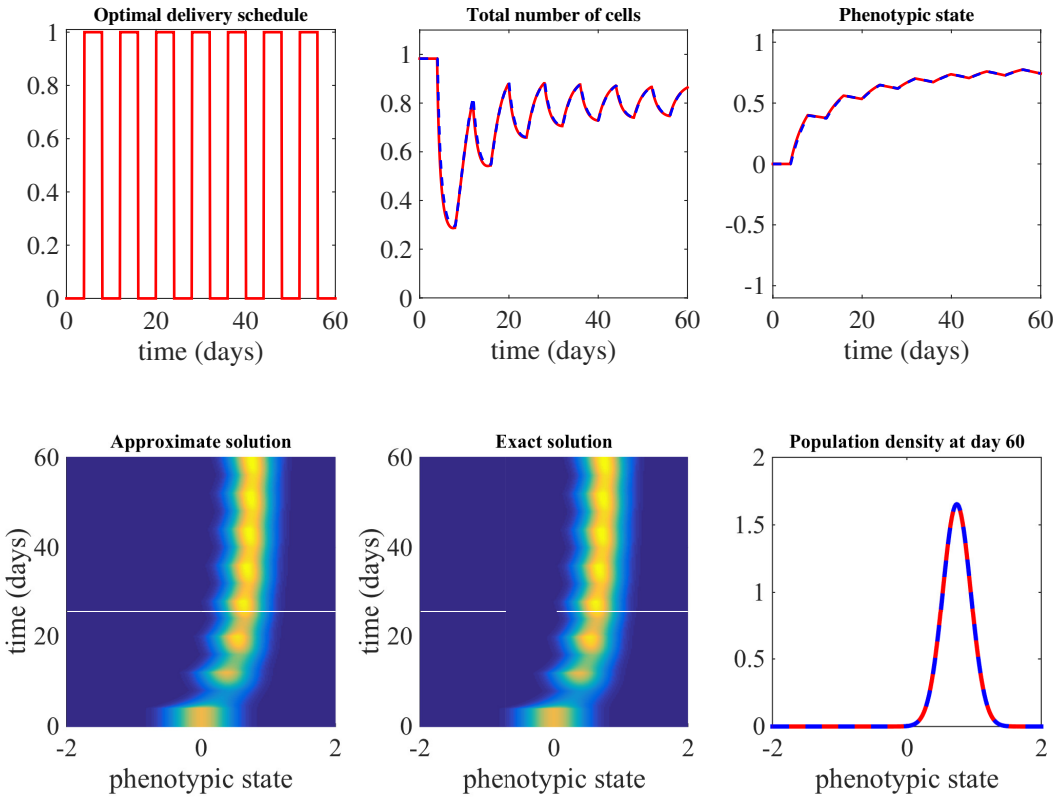

Figura 6.2.: Top row: dosing schedule (left); dynamics of the corresponding total number of cells $\rho(t)$ (middle); dynamics of the corresponding average phenotypic state $\mu(t)$ (right). The red line correspond to the exact solution obtained solving numerically the system (6.33), while the blu dashed line refers to the numerical solution of the PDE (6.3). Bottom line: evolution of the cells population $n(t, x)$ in space and time numerically solving the PDE (6.3) (left), the same plot, but solving numerically the system of ODEs (6.33), distribution of the population density at the last day (right). The red line is the exact solution computed solving the system (6.33), while the blu dashed line refers to the numerical solution of the PDE (6.3).

$C_1 = C_2 = LC80$ in (6.12),(6.13). We remark that in the simulations we consider a small diffusion term ($\beta = 10^{-3}$).

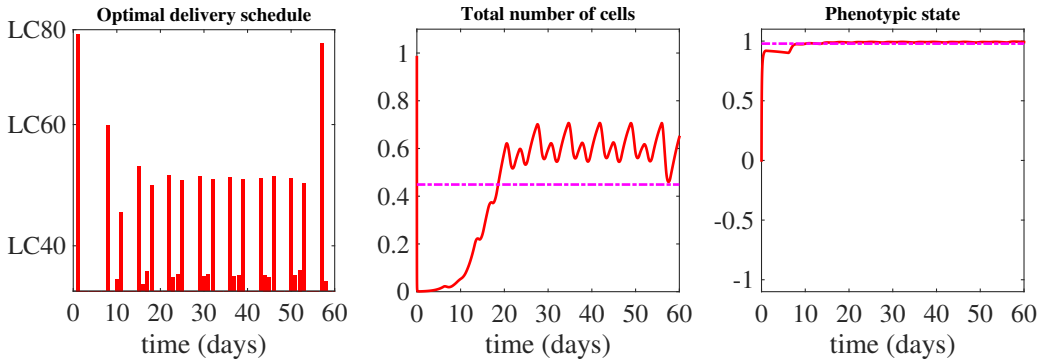

Figura 6.3.: Sample dynamics of the optimal dosing schedule (left), normalized total number of cells, with the corresponding average in time (middle) and phenotypic state with the corresponding average in time (right) for $\alpha_1 = 1$ and $\alpha_2 = 0$. The values of the constant C_1 and C_2 in equations (6.9) correspond to the LC80 dose. The results are obtained solving the optimal control problem associated to the ODE system (6.33).

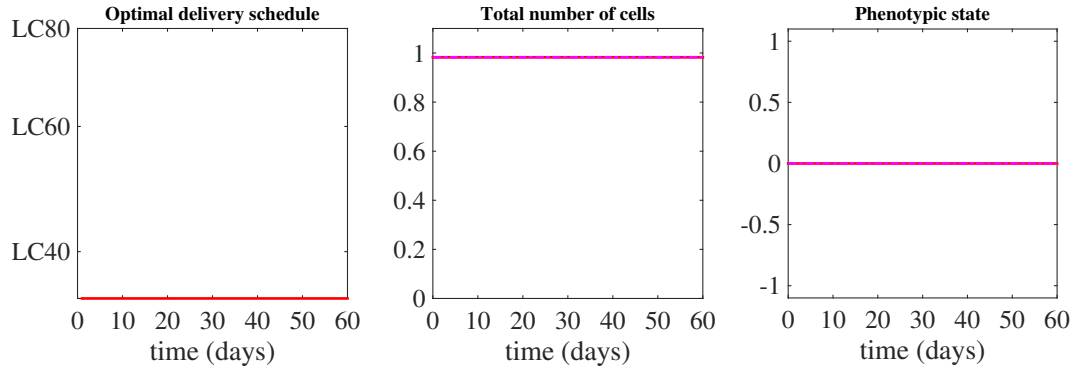

Figura 6.4.: Sample dynamics of the optimal dosing schedule (left), normalized total number of cells, with the corresponding average in time (middle) and phenotypic state with the corresponding average in time (right) for $\alpha_1 = 0$ and $\alpha_2 = 1$. The values of the constant C_1 and C_2 in equations (6.9) correspond to the LC80 dose. The results are obtained solving the optimal control problem associated to the ODE system (6.33).

Firstly, we consider the case where we want penalize only the density and we do not care at all about what happens to the resistance, which means taking $\alpha_1 = 1$ and

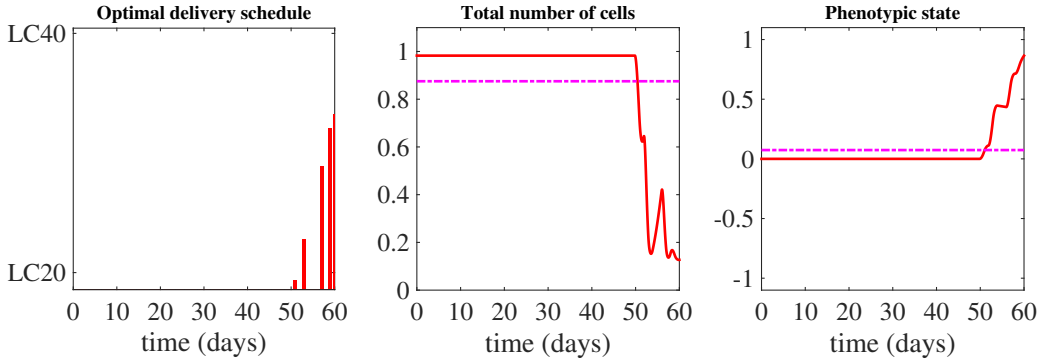

Figura 6.5.: Sample dynamics of the optimal dosing schedule (left), normalized total number of cells, with the corresponding average in time (middle) and phenotypic state with the corresponding average in time (right) for $\alpha_1 = 1$ and $\alpha_2 = 1$. The values of the constant C_1 and C_2 in equations (6.9) correspond to the LC80 dose. The results are obtained solving the optimal control problem associated to the ODE system (6.33).

$\alpha_2 = 0$. Looking at the control (Figure 6.3 left panel) we observe that we saturate the L^1 bound in each interval, but the L^∞ one just in the first day; the best strategy is to spread the treatment in 4 days instead of giving all the drugs in one day. Concerning the corresponding density (Figure 6.3 middle panel) we observe a significant decay in the first day, which corresponds to the peak of the control, followed by an increase. Looking at the average density, which is the quantity we are minimizing, is one-half of the one we had at the beginning. As we expected, the corresponding resistance (Figure 6.3 right panel) starts increasing from the beginning and remains high (close to 1) for the whole period. We observe that we have a second peak in the control in the last time interval, but this does not lead to a significant decay of the density. This is due to the fact that the resistance plays an opposite role and it affects the efficiency of the drug.
If we look at the opposite scenario, taking $\alpha_1 = 0$ and $\alpha_2 = 1$, the best strategy is not giving drugs at all (left panel Figure 6.4). This is reasonable since we do not want to increase the resistance and we do not have a term in the cost that penalize the increase of the density. As a consequence, the resistance remains equal to zero, while the density remains constant at the equilibrium level $\bar{\rho}$ (central and right panel of Figure 6.4). The last case we consider is the one where we give the same weight to the two terms in the integral, $\alpha_1 = \alpha_2 = 1$. In this case we want minimize both the density and the average resistance. The optimal strategy is waiting until the last interval and then giving some control (left panel Figure 6.5). As a consequence, the density is high for a long period and at the end it decreases drastically (central panel Figure 6.5). Looking at the average density, we observe that the value is lower than the one we had at the beginning. The corresponding resistance remains low almost until the end and then it increases; we remark that, even if the value of the resistance at the end is high, the average resistance

is low (magenta line in right panel Figure 6.5). With this choice of parameters we have a good compromise: we have a reduction of the average density of 10.92% and we have an increase of the average resistance of 7.39%. These simulations have been done solving the optimal control problem associated to the system of ODEs (6.33). We remark that we obtain the same results solving the optimal control problem for the PDE (6.3) with a huge difference in the CPU time. In fact when we solve the ODEs system, we have a reduction of the CPU time of $98,87\%$. This results is reasonable, since solving a system of three ODEs is faster and less expensive than solving an optimal control problem for a PDE. In fact, what we do in the second case is the following: we discretize the PDE in time and we obtain an high dimensional system of semidiscrete ODEs, then we use the same numerical optimization technique of the first case.
It is worth to present also the case where we consider a low concentration of cytotoxic drug as upper bound; we present the results with the $LC20$ (we obtain the same results for the $LC30$). When we consider $\alpha_1 = 0, \alpha_3 = 1$, the results are the same that in all cases: for not increasing the resistance, it is better not to give drugs at all. Concerning the case where we penalize both density and resistance, *i.e.*, $\alpha_1 = \alpha_2 = 1$, we observe that the optimal strategy is to administer therapy in the last two periods (Figure 6.6 left panel). We remark also that the control saturates the L^1-bound in both periods. The interesting case is $\alpha_1 = 1$, $\alpha_2 = 0$: the optimal therapy is the same in all the periods: we have 9 peaks (left panel Figure 6.7) and again we saturate the L^1 bound in each period. Since the total amount of drug we are allowed to inject to the patient is low, it is not surprising that we have an average reduction of density of 4.84%. We also observe that the peaks in the control leads to an oscillatory behaviour in the density (Figure 6.7 central panel).

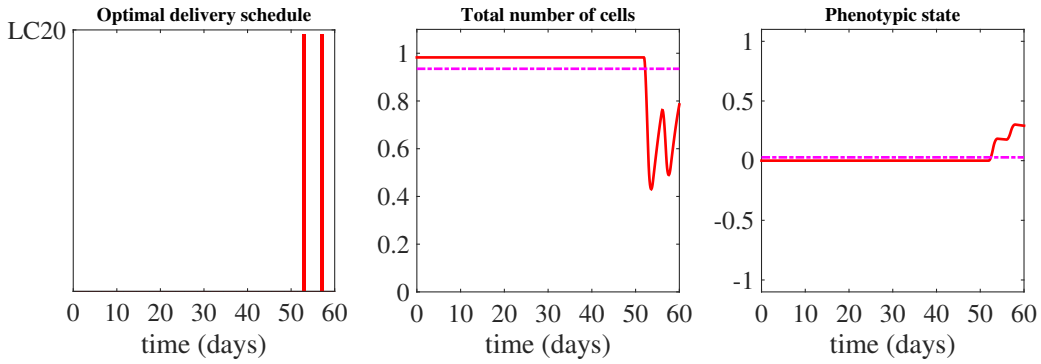

Figura 6.6.: Sample dynamics of the optimal dosing schedule (left), normalized total number of cells, with the corresponding average in time (middle) and phenotypic state with the corresponding average in time (right) for $\alpha_1 = 1$ and $\alpha_2 = 1$. The values of the constant C_1 and C_2 in equations (6.9) correspond to the LC20 dose. The results are obtained solving the optimal control problem associated to the ODE system (6.33).

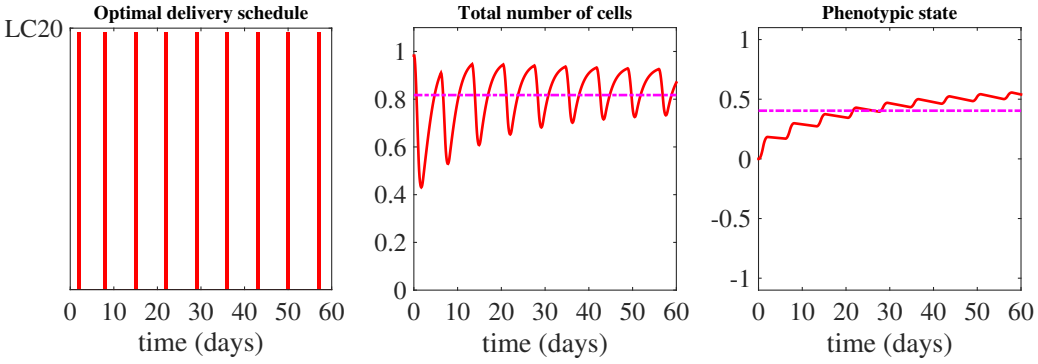

Figura 6.7.: Sample dynamics of the optimal dosing schedule (left), normalized total number of cells, with the corresponding average in time (middle) and phenotypic state with the corresponding average in time (right) for $\alpha_1 = 1$ and $\alpha_2 = 0$. The values of the constant C_1 and C_2 in equations (6.9) correspond to the LC20 dose. The results are obtained solving the optimal control problem associated to the ODE system (6.33).

The difference of the optimal protocol in the case of the $LC20$ and $LC80$ for the case with $\alpha_1 = 1, \alpha_2 = 0$, it can be explained as follows: when we have a low concentration of drugs is better to administer to the patient all in one day. On the other side, in the second case, since we have a huge quantity of drug, it is better to spread it in the interval, in order to have a sudden decrease of the density and to mantain it at a lower level as well.

Finally, in the last test (Figure (6.8)) we removed the days of rest from the therapy and we put an L^1-bound on periods of 7 days. We observe that the optimal strategy is to "spread" the therapy over the whole interval instead of giving peaks of maximum therapy. We have a substantial reduction of the density, since the average value is less than half we had at the beginning. On the other side it is natural that the resistance starts increasing from the beginning and remains high for the whole interval.

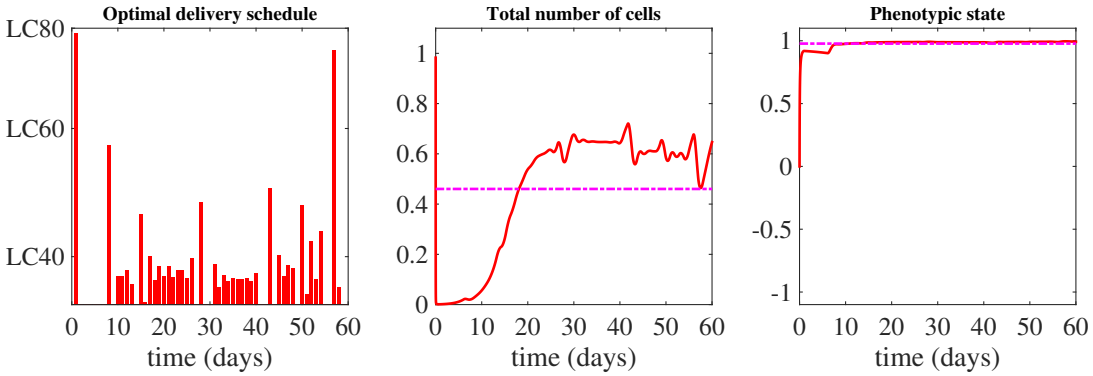

Figura 6.8.: Sample dynamics of the optimal dosing schedule (left), normalized total number of cells, with the corresponding average in time (middle) and phenotypic state with the corresponding average in time (right) for $\alpha_1 = 1$ and $\alpha_2 = 0$. The value of the constant C_1 in equation (6.9) correspond to the LC80 dose. The results are obtained solving the optimal control problem associated to the ODE system (6.33).

7. Conclusions and future directions

In Chapter 3 we have proposed a local version of the dynamic programming approach for the solution of the infinite horizon problem, showing that the coupling between MPC and DP methods can produce accurate results. The coupling improves the original guess obtained by the MPC method and allows to save memory allocations and CPU time with respect to the global solution computed via Hamilton-Jacobi equations. There are two future developments: on one side, it could be interesting investigating the role played by the discount factor λ in MPC (*e.g.* economic MPC), since the theory of MPC is developped for quadratic cost functional without discount factor. Moreover, from the simulation made, it is clear that in most of the cases when we have a discount factor, especially when $\lambda = 1$, the MPC solver does not converge to the optimal solution. On the other side, we do not use a particular criteria to choose the radius of the tube ρ (*i.e.* the restricted domain built around a reference trajectory in which we solve the Bellman equation). This choice can be made rigourous using some a-posteriori error estimates on the control obtained via MPC (*e.g.* using the result in [124]).
Moreover, in Chapter 4 we have proposed a HJB-POD approach for the control of a nonlinear hyperbolic problem that typically has weak solutions in the viscosity sense. This problem is more difficult with respect to other evolutive problems, such as parabolic equations, where the regularity of the initial condition is preserved or even improved. Therefore, it is not trivial that POD model order reduction with a few number of basis functions provide a satisfactory approximation of the model. Indeed, numerical simulations show that if we represent the front with a POD-basis with rank 4 or 5 we obtain satisfactory results.
Furthermore, we have investigated different norms in the cost functional, motivated by the lack of general theory particularly for nonlinear dynamics. It turns out that the best approximation is obtained using the standard L^2 norm in most of the cases.
The computation of the basis functions remains an open question that definitely deserves further investigation. We will try to extend the results in [6] to build theoretical results in a future work.
Finally, in Chapter 6 we have proposed a model dealing with the optimal control of an evolutionary dynamics of cancer cells population. We have presented the model and we have given a complete characterisation of the cancer cell population at the equilibrium in two particular cases: in the absence of cytotoxic drugs and under the action of constant cytotoxic drugs. For the most general case, with a general time-dependent drug we have shown that the solution can be expressed by means of three functions which are the solutions of an ODE system. Finally we have investigated numerically the optimal dosing protocol for different weights in the cost functional where we have penalized both the density and the emergence of resistant cells.

List of Algorithms

Bibliografia

[1] C.A. Aktipis, A.M. Boddy, R.A. Gatenby, C.C. Maley, *Life history trad-offs in cancer evolution,* Nat. Rev. Cancer **13 (12)**, 883-92 (2013).

[2] A. Alla and M. Falcone, *An adaptive POD approximation method for the control of advection-diffusion equations*, in K. Kunisch, K. Bredies, C. Clason, G. von Winckel, (eds) *Control and Optimization with PDE Constraints,* International Series of Numerical Mathematics, **164**, Birkhäuser, Basel, 1-17 (2013).

[3] A.Alla, G.Fabrini, M.Falcone, *Coupling MPC and DP methods for an efficient solution of optimal control problems.* to appear in Conference Proceedings of IFIP 2015.

[4] A.Alla, G.Fabrini, M.Falcone *A HJB-POD approach to the control of the level set equation.* submitted to Conference Proceedings of Model Reduction of Parametrized Systems III (MoRePas III).

[5] A. Alla, M. Falcone and D. Kalise. *An Efficient Policy Iteration Algorithm for Dynamic Programming Equations*, SIAM J. Sci. Comput. **37**, no. 1, 181-200 (2015).

[6] A. Alla, M. Falcone and S. Volkwein. *Error Analysis for POD approximations of infinite horizon problems via the dynamic programming principle.* Submitted to SIAM Journal on Control and Optimization, 2015.

[7] A. Alla, A. Schmidt, B. Haasdonk. *Model order reduction approaches for infinite horizon optimal control problems via the HJB equation* to appear in Conference Proceedings of MoRePas III, 2016.

[8] F. Allgöwer, H. Chen, *A quasi-infinite horizon nonlinear model predictive control scheme with guaranteed stability,* Automatica, **34**, 1205-1217 (1998).

[9] F. Allgöwer, R. Findeisen, Z.K. Nagy, *Nonlinear Model Predictive Control: From Theory to Application,* J. Chin. Inst. Chem. Engrs., **35**, 299-315 (2004).

[10] K. Alton, I. M. Mitchell, *An ordered upwind method with precomputed stencil and monotone node acceptance for solving static convex Hamilton-Jacobi equations,* J. Sci. Comput., **51**, 313–348, (2012).

[11] A.R. Anderson, V. Quaranta, *Integrative mathematical oncolgy.* Nat. Rev. Cancer **8**, 227-234 (2008).

[12] A.C. Antoulas, *Approximation of large-scale Dynamical Systems,* SIAM, Philadelphia, 2005.

[13] M. Bardi, M. Falcone, *An approximation scheme for the minimum time function,* SIAM J. Control Optim., **28**, 950-965 (1990).

[14] M. Bardi, I. Capuzzo Dolcetta, *Optimal control and viscosity solutions of Hamilton-Jacobi-Bellman equations.*, Birkhauser, Basel, 1997.

[15] G. Barles, *Solutions de visocité des equations de Hamilton-Jacobi.* Springer, Berlin, 1994.

[16] R. Bellman, *Dynamic Programming.* Princeton University Press, Princeton, NJ, 1957.

[17] H.M. Byrne, *Dissecting cancer through mathematics: from the cell to the animal model.* Nat. Rev. Cancer **10**, 221-230 (2010).

[18] O. Bokanowski, S. Maroso, H. Zidani, *Some convergence results for Howard's algorithm,* SIAM Journal on Numerical Analysis **47**, 3001–3026 (2009).

[19] N.D. Botkin, K. Hoffman, V. Turova, *Stable numerical schemes for solving Hamilton Jacobi Bellman Isaacs equations*, SIAM J. of Scientific Computing, **33**, 992-1007 (2011).

[20] I. Bozic. B. Allen, MA Nowak, *Dynamics of targeted cancer therapy*, Trends Mol Med. **18**(6) (2012).

[21] I. Bozic, J. Reiter, B. Allen, T. Antal, K. Chatterjee, P. Shah, YS Moon, A. Yaqubie, N. Kelly, DT Le, EJ Lipson, PB Chapman, LA Diaz, B. Vogelstein, MA Nowak *Evolutionary dynamics of cancer in response to targeted combination therapy*, eLife **2** (2013).

[22] A. Brock, H. Chang, S. Huang, *Non genetic heterogeneity–a mutation-independent driving force for the somatic evolution of tumours*, Nat. Rev. Genet. **10(5)**, 336-42 (2009).

[23] S. Cacace, E. Cristiani, M. Falcone, A. Picarelli, *A patchy dynamic programming scheme for a class of Hamilton-Jacobi-Bellman equations,* SIAM J. of Scientific Computing, **34**, 2625-2649 (2012).

[24] S. Cacace, E. Cristiani, M. Falcone, *Can local single pass methods solve any stationary Hamilton-Jacobi-Bellman equations?*, SIAM J. Sci. Comput., **36**, A570-A587, (2014).

[25] F. Camilli, L. Grüne, *Numerical approximation of the maximal solution of a class of degenerate Hamilton-Jacobi equations,* SIAM J. Numer. Anal. **38**, 1540-1560 (2000).

[26] F. Camilli, A. Siconolfi, *Maximal subsolutions for a class of degenerate Hamilton-Jacobi equations with discontinuities*, Interface and free boundaries, **6**, 329-349 (2004).

[27] I. Capuzzo Dolcetta, M. Falcone, *Discrete dynamic programming and viscosity solutions*, Annales de l'Institut Henry Poincaré- Analyse non-lineaire, **6** (supplement), 161-184 (1989).

[28] E. Carlini, M. Falcone, R. Ferretti, *An efficient algorithm for Hamilton-Jacobi equations in high dimension.* Computing and Visualization in Science, **7**, 15-29, (2004).

[29] HH Chang, PY Oh, DE Ingber, S. Huang, *Multistable and multistep dynamics in neutrophil differentiation,* BMC Cell. Biol. **7**(1), (2006)

[30] N. Champagnat, R. Ferrière, G. Ben Arous, *The canonical equation of adaptive dynamics: A mathematical view* Selection **2**, 73-83 (2001).

[31] N. Champagnat, R. Ferrière, S. Méléard, *Unifying evolutionary dynamics: from individual stochastic process to macroscopic models*, Theor. Popul. Biol. **69**(3), 297-321 (2006).

[32] R.H. Chisholm, T. Lorenzi, J. Clairambault, *Cell population heterogeneity and evolution towards drug resistance in cancer: biological and mathematical assessment, theoretical treatment optimisation* Biochim. Biophys. Acta - General Subjects, Vol. 1869, Issue 11, Part B, 2627-2645 (2016).

[33] R.H. Chisholm, T. Lorenzi, L. Desvillettes, B.D. Hughes, *Evolutionary dynamics of phenotype-structured populations: from individual-level mechanisms to population-level consequences*, Z. angew. Math. Phys., in press.

[34] R.H. Chisholm, T. Lorenzi, A. Lorz, *Effects of an advection term in nonlocal Lotka-Volterra equations*, Commun. Math. Sci., **14**, 1181-1188, (2016).

[35] R.H. Chisholm, T. Lorenzi, A. Lorz, A.K. Larsen, L. Neves de Almeida, A. Escargueil, J. Clairambault, *Emergence of drug tolerance in cancer cell populations: an evolutionary outcome of selection, non-genetic instability and stress-induced adaptation*, Cancer Res.,**75**, 930-939, (2015).

[36] M.G. Crandall, P.L. Lions, *Viscosity solutions of Hamilton-Jacobi equations*, Trans. Amer. Math. Soc., **277**, 1-42, (1983).

[37] M.G.Crandall, P.L. Lions, *Two approximations of solutions of Hamilton-Jacobi equations,* Math. Comput. **43**, 1-19 (1984).

[38] E. Cristiani, M. Falcone *Fast semi-lagrangian schemes for the eikonal equation and applications*, SIAM J. Numer. Anal., **45**, 1979-2011 (2007).

[39] K. Deckelnick, C.M. Elliott, V. Styles. *Optimal control of the propagation of a graph in inhomogeneous media.* SIAM J. Control. Optim. **48**, no. 3, 1335-1352 (2009).

[40] K. Deckelnick, C.M. Elliott. *Propagation of graphs in two-dimensional inhomogeneous media.* Appl. Numer. Math., **56**, pp. 3, 1163-1178 (2006).

[41] DL Dexter, HM Kowalski, BA Blazar, Z. Fliegiel, GH Heppner, *Heterogeneity of tumor cells from a single mouse mammary tumor,* Cancer. Res. **38 (10)**, 3174-81 (1978).

[42] G. Fabrini, T. Lorenzi, P. Bagnerini, M. Gaggero, B.D. Hughes, L. Neves de Almeida *Emergence of acquired cytotoxic-drug resistance in cancer cell populations and identification of optimal dosing schedules: insights from phenotype-structured equations*, in preparation

[43] M. Falcone, *A numerical approach to the infinite horizon problem of deterministic control theory*, Applied Mathematics and Optimization, **15**, 1-13 (1987).

[44] M. Falcone, *Numerical solution of Dynamic Programming equations*, Appendix A in the volume M. Bardi and I. Capuzzo Dolcetta, *Optimal control and viscosity solutions of Hamilton–Jacobi–Bellman equations*, Birkhäuser, Boston, 471-504 (1997).

[45] M. Falcone, R. Ferretti, *Discrete time high-order schemes for viscosity solutions of Hamilton-Jacobi-Bellman equations*, Numer. Math., **67**, 315-344 (1994).

[46] M. Falcone, P. Lanucara and A. Seghini, *A splitting algorithm for Hamilton-Jacobi-Bellman equations,* Applied Numerical Mathematics, **15**, 207-218 (1994).

[47] M. Falcone, R. Ferretti, *Semi-Lagrangian Approximation Schemes for Linear and Hamilton-Jacobi Equations*, SIAM, 2014.

[48] R. Findeisen, F. Allgöwer, *An Introduction to Nonlinear Model Predictive Control* In C.W. Scherer and J.M. Schumacher, editors, Summerschool on *The Impact of Optimization in Control*, Dutch Institute of Systems and Control, DISC, 2001.

[49] R. Findeisen, F. Allgöwer, *The quasi-infinte horizon approach to nonlinear model predictive control,* In A. Zinober and D. Owens, editors, *Nonlinear and Adaptive Control, Lecture Notes in Control and Information Sciences,* Springer-Verlag, Berlin, 2002, 89-105.

[50] K.R. Fister, J.C. Panetta, *Optimal control applied to cell-cycle-specific cancer chemotherapy,* SIAM J. Appl. Math. **60**, 1059-1072 (2000).

[51] W.H. Fleming, R.W. Rishel, *Deterministic and stochastic optimal control,* Springer-Verlag, New York, 1975.

[52] A.Friedman, E.Kashdan, U.Ledzewicz, H. Schättler, *Mathematical methods in biomedicine*, Springer, New York 257-299 (2012).

[53] R. Glasspool, JM Teodoridis, R. Brown, *Epigenetics as a mechanism driving polygenic clinical drug resistance,* Br J Cancer **94(8)**, 1087-92 (2006).

[54] M. Graeves, CC Maley, *Clonal evolution in cancer,* Nature **481 (7381)** 306-13 (2012).

[55] M. Grepl and K. Veroy, *A level set reduced basis approach to parameter estimation*, Comptes Rendus Mathematique, **349**, 1229-1232 (2011).

[56] L. Grüne, *An adaptive grid scheme for the discrete Hamilton-Jacobi-Bellman equation*, Numer. Math., **75**, 319-337 (1997).

[57] L. Grüne, J. Panneck, M. Seehafer, K. Worthmann, *Analysis of unconstrained nonlinear MPC schemes with time varying control horizon,* SIAM Journal on Control and Optimization, **48**, 4938-4962 (2010).

[58] L. Grüne and J. Pannek. *Nonlinear Model Predictive Control*, Springer London, 2011.

[59] R. Gonzáles, C. Sagastizábal, *Un algorithme pour la résolution rapide d'équations discrètes de Hamilton-Jacobi-Bellman*, C.R. Acad. Sci. Paris, Sér. I, **311**, 45-50 (1990).

[60] PB Gupta, CM Fillmore, G. Jiang, SD Shapira, K Tao, C Kuperwasser, ES Lander, *Stochastic state transitions give rise to phenotypic equilibrium in populations of cancer cells,* Cell **46(4)**, 633-44 (2011).

[61] P. Hahnfeldt, D. Panigrahy, J. Folkman, L. Hlatky, *Tumor development under angiogenic signaling: a dynamical theory of tumor growth, theory response, and postvascular dormancy,* Canc. Res. **59**, 4770-4775 (1999).

[62] D. Hanahan, RA Weinberg, *Hallmarks of cancer: the next generation*, Cell **144(5)**, 646-74 (2011).

[63] M. Hinze, R. Pinnau, M. Ulbrich, S. Ulbrich, *Optimization with PDE Constraints Mathematical Modelling: Theory and Applications,* **23**, Springer Verlag, 2009. Mathematical Modelling: Theory and Applications, 23, Springer Verlag, 2009.

[64] P. Holmes, J.L. Lumley, G. Berkooz, C.W. Romley, *Turbulence, Coherent Structures, Dynamical Systems and Symmetry,* Cambridge Monographs on Mechanics, Cambridge University Press, 2nd edition, 2012.

[65] R.A. Howard, *Dynamic programming and Markov processes,* Wiley, New York, 1960.

[66] S. Huang, *Genetic and non-genetic instability in tumor progression: link between the fitness landscape and the epigenetic landscape of cancer cells*, Cancer Metastasis Rev, **32 (3-4)**, 423-48 (2013).

[67] R. Kalaba, *On nonlinear differential equations, the maximum operation and monotone convergence,* J. of Math. Mech., **8**, 519-574 (1959).

[68] C.T. Kelley, *Iterative Method for Optimization,* SIAM, 1999.

[69] KS Korolev, JB Xavier, J. Gore, *Turning ecology and evolution against cancer,* Nat. Rev. Cacner. **14(5)**, 371-80 (2014).

[70] G. Kossioris, C. Makridakis, P. Souganidis, *Finite volume schemes for Hamilton Jacobi equations,* Numer. Math. **83**, 427 - 442 (1999).

[71] A. Kröner, K. Kunisch and H. Zidani. *Optimal feedback control of undamped wave equations by solving a HJB equation,* preprint, available at: `http://www.cmap.polytechnique.fr/~kroener/KroenerKunischZidani2013.pdf`

[72] K. Kunisch, S. Volkwein, *Galerkin proper orthogonal decomposition methods for parabolic problems,* Numer. Math. **90**, 117-148 (2001).

[73] K. Kunisch, S. Volkwein, and L. Xie. *HJB-POD based feedback design for the optimal control of evolution problems*, SIAM J. on Applied Dynamical Systems, **4**, 701-722 (2004).

[74] K. Kunisch and L. Xie. *POD-Based Feedback Control of Burgers Equation by Solving the Evolutionary HJB Equation,* Computers and Mathematics with Applications. **49**, 1113-1126, (2005).

[75] T. Lorenzi, R.H. Chisholm, J. Clairambault. *Tracking the evolution of cancer cell populations through the mathematical lens of phenotype-structured equations,* Biology Direct, (2016).

[76] I. Lasiecka, R. Triggiani, *Control theory for partial differential equations: continuous and approximation theories. I,* Abstract parabolic systems. Encyclopedia of Mathematics and its Applications, 74. Cambridge University Press, Cambridge, 2000.

[77] I. Lasiecka, R. Triggiani, *Control theory for partial differential equations: continuous and approximation theories. II.* Abstract hyperbolic-like systems over a finite time horizon. Encyclopedia of Mathematics and its Applications, 74. Cambridge University Press, Cambridge, 2000.

[78] U. Ledzewicz, H. Schättler, *Optimal controls for a model with pharmacokinetics maximizing bone marrow in cancer chemotherapy,* Math. Biosci. **206**, 320-342 (2007).

[79] U. Ledzewicz, H. Maurer, H. Schttler *Optimal and suboptimal protocols for a mathematical model for tumor anti-angiogenesis in combination with chemoterapy,* Math. Biosci. Eng. **8**, 307-323 (2011).

[80] J.L. Lions, *Optimal control of systems governed by partial differential equations,* Springer-Verlag, New York 1971.

[81] T. Lorenzi, R.H. Chisholm, L. Desvillettes, B.D. Hughes, *Dissecting the dynamics of epigenetic changes in phenotype-structured populations exposed to fluctuating environments*, J. Theoret. Biol., **386**, 166-176, (2015).

[82] A. Lorz, S. Mirrahimi, B. Perthame *Dirac mass dynamics in multidimensional nonlocal parabolic equations*, Comm. Partial Differential Equations, **36(6)**,1071-1098 (2011).

[83] R. Martin, *Optimal control drug scheduling of cancer chemotherapy*, Automatica **28**, 1113-1123 (1992).

[84] A. Marusyk, V. Almendro, K. Polyak, *Intra-tumor heterogeneity: a looking glass for cancer?*, Nat. Rev. Cancer, **2(5)**, 323-34 (2012).

[85] H. Maurer, *Numerical Solution of singular control problems using a multiple shooting techniques,* J. of Optimization Theory and Applications, **18**, 235-257 (1976).

[86] JP Medema, *Cancer stem cells: the challenges ahead*, Nat Cell Biol. **15(4)** 338-44 (2013).

[87] LM Merlo, JW Pepper, BJ Reild, CC Maley, *Cancer as an evolutionary and ecological process,* Nat. Rev. Cancer. **6(12)**, 924-35 (2006).

[88] J.C.P. Miller, *Parabolic cylinder functions,* Handbook of Mathematical Functions, National Bureau of Standards, Appl. Math. Ser. No 55, M. abramowitz and I. A. Stegun, eds., U.S. Govt. Printing Office, Washington, DC, 685-720, (1964).

[89] J. Murray *Optimal control for a cancer chemotherapy problem with general growth and loss functions*, Math. Biosci. **98**, 273-287 (1990).

[90] J. Murray *Some optimal control problems in cancer chemotherpy with a toxicity limit*, Math. Biosci. **100**, 49-67 (1990).

[91] JR Newman, S Ghaemmaghami, J. Ihmels, DK Breslow, M. Noble, JL Derisi, JS Weissman, *Single-cell protemic analysis of s. cerevisiae reveals the architecture of biological noise,* Nature **441(7095)**, 840-6 (2006).

[92] J. Nocedal, S.J. Wright. *Numerical Optimization,* Springer Series in Operation Research, second edition, 2006.

[93] PC Nowell, *The clonal evolution of tumor cell populatoins,* Science **194(4260)**, 23-8 (1976).

[94] S. Osher, J.A. Sethian, *Fronts propagation with curvature dependent speed: algorithms based on Hamilton-Jacobi formulations,* J. Comput. Phys., **79** (1988).

[95] S. Osher, R.P. Fedkiw, *Level Set Methods and Dynamic Implicit Surfaces*, Springer-Verlag, New York, 2003.

[96] J. Otwinowski, J.B. Plotkin *Interferring fitness landscapes by regression produces biased estimates of epistasis*, Proceedings of the National Academy of Sciences **111 (22)**, E2301-E2309 (2014).

[97] J. Panetta, J. Adam *A mathematical model of cell-specific chemotherapy*, Math. Comput. Model. **22**, 67 (1995).

[98] G. Pannocchia, J.B. Rawlings, S.J. Wright, *Conditions under which suboptimal nonlinear MPC is inherently robust,* In 18th IFAC World Congress, Milan, Italy, Sep. 2011.

[99] A.T. Patera, G. Rozza, *Reduced Basis Approximation and A Posteriori Error Estimation for Paramtrized Partial Differential Equations.* MIT Pappalardo Graduate Monographs in Mechanical Engineering, 2006.

[100] B. Perthame, *Transport Equations in Biology*, Birkhäuser (2006).

[101] B. Perthame *Some mathematical models of tumor growth* , Note February 2015.

[102] B. Perthame *Parabolic equations in biology*, Lecture Notes on Mathematical Modelling in the Life Sciences (2015).

[103] AO Pisco, A Brock, J. Zhou, A. Moor, M. Mojtahedi, D. Jackson, S. Huang, *Non darwinian dynamics in therapy-induced cancer drug resistance,* Nat. Commun., 4:2467 (2013)

[104] A.O. Pisco, S. Huang, *Non-genetic cancer cell plasticity and therapy-induced stemness in tumour relapse: 'What does not kill me strengthens me'*, British Journal of Cancer **112**, 1725-1732 (2015).

[105] M. Pollatschek, B. Avi-Itzhak, *Algorithms for Stochastic Games with Geometrical Interpretation,* Management Sci **15** (1969), 399-415.

[106] L. Pontryagin, V. Boltyanskii, R. Gamkrelize, E. Mishenko, *The Mathematical Theory of Optimal Processes,* Wiley, 1962.

[107] M.L. Puterman, S.L. Brumelle, *On the convergence of Policy iteration in stationary Dynamic,* Porgramming. Math. of Operation Research, **4** (1979), 60-69.

[108] A. Raj, A. van Oudenaarden, *Nature, nurture, or chance: stochastic gene expression and its consequences,* Cell. **135(2)**, 216-26 (2008).

[109] R. Ramakrishnan, D. Assudani, S. Nagaraj, T. Hunter, HI Cho, S. Altiok, E. Celis, DI Gabrilovich, *Chemotherapy enhances tumor cell susceptibility to CTL-mediated killing during cancer immunotherapy in mice*, J Clin Invest, **120 (4)**, 1111-24 (2010).

[110] J.B. Rawlings, D.Q. Mayne *Model Predictive Control: Theory and Design,* Nob Hill Publishing, LLC, 2009.

[111] M.S. Santos and J. Rust, *Convergence properties of policy iteration*, SIAM J. Control Optim., **42** (2004), 2094-2115.

[112] P. Savage, J. Stebbing, M. Bower, T. Crook. *Why does cytotoxic chemotherapy cure only some cancers?*, Nat. Clin Pract Oncol, **6(1)**: 43-52 (2009).

[113] SV Sharma, DY Lee, B. Lee, MP Quinlan, F. Takahashi, S. Maheswaran, U. McDermott, N. Azizian, L. Zou, MA Fischbach et al, *A chromatin-mediated reversible drug-tolerant state in cancer cell subpopulations*, Cell. 2010; **141(1)** 69-80 (2010)

[114] J.A. Sethian, *A fast marching level set method for monotonically advancing fronts,* Proc. Natl. Acad. Sci. USA, **93** (1996), 1591-1595.

[115] J.A. Sethian, *Level set methods and fast marching methods*, Cambridge University Press, 1999.

[116] J.A. Sethian, *Fast marching methods*, SIAM Rev. **41**, 199-235 (1999).

[117] J.A. Sethian, A. Vladimirsky, *Ordered upwind methods for static Hamilton-Jacobi equations: theory and algorithms*, SIAM J. Numer. Anal., **41** (2003), 325-363.

[118] L. Sirovich, *Turbulence and the dynamics of coherent structures. Parts I-II,* Quarterly of Applied Mathematics, **XVL**, 561-590 (1987).

[119] G. Steel, L. Lamerton, *The growth rate of human tumours,* Br J Cancer. 1966;20(1):74.

[120] N.M. Temme, *Parabolic cylinder function*, in Olver, Frank W. J.; Lozier, Daniel M.; Boisvert, Ronald F.; Clark, Charles W., NIST Handbook of Mathematical Functions, Cambridge University Press (2010).

[121] F. Tröltzsch. *Optimal Control of Partial Differential Equations: Theory, Methods and Application*, American Mathematical Society, 2010.

[122] J.N. Tsitsiklis, *Efficient algorithms for globally optimal trajectories,* IEE Tran. Automatic. Control, **40** (1995), 1528-1538.

[123] S. Volkwein, *Model Reduction using Proper Orthogonal Decomposition: Theory and Reduced-Order Modelling,* Lecture Notes, Universität Konstanz, 2012. See `www.math.uni-konstanz.de/numerik/personen/volkwein/index.php`.

[124] S. Volkwein, F. Tröltzsch, *POD a-posteriori error estimates for linear-quadratic optimal control problems,* Computational Optimization Theory and Applications, **147**: 169-193 (2009).

[125] H. Zhao *A fast sweeping method for Eikonal equations,* Math. Comp., **74**, 603-627 (2005).